THE ASTROPHYSICAL JOURNAL

AN INTERNATIONAL REVIEW OF SPECTROSCOPY AND ASTRONOMICAL PHYSICS

VOLUME 90 SEPTEMBER 1939 NUMBER 2

SPACE REDDENING IN THE GALAXY*

JOEL STEBBINS, C. M. HUFFER, AND A. E. WHITFORD

ABSTRACT

The space reddening was determined from the colors of 1332 B stars measured photoelectrically at Madison and Mount Wilson.

From spectrophotometric measures of reddened B stars the selective absorption varies approximately as λ^{-1}. On the basis of this law the total visual and photographic absorptions are, respectively, seven and nine times the color excess.

When allowance is made for interstellar absorption, the early B stars are found to be intrinsically nearly 1 mag. brighter than previously assumed.

The correlation between color excess and the intensities of interstellar lines is as close as the correlation between the intensities of the different lines in the same stars.

The reddest B stars are all near the galactic circle, and there are more of them toward the center than toward the anticenter of the galaxy. Near the center there is more absorption on the north side than on the south side of the galactic circle.

The B stars in several bright clouds are all slightly colored, showing that even the brightest parts of the Milky Way are affected by absorption.

The absorption near the sun is given by the colors of bright B stars and of A stars near the north pole of rotation. The absorption near the pole at less than 300 parsecs is confirmed.

In general the absorbing clouds are near the galactic plane, but they are so irregular in distribution that the conception of a uniform layer with a constant coefficient of absorption is no longer tenable.

The present paper is an extension of the previous study of the colors of 733 B stars[1] measured at Madison with a photoelectric photometer. The new program included about 600 fainter B stars measured with the 15-inch refractor at Madison and with the 60- and 100-inch reflectors at Mount Wilson. The combined list com-

* *Contributions from the Mount Wilson Observatory, Carnegie Institution of Washington*, No. 617. This paper was presented at the symposium on galactic and extragalactic structure held in connection with the dedication of the McDonald Observatory on May 5–8, 1939.

[1] *Pub. Washburn Obs.*, **15**, Part V, 1934.

prises 1332 stars of early type, and their colors give considerable information about selective and general space absorption in the galaxy.

The first list, which will be designated as the "733 stars," included nearly all stars of spectrum O–B5 brighter than visual magnitude 7.5 and north of $-15°$ declination. The extended list includes nearly all stars of spectrum O–B2 north of $-40°$ and to the limit of the *Henry Draper Catalogue*. To these were added miscellaneous cB, cA, and faint Be stars furnished by Mr. Merrill, distributed along the Milky Way, and additional B3, B5, and B stars in several selected regions.

The photoelectric cells, each with two filters, gave essentially the same system of colors that was used for the 733 stars. The scale, about two-thirds that of the international scale for color index, varied little from cell to cell or from telescope to telescope, but the zero point had to be carefully determined for each change of instrumental conditions—for instance, when the large mirrors were resilvered and especially when they were aluminized. The zero point was continually controlled by measures of standard B stars or of A stars in the North Polar Sequence.

The measures of the 733 stars at Madison and the first ones at Mount Wilson were made with the combination of a Kunz potassium cell and a Lindemann electrometer. From 1933 on, all measures were made with a Kunz cell and the thermionic amplifier perfected by Whitford. For bright stars—e.g., down to fourth or fifth magnitude with the 15-inch telescope—the amplifier has no special advantage over the electrometer, but for seventh- or eighth-magnitude stars with the 15-inch telescope and for 3 mags. fainter with the 60-inch telescope the amplifier is easily 1 or 2 mags. more sensitive than the electrometer. A more detailed account of the work, with the data for individual stars, will be published in the *Mount Wilson Contributions*.

LAW OF SPACE REDDENING

As the law of variation of selective absorption with wave length is of fundamental importance in a study of space reddening from the colors of B stars, we have made spectrophotometric measures of a few strongly reddened stars. This study, due mainly to Whitford, was carried on with the focal-plane or so-called "zero-power" spec-

trograph on the 60-inch reflector. A cesium oxide cell refrigerated with dry ice was used to cover the long range of spectrum. By using two stars, one of small and the other of large color excess, close to-

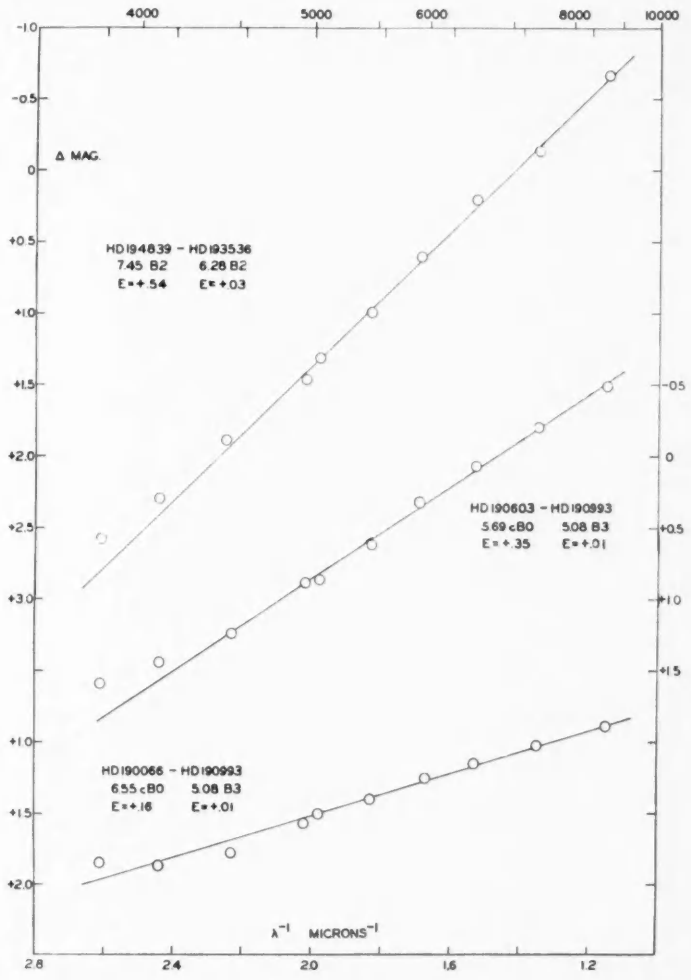

FIG. 1.—Variation of absorption with wave length

gether in the sky to eliminate atmospheric absorption, a series of measures was taken at about ten points along the spectrum of each star. The results for three such pairs of stars are shown in Figure 1.

The difference of magnitude between two stars at each spectral region is plotted against the inverse wave length, and from the straight-line relation it is seen at once that the difference of the selective absorption in two stars varies nearly as λ^{-1}. This law of space reddening has also been derived by Mrs. Rudnick,[2] Hall,[3] Greenstein,[4] and others. To the violet of, say, 4500 A the observed points run off in the same direction for the different stars, but the measures are increasingly uncertain at small wave lengths because of the reduced intensity. A new spectrophotometer with UV glass for the prism and lenses is being constructed for use with the 60- and 100-inch telescopes.

Without considering for the present the nature of the material necessary to absorb according to λ^{-1}, we assume that this is the law of space reddening and that it applies uniformly to the colors of the B stars. The ratio of the total to the selective absorption in space may then be derived from the same reasoning as that used for the globular clusters.[5]

Let I_v, I_y, and I_b represent the observed intensities with the eye, with the cell and yellow filter, and with the cell and blue filter, respectively. Let I_v^0, I_y^0, and I_b^0 represent the same intensities prior to reduction by selective absorption in interstellar space. Then we have

$$2.5 \log_{10} \frac{I_v}{I_v^0} = -t\,\lambda_v^{-1}\,, \tag{1}$$

$$2.5 \log_{10} \frac{I_y}{I_y^0} = -t\,\lambda_y^{-1}\,, \tag{2}$$

$$2.5 \log_{10} \frac{I_b}{I_b^0} = -t\,\lambda_b^{-1}\,, \tag{3}$$

where t is proportional to the optical path in the material which absorbs according to the law of λ^{-1}. Subtracting (3) from (2), we have

$$2.5 \log_{10} \frac{I_y}{I_b} - 2.5 \log_{10} \frac{I_y^0}{I_b^0} = -t\,(\lambda_y^{-1} - \lambda_b^{-1})\,. \tag{4}$$

[2] *Ap. J.*, **83**, 394, 1936. [3] *Ap. J.*, **85**, 145, 1937. [4] *Ap. J.*, **87**, 151, 1938.

[5] *Mt. Wilson Contr.*, No. 547, p. 22; *Ap. J.*, **84**, 153, 1936.

The terms on the left-hand side of the equation are seen to be the observed color index and the normal color index, respectively, and their difference therefore represents the color excess E. Equation (1) gives simply the visual absorption A_v, in magnitudes, due to selective absorption. It has been previously shown that for a source of equal energy along the spectrum, λ_b and λ_y are equal to 4260 A and 4770 A, respectively. When applied to the energy-curve of a hot star, taken as a black body at 20,000°, the effective wave lengths are changed slightly to $\lambda_b = 4170$ and $\lambda_y = 4710$. The effective wave length corresponding to the Harvard visual-magnitude system is more uncertain but is taken as $\lambda_v = 5100$, approximately the value found by Wesselink.[6]

$$\frac{A_v}{E} = \frac{\lambda_v^{-1}}{\lambda_b^{-1} - \lambda_y^{-1}} = \frac{5100^{-1}}{4170^{-1} - 4710^{-1}} = 7.1 . \qquad (5)$$

In the same way, assuming the photographic wave length to be 4250,

$$\frac{A_{pg}}{E} = \frac{4250^{-1}}{4170^{-1} - 4710^{-1}} = 8.6 . \qquad (6)$$

In what follows we shall take

$$A_v = 7E, \qquad A_{pg} = 9E , \qquad (7)$$

as sufficiently close for estimates of the total visual and photographic absorption. We have tacitly assumed that the λ^{-1} law continues to apply for very long wave lengths, i.e., down to very small values of λ^{-1}. This is a not unnatural assumption from the point of view of Greenstein's[7] theory of scattering by a mixture of particles with a size-distribution function extrapolated from that observed for telescopic meteors. It may be noted that the value $A_{pg} = 9E$ is not far from the mean obtained by Oort[8] from a study of the radial velocities of normal and reddened B stars.

In the study of the colors of the globular clusters it was found that the extragalactic nebulae disappear when E exceeds $+0.20$ — a fact which argues for a high value of the ratio of total to selective

[6] *B.A.N.*, **7**, 243, 1935.

[7] *Harvard Circ.*, No. 422, 1938; *Ap. J.*, **88**, 599, 1938. [8] *B.A.N.*, **8**, 248, 1938.

absorption. In Hubble's[9] survey the number of nebulae on an average plate in high latitude was about fifty. From his distribution-curve an absorption of $9 \times 0.20 = 1.80$ mag. would reduce this number about tenfold, so that there would be few nebulae above the threshold of identification. In view of the greater brightness of the sky in the Milky Way and the richer star fields, the observed limit is at least not a contradiction.

At first sight it might appear that such large ratios of total to selective absorption would lead to difficulties with the density function;[10] but if the dark material is arranged in successive clouds along the plane of the galaxy rather than in a thin uniform layer, these difficulties may disappear. Some such high ratio of total to selective absorption is to be expected from the lack of strong coloring of stars in or near such regions as the Barnard dark nebulae, where stars are almost entirely obscured without showing much space reddening. If the interstellar material is not thoroughly "stirred," so to speak, and the ratio of total to selective absorption is not reasonably constant over large regions, then the problem of determining absorption and distances in the galaxy from measures of color is of course hopeless. Therefore, until we run into difficulties, we proceed as though the absorbing material were uniform in quality if not in distribution.

ABSOLUTE MAGNITUDES

The more important determinations of the mean absolute magnitude of B stars in the galaxy from proper motions, radial velocities, moving clusters, etc., have hitherto been made without regard to the space absorption, which now turns out to be far from negligible. In all strictness such absolute magnitudes should be worked out all over again with proper allowance for the actual absorption for each star, but we can obtain useful results by applying a mean absorption to each spectral subclass.

In Table 1 are brought together several determinations of the absolute magnitudes of B stars, which seem to us to be of greatest weight. In column 2 are the results by Plaskett and Pearce[11] and

[9] *Mt. Wilson Contr.*, No. 485; *Ap. J.*, **79**, 8, 1934.

[10] Seares, *Mt. Wilson Contr.*, No. 428; *Ap. J.*, **74**, 91, 1931.

[11] *Pub. Dom. Ap. Obs.*, **5**, 289, 1936.

in column 3 those by Strömberg,[12] both from the proper motions in the *Boss General Catalogue*. Strömberg used only stars brighter than visual magnitude 6.0; Plaskett and Pearce included the fainter B stars in the catalogue. The means of these two determinations in column 4 show what is found when the absorption is neglected. In column 5 are the smoothed values of the average absorption $A_v = 7E$ which we find for the B stars of the magnitudes used by Plaskett and Pearce and by Strömberg. There is, of course, the defect that

TABLE 1

ABSOLUTE VISUAL MAGNITUDES

Spectrum (1)	Plaskett and Pearce (2)	Strömberg (3)	Mean (4)	Absorption (5)	Corrected Mean (6)	Radial Velocities (7)	Pairs (8)	Final (9)	733 (10)	Difference (11)
cB, cA	.....	.....	.....	−1.0	.....	.....	.....	−5.5	.....	.....
O	−4.0	.....	−4.0	−0.6	−4.6	−4.4	−4.1	4.5	−4.0	−0.5
Bo	.....	.....	3.5	−0.5	4.0	3.8	3.6	3.9	−3.2	0.7
	3.4	.....	.....	.....	.....	.....	.....	.....	.....	.....
B1	.....	−3.3	3.3	−0.4	3.7	.....	3.3	3.6	−2.5	1.1
B2	2.8	.....	2.8	−0.3	3.1	−2.5	3.1	3.0	−1.8	1.2
B3	1.5	1.9	1.7	−0.2	1.9	.....	2.8	2.2	−1.3	0.9
B4	.....	.....	.....	.....	.....	.....	.....	1.9	−0.9	1.0
B5	−1.0	1.6	1.3	−0.1	1.4	.....	−1.9	1.6	−0.7	0.9
B6	.....	.....	.....	.....	.....	.....	.....	1.4	−0.5	0.9
B7	.....	.....	.....	.....	.....	.....	.....	1.1	−0.3	0.8
B8	.....	.....	0.8	0.0	0.8	.....	.....	0.8	−0.2	0.6
	.....	−0.7	.....	.....	.....	.....	.....	.....	.....	.....
B9	.....	.....	−0.4	0.0	−0.4	.....	.....	−0.4	+0.1	−0.5

our colors extend only to declination −40°, while the proper motions extend over the entire sky. Nevertheless, the corrected means in column 6 formed from the two preceding columns are undoubtedly an improvement over the uncorrected values.

The absolute magnitudes in column 7 were determined by Whitford from the Victoria radial velocities on the assumption that the constant $A = 19$ km/sec at 1000 parsecs for the rotation of the galaxy.

The results in column 8 were derived from the colors and magnitudes of pairs or groups of B stars in different parts of the sky.

[12] *Mt. Wilson Contr.*, No. 442, p. 8; *Ap. J.*, **75**, 122, 1932.

When two stars in a recognized obscured region have the same color excess and are separated by not more than, say, one degree, the presumption is that they are at about the same distance from the sun and that the difference in their apparent magnitudes is actually the difference in their absolute magnitudes. In many such pairs of spectra O–B5, with color excesses greater than 0.10 mag. and differing not more than 0.04 mag., the slight correction to distance on account of differential color was applied, and each pair thus gave an equation of condition for the difference between the absolute magnitudes of the corresponding spectral classes. The general solution for the five independent unknowns, O–Bo, Bo–B1, etc., gave each difference with an average probable error of ± 0.10 mag.—a surprisingly small value considering the nature of the method. In all strictness the results from radial velocities and pairs of B stars are only differential between the subclasses, and the values from pairs have been arbitrarily adjusted to agree in the mean with those from proper motions.

The final absolute magnitudes in column 9 are the smoothed means of columns 6, 7, and 8, giving double weight to column 6. In columns 10 and 11 are the absolute magnitudes used for the 733 stars and the differences from the revised values. The adopted value of -5.5 for supergiant c stars is more or less a rough guess. These stars are included in the means from proper motions but not for the radial velocities or pairs. In using mean absolute magnitudes to infer distances of B stars, it is somewhat disturbing to suspect that a star classified in the *Henry Draper Catalogue* as B3 or B5 is actually a supergiant c star 3 or 4 mags. brighter than assumed, and such difficulties increase proportionally among the fainter stars where the spectra have not been accurately classified. In fact, there are some thirty or forty cases of stars in the list whose large color excesses compared with neighboring B stars indicate that they are probably unrecognized c stars. For this and other reasons it is well to study the relation of color excess to the obscured areas and bright areas with as little assumption as possible about mean distances which are so much affected by inaccuracies in the classification of the spectra.

INTERSTELLAR LINES

In the 733 stars very little correlation was found between color excess and the intensity of the interstellar K line of calcium. However, Williams[13] did find such a correlation in stars whose lines had been measured photometrically, and we have known for some time that a similar relation exists between color excess and the intensities of interstellar D and other lines measured by Merrill[14] and others at Mount Wilson. In Figure 2 the intensities of interstellar lines have been plotted, first against color excess E and then against the intensity of the D lines. Owing to the nature of the material, the same stars are not always involved in the corresponding figures. It is seen that there is a strong statistical connection—the redder the star, the stronger the interstellar line—but the relation may be an indirect one due to common distance. The probable error of a color excess is not more than 0.01 or 0.02 mag., and there are numerous cases of stars of the same color excess where the ratio of the intensities of the corresponding interstellar lines is at least 5:1. In any event the correlation between color excess and line intensity is just as strong as that between the intensities of the lines themselves, as evidenced by the plots on the right-hand side of Figure 2.

Further evidence of the connection between space reddening and interstellar sodium is in Figure 3. The distribution of the stars with lines of weak, medium, and strong intensity, respectively, are shown in galactic co-ordinates in relation to Hubble's[15] zone of avoidance of the extragalactic nebulae. Not many stars were observed in the direction of the galactic center, but toward the anticenter it is seen that there are no stars with D lines stronger than 0.54 on the Mount Wilson scale in the range of longitude from 115° to 215°. The same effect in the color excesses has been pointed out before and is shown in the last graph of Figure 3. There are not enough stars with interstellar lines other than the D lines to make a comparison in the galactic distribution. There are 1332 stars with color excess available,

[13] *Mt. Wilson Contr.*, No. 487; *Ap. J.*, **79**, 280, 1934.

[14] Merrill, Sanford, Wilson, and Burwell, *Mt. Wilson Contr.*, No. 576; *Ap. J.*, **86**, 274, 1937.

[15] *Mt. Wilson Contr.*, No. 485, p. 172; *Ap. J.*, **79**, 41, 1934.

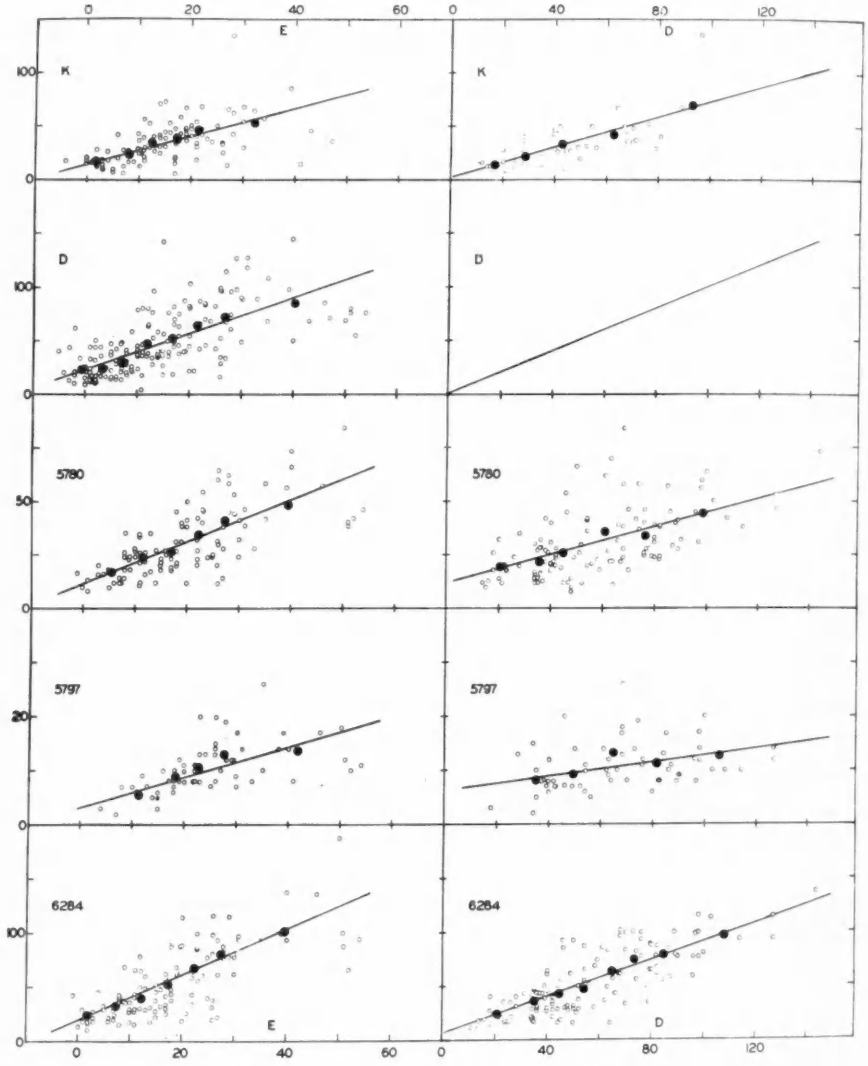

FIG. 2.—Relation between interstellar lines and color excess (*left*), with D lines (*right*)

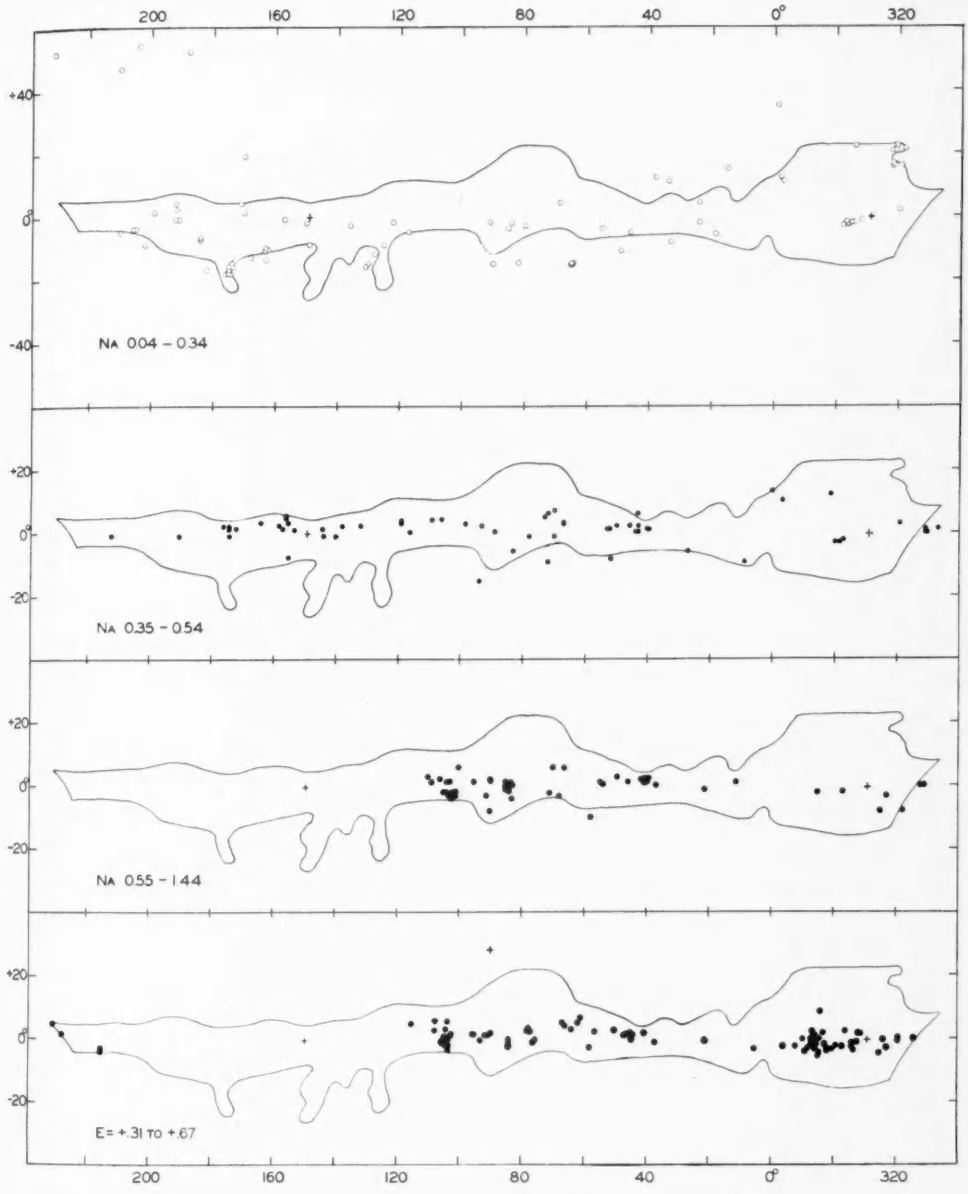

FIG. 3.—Galactic distribution of interstellar sodium and of stars with large color excess

about 200 with measures of the D lines, and from 130 down to 60 for the other lines. Further progress will depend upon the accumulation of spectroscopic data.

DISTRIBUTION OF RED B STARS

In Figure 3 the stars of color excess greater than +0.30 are strongly condensed toward the galactic circle; they are especially numerous in the region of the center of the galaxy but do not occur near the anticenter. This absence of strong selective absorption toward the anticenter leads to some puzzling deductions. The limits of visual and photographic absorption, $7E$ and $9E$, would be 2.1 mag. and 2.7 mag., respectively. Let us call them roughly 2 and 3 mags. A star of visual magnitude 9 corrected for absorption would be of true magnitude 7. With absolute magnitude −3 for spectrum B2 the modulus is 10 and the distance 1000 parsecs. Surely we can scarcely expect the space reddening to stop at less than one-fifth of the estimated extent of the galaxy in that direction. We can always get around such a difficulty temporarily by assuming that there is a cloud of dark material which conveniently stops at our limit and is succeeded by other clouds beyond. However, that particular question might be answered by long-exposure photographs with a large reflector capable of showing faint nebulae in spite of the 3 mags. of absorption. There are already known "holes" in low latitude near the anticenter where Hubble has photographed extragalactic nebulae, and it would be interesting to find just how nearly opaque the absorbing cloud is in that part of the sky.

Turning to the galactic center, where as yet the limit of selective absorption seems not to have been reached, we see in Figure 4 the colors of B stars in that region. The upper graph shows the distribution of known novae listed by Payne-Gaposchkin and Gaposchkin.[16] The larger circles indicate novae brighter than sixth magnitude at maximum. The large group to the south of the center is in the great cloud in Sagittarius. We take the center of the galaxy simply at the centroid of the apparent positions of 26 globular clusters near the center,

$$l = 329^\circ.2, \qquad b = -0^\circ.5,$$

[16] *Variable Stars*, pp. 232–236, 1938.

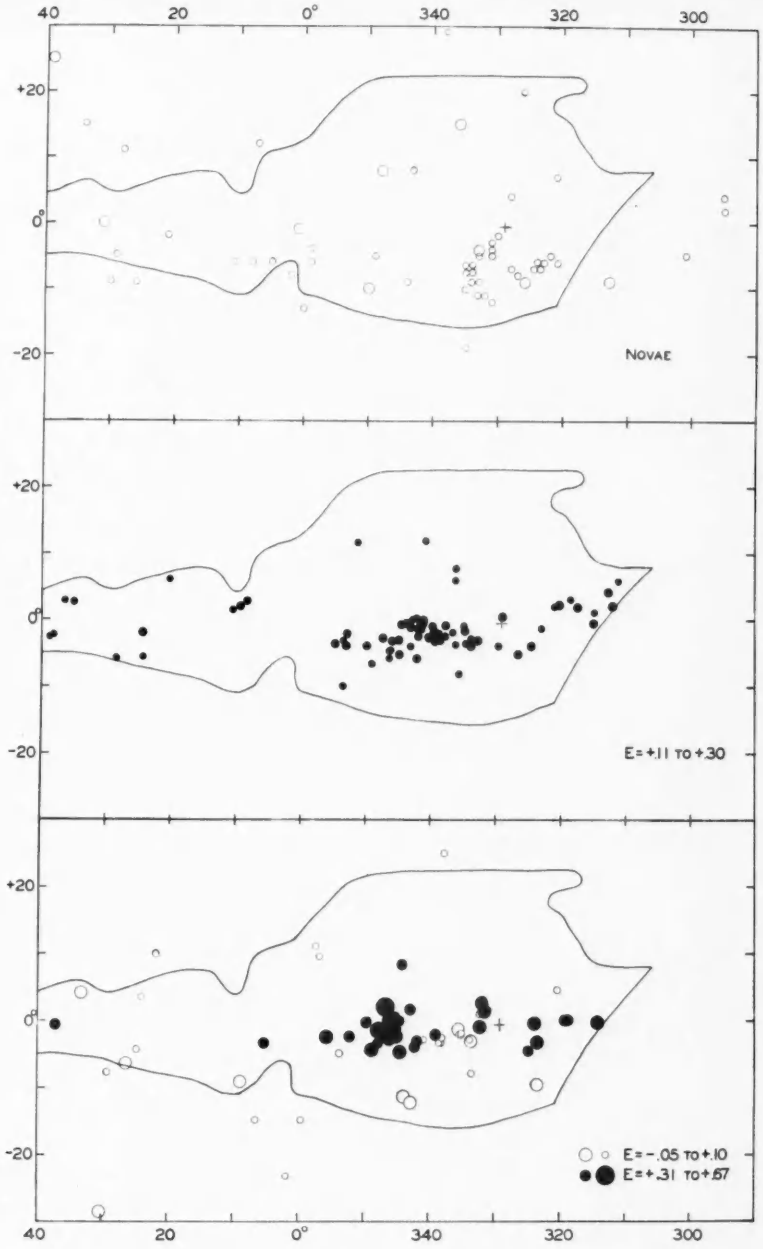

FIG. 4.—Stars with spectra O–B2, $r > 400$ parsecs, near center of galaxy

on the system of the Lund tables. The blank in the distribution of novae on the north side of the galactic circle is readily explained by absorption. This region is in the southern part of what Lindsay and Bok[17] call the dark nebula in Ophiuchus. In the lower diagrams for the B stars a few objects in the foreground have been discarded by taking the limiting modulus to be 8. The distribution is, then, for stars of spectrum O–B2 and at distances greater than 400 parsecs. The known c stars are always included with these stars of greatest luminosity.

The stars of normal color, $E = -0.05$ to $+0.05$, in the lower figure are all on the south side of the galactic plane and, together with the suspicious stars with E up to $+0.10$, indicate some real holes of small absorption between the strongly reddened stars, as at $l = 335°$, $b = -2°$. The intermediate stars in the second figure $E = +0.11$ to $+0.30$ are mostly on the south side of the galaxy. Presumably there may be corresponding stars on the north side, but they are either more strongly reddened or blotted out entirely.

The reddest stars, as before, show the strong galactic concentration, and the region near $l = 345°$, containing many red stars, is not far from the reddest globular cluster. The two reddest B stars found thus far are in this region, and they have color excesses of $+0.67$ and $+0.61$ for distances 360 parsecs and 480 parsecs, respectively. There is thus a photographic absorption greater than 5 mags. in less than 500 parsecs. There are half-a-dozen other stars along the Milky Way which have $E > +0.50$, and presumably among fainter B stars still stronger reddening will be found.

BRIGHT REGIONS IN THE MILKY WAY

A special study has been made of the B stars in three bright regions in the Milky Way, where additional stars of classes B3 and B5 were available from the *Henry Draper Catalogue* and from a list of earlier stars from lists kindly supplied by Merrill. Their designations and the rough positions of the centers for 1900 are in Table 2.

The small cloud in Sagittarius is shown in Plate I, where each B star is marked by a circle—the larger the circle, the redder the star. There are several stars in the *Henry Draper Catalogue* which were

[17] *Harvard Annals*, **105**, 289, 1937.

PLATE I

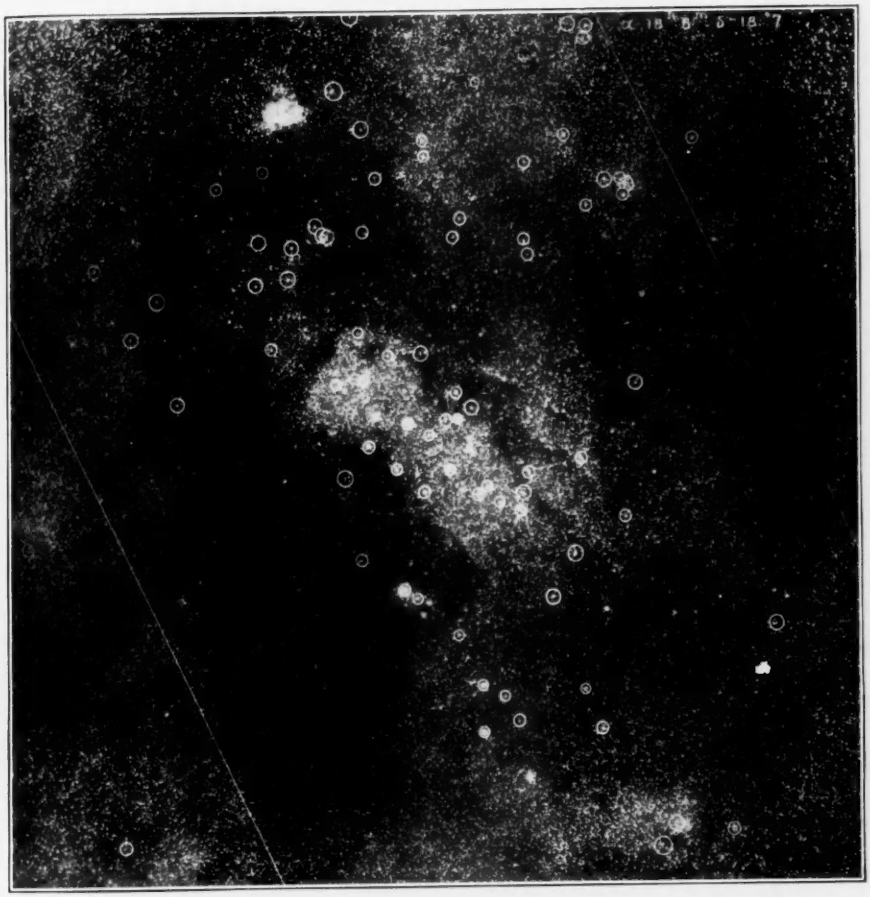

$b = 0^\circ$

$b = -5^\circ$

B Stars in the Small Cloud in Sagittarius

PLATE II

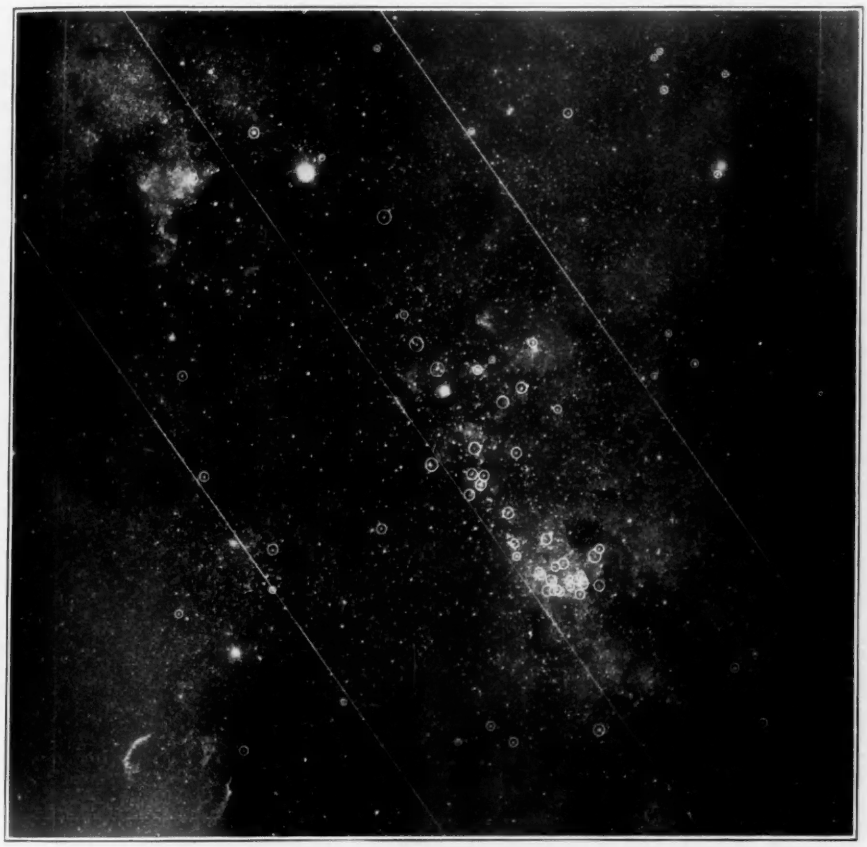

$b = +5^\circ$

$b = -5^\circ$ $b = 0^\circ$

STARS WITH SPECTRA O–B3 IN CYGNUS HAVING DISTANCES GREATER THAN 400 PARSECS

missed, but there are few if any HD stars in the blank dark areas. Very few of the B stars in Plate I have computed moduli less than 9; those which have may be c stars. Therefore, the B stars are mostly beyond 600 parsecs, but the absorption probably begins to be noticeable at less than that distance. At first glance it is evident that the small circles are in the bright cloud; the large circles are in intermediate areas, while the darkest areas are devoid of B stars. The average color excess of 15 stars in the bright cloud is +0.10 mag.; hence the visual absorption $7E = 0.70$, and the cloud is about half as bright as it would be if we could see it in the clear. The mean

TABLE 2

Region	R.A.	Decl.	l	b
Small cloud in Sagittarius	18^h10^m	$-18°.5$	$340°.2$	$-2°.5$
Bright part of the cloud in Cygnus	20 4	+35.3	40.3	+0.8
Double cluster in Perseus	2 14	+56.7	102.7	−3.1

modulus for these 15 stars is 10.2 ± 0.12, giving a distance of 1100 ± 60 parsecs. The two stars near the dark nebula, Barnard 92, at the upper right edge of the cloud, have color excesses of +0.27 and +0.16 and an average distance of 600 parsecs.

We have made a thorough check for a systematic error in the colors of this region, and we are convinced that the effect is real. There is not a single B star in the entire region of Plate I which is normal in color (one star has $E = +0.05$). The whole area is covered by a veil, and the maximum reddening is about $E = +0.40$, giving a photographic absorption of $3\frac{1}{2}$ mags. There are probably fainter and redder B stars in the dark areas about the small cloud.

The Cygnus cloud and its surroundings are shown in Plate II. The stars are those from O to B3 in the *Henry Draper Catalogue*, and the near limit of modulus 8, or 400 parsecs, was adopted to eliminate a few foreground objects. Additional stars from a list by Merrill and Sanford made a group of 19 stars in the brightest part of the cloud. The whole bright region north of the galactic circle has many more B stars in the *Henry Draper Extension*, but there

are very few in the dark lane to the south of that circle. Here again there is not a single normal color in the brightest part of the cloud. The mean for the group of 19 stars is $E = +0.16$, $9E = 1.4$ mag., $r = 1300 \pm 80$ parsecs. Along the dark lanes we have $E = +0.50$, $9E = 4.5$ mag., at distances of 600 parsecs or less.

The double cluster in Perseus, Plate III, is in a recognized region of obscuration, and again there are no normal colors near the main clusters. There is the well-known grouping of c stars in this region. Also, there is a strong gradient in the absorption running from $E = +0.15$ in h Persei to $+0.23$ in χ Persei and then up to $+0.51$ near the galactic circle and dropping off on the other side. The mean modulus for 14 stars is 10.9 ± 0.13, giving 1500 ± 90 parsecs. Trumpler's[18] distance of 1330 parsecs was based upon a fainter scale of absolute magnitudes.

The colors of the B stars in these three regions in low galactic latitude indicate that even the brightest parts of the Milky Way may suffer a photographic absorption of at least 1 mag. What we see are not necessarily clouds of faint stars but holes in the veil. It should be pointed out, however, that this absorption in bright areas has so far been found only very near the galactic circle—another evidence that the absorbing layer, whether it be uniform or spotted, is concentrated quite close to the galactic plane.

ABSORPTION TOWARD THE CENTER AND THE ANTICENTER OF THE GALAXY

A comparison of the absorption toward the center and the anticenter of the galaxy can be made from the colors of B stars within 5° of the galactic circle and over a range of about 40° of longitude in each direction. In Figure 5 the color excess E is plotted against the distance r, computed from the formula

$$5 \log r = m - 7E - M + 5 . \qquad (8)$$

If m is the limiting magnitude of the observing list and M is the assumed absolute magnitude, then E determines the maximum distance r. In the figure the curve is drawn for $m = 9$ and $M = -3.9$ for Bo stars. All stars plotted above this curve must be fainter than

[18] *Lick Obs. Bull.*, **14**, 170, 1930.

PLATE III

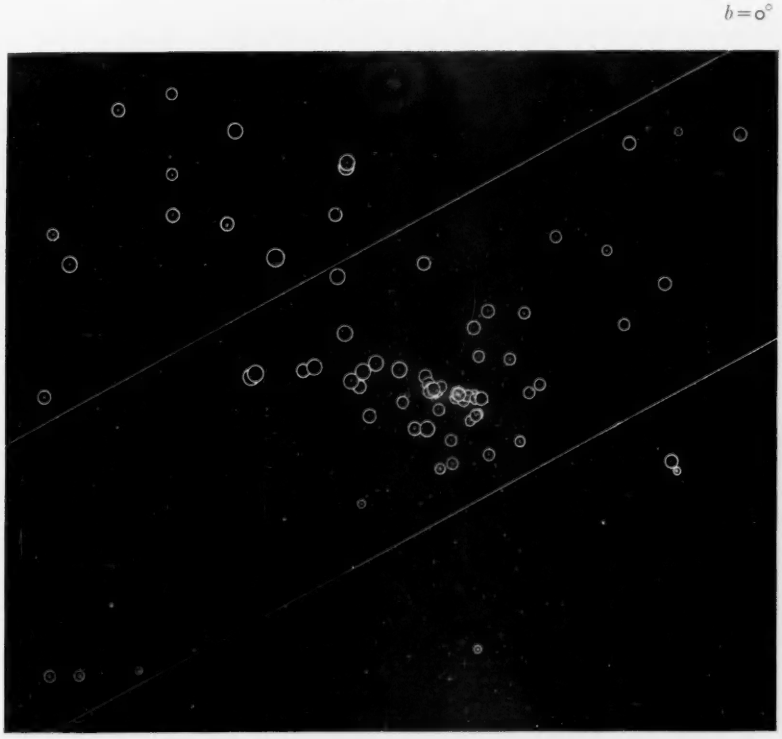

B Stars in the Double Cluster in Perseus

9 or have an assumed absolute magnitude brighter than −3.9. There are no c or O stars as faint as the ninth magnitude on our list,

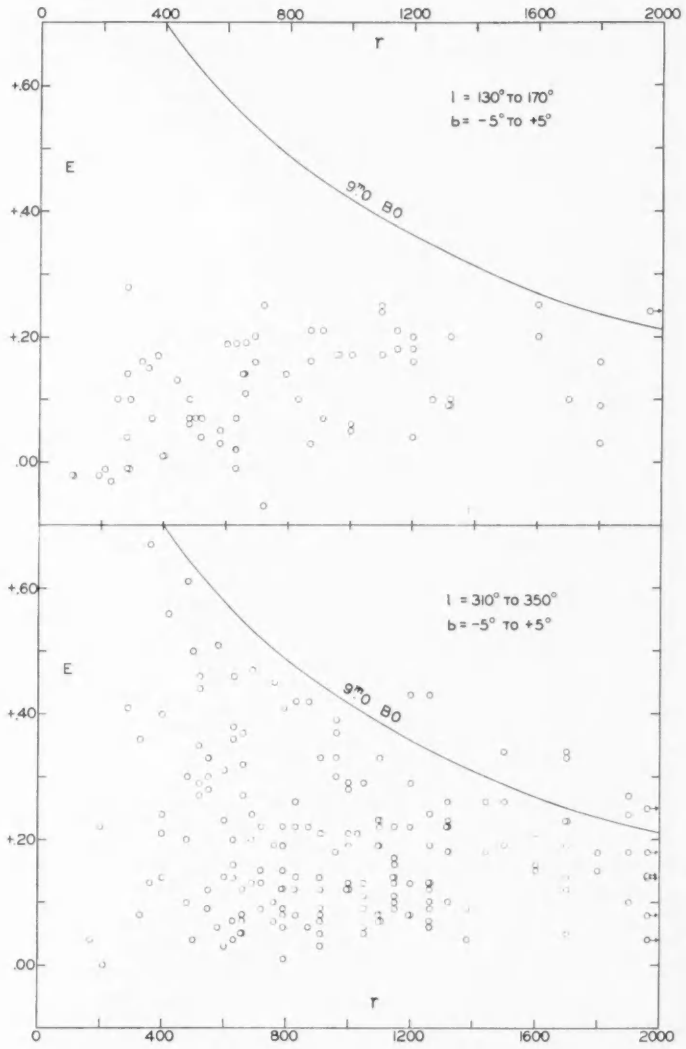

FIG. 5.—Colors of B stars toward the center and anticenter of the galaxy

and the points above the curve are for Bo stars fainter than 9. The *Henry Draper Catalogue* begins to be incomplete beyond the

eighth magnitude, and magnitude 9 marks the approximate limit of our survey.

The term $7E$ in equation (8) represents the correction to the photometric distance computed from interstellar reddening and has the effect of reducing greatly the inferred distances of strongly reddened stars. In other words, for a given apparent magnitude a star in a heavily obscured region is nearer to us than another star of the same intrinsic brightness out in the clear. In fact, a strongly reddened B star will be fainter than ninth magnitude, and therefore unobserved, unless it is relatively close. The stars toward the galactic center in Figure 5 give little evidence of a constant coefficient of absorption. Even if the term $7E$ is wrong and allowance is made for a large dispersion in M, there is no easy way of making E a linear function of r. There are eighth-magnitude stars with almost no color excess as well as those which are strongly reddened.

Toward the anticenter the case is different. There are no stars with E as large as $+0.30$, and the maximum reddening is reached at 1000 or perhaps even at 500 parsecs. There is apparently no further absorption out to 2000 parsecs. The effect is just what we would get if we could see through the absorbing clouds and could find no further dark material beyond. Whether or not this is the end of the absorption toward the anticenter will depend upon the detection of extragalactic nebulae in this direction. In any event, in the first 1000 parsecs there is more absorption toward the center than toward the anticenter of the galaxy.

ABSORPTION NEAR THE SUN

The absorption in the bright areas of the Milky Way brings up the question of the amount of the dark material in the immediate neighborhood of the sun. We can eliminate most of the effect of absorption by taking stars in high latitude, say above 30°, but we also eliminate most of the B stars. As Oort[19] has pointed out, the question of selective absorption near the sun is involved with the adopted zero points for the colors of the B stars. We now have additional stars in high latitude and in low latitude not far from the

[19] *Op. cit.*, p. 243.

sun. In Table 3 are the mean colors for stars at small distances and in different latitudes, the latter, of course, taken without regard to sign. From 27 stars the mean seems to be not far from $E = -0.01$ at 100 parsecs, and the last group indicates little additional absorption at greater distances out from the plane. Oort found -0.019 for the same error from 14 stars, and he added 0.030 mag. for the assumed absorption at their average distance of 100 parsecs, making a total of $+0.049$ for the systematic correction to E. We are pretty sure from the new material that 0.30 mag/kpc is too high and that 0.01 or 0.02 mag. is sufficient for the selective absorption at 100

TABLE 3

b	Range of $m_0 - M$	$\overline{m_0 - M}$	$\bar{r}$	$\bar{E}$	P.E.	No.
0°–30°	4.1– 5.4	5.0	100	−0.013	±0.005	13
>40	3.9– 5.9	5.2	110	.006	.006	14
>40	6.0–10.1	7.8	360	−0.008	±0.006	19

parsecs. As there is an increased proportion of classes B5–B8 in the stars at small distances, we prefer to let the old zero points stand until we have more information about the region near the sun.

A STARS NEAR THE NORTH POLE

At the suggestion of Dr. Jesse Greenstein we have made a further test of absorption close to the sun by measuring the colors of about one hundred and fifty A stars near the north pole of rotation. It is known that the stars of the North Polar Sequence show a slight color excess. In the first tests, A0 to A5 stars down to sixth magnitude were taken in a quadrilateral 40° on a side with the pole at the center. When these stars showed no color effect, all A0 stars within a circle of 10° radius about the pole were taken from the *Henry Draper Catalogue*, and about fifty check stars of spectrum A0 were found in high latitude in positions which would be observed at the same altitude as the pole. In Figure 5 each plotted point is for the mean of twelve to fifteen stars; the zero point for the color excess

happens to be shifted from that of the system of the B stars. The distances were computed from the formula

$$5 \log r = m - 7(E - 0.06) - M + 5 ,$$

where M was taken as $+0.6$ for an Ao star.

The presence of obscuration is confirmed by the color excess of the faint A stars. The uniform absorption indicated by the straight line represents the observations fairly well; but if the deviation of the two points at 200 parsecs is real, there is little or no absorption out to that distance. The broken line conforms with the condition

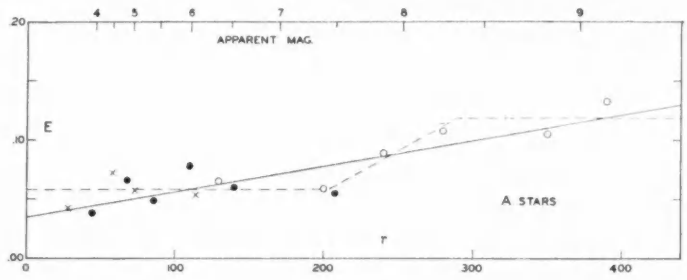

FIG. 6.—Selective absorption in A stars near the north pole of rotation; crosses: in high latitude; dots: in area $40° \times 40°$ about pole; circles: within $10°$ of pole.

of no absorption out to 200 parsecs, a cloud from 200 to about 300 parsecs, and then no more absorption. We do not think the evidence is conclusive either way in regard to these small irregularities.[20]

The deviations of the observed points in the figure are due mostly to the dispersion in the colors of the A stars. From the residuals within each normal, the standard deviation of the color of an Ao star is about ± 0.030 mag., and the average of a dozen stars will have a mean error of ± 0.01 or less, which is about the size of the mean error of a single observation. Though the dispersion in the colors of the A stars is perhaps twice as large as that of the B stars, the A stars are so widely distributed in latitude that they can be used for further tests of selective absorption. At the suggestion of

[20] For discussion of the absorption about the north pole see also Seares, *Mt. Wilson Comm.*, No. 119, 1936; Shapley and Jones, *Harvard Bull.*, No. 905, 1937; and W. Becker, *Zs. f. Ap.*, **17**, 292, 1939.

Professor van Rhijn we plan to measure all available B8 and B9 stars and many A0 stars near both poles of the galaxy. From such observations we hope to get further evidence of the absorption near the sun at different distances from the galactic plane.

GENERAL REMARKS

There is considerably more material for discussion in the colors of the B stars, and much information can be found about the distances of dark clouds and the corrections to the brightness of stars or nebulae seen through them, but these studies are left for another paper. The absorption in the galaxy is so obviously spotted in appearance that we should expect it to be irregular along the line of sight. We have become convinced that the assumption of a uniform layer of dark material near the plane or the use of mean coefficients of space absorption should be made with caution. Further work can be done on known A stars, but perhaps the most fruitful source of information would be the colors of faint B stars near the galactic center. The detection and study of such objects would be a splendid field of research for the new McDonald telescope.

We are pleased to record the encouragement and support by several agencies. The photometer at Madison was rebuilt and improved by means of a grant from the Rumford Fund of the American Academy of Arts and Sciences. Other grants were received from the Alumni Research Fund of the University of Wisconsin and from the Observatory Council of the California Institute of Technology.

CARNEGIE INSTITUTION OF WASHINGTON
MOUNT WILSON OBSERVATORY

UNIVERSITY OF WISCONSIN
WASHBURN OBSERVATORY
May 1939

THE INTENSITIES OF SUNSPOTS FROM CENTER TO LIMB IN LIGHT OF DIFFERENT COLORS*

R. S. RICHARDSON

ABSTRACT

The ratio of intensity, spot to disk, was determined for thirteen different sunspots on twenty-five days during the summer of 1938. Observations were made only on large stable spots when the seeing was 5 or better on a scale of 10. Spectral regions nearly free from lines were selected at λλ 4100, 5100, 5800, and 6600. The observations can better be represented on the assumption that the spot is in radiative, rather than in adiabatic, equilibrium. An effective temperature of 4300° K was found for the umbra, about 500° lower than that commonly given.

1. INTRODUCTION

In 1932 Minnaert and Wanders[1] presented a comparatively easy method for obtaining valuable information about the structure of sunspots. Their proposal was simply that, if a spot consists of an ascending column of gas cooling by adiabatic expansion, as generally assumed, then three consequences follow, all of which can be tested by observation:

1. The intensity of the umbra relative to the surrounding photosphere in radiative equilibrium should fall rapidly as the spot approaches the limb.

2. The ratio, spot to disk, should increase slowly with wave length.

3. But, if the spot is in radiative equilibrium at an effective temperature considerably below the photosphere, then the decrease toward the limb is much slower, and the increase with wave length much faster, than in the case of adiabatic equilibrium.

On comparing this theory with observations made by Pettit and Nicholson[2] and later by Wanders,[3] they found that spots behave as if they are in radiative equilibrium. No modification of the adiabatic hypothesis would represent the data nearly as well as the simple assumption of radiative equilibrium alone. This result was so surpris-

* *Contributions from the Mount Wilson Observatory, Carnegie Institution of Washington*, No. 612.

[1] *Zs. f. Ap.*, **5**, 297, 1932.

[2] *Mt. W. Contr.*, No. 397; *Ap. J.*, **71**, 153, 1930.

[3] *B.A.N.*, **7**, 237, 1934.

ing that it seemed desirable to give it a thorough test under the best observational conditions possible. During the summer of 1938 sunspot activity was near maximum, and an exceptional number of large stable spots appeared, ideally suited for this particular investigation. Although the writer was then engaged on Mount Wilson primarily with another problem, the opportunity seemed too good to miss; and the early morning hours, when the seeing is best, were devoted to this additional program.

2. OBSERVATIONAL MATERIAL

The observations were all made at the 150-foot tower telescope in the first order of the 75-foot spectrograph, where the linear scale is 1 mm = 0.7 A. Four spectral regions relatively free from lines were selected at λλ 4100, 5100, 5800, and 6600. The exposures were made through suitable filters on Eastman III-F plates, which are nearly uniform in sensitivity over the entire range. Each plate was calibrated for its particular wave length by an exposure on the center of the disk taken through a raster. The plates were developed for six minutes in a soft developer and were continually brushed during development.

The spectrograph was always oriented so that the slit was parallel to the sun's meridian. The intensity of the spot has been measured with respect to the intensity of the disk on either side. Values obtained in this way are not quite the same as the intensity of the disk at the position of the umbra. The ideal method would be to work with the slit radial. This is impracticable, however, when the spot is near the limb and reduced to a narrow line. It is believed that any errors caused by the orientation of the slit are negligible compared with the others involved.

Exposures were made on thirteen large stable spots, on days when the sky was free from haze, and the seeing at least 5 on a scale of 10. On most days, the seeing was called 7, 8, or even 9, the spots often appearing so black and sharply defined that they resembled an engraving.

3. DISCUSSION OF RESULTS

The results of the investigation may be seen most clearly from an inspection of the diagrams for the four spectral regions, in which the

abscissas are fractional distances from the center of the disk, and the ordinates are the ratios of intensity, spot to disk. After trying several schemes for presenting the data, it was finally decided merely to plot each point separately, without taking means or making a least-squares solution. All have been given equal weight, and none has been omitted. Most of the scatter can be attributed to differences in seeing and errors in guiding, but some is probably real. The largest umbrae should contain the least scattered light, and occasionally a spot appears that is abnormally dark for its size.

A slight increase of intensity occurs from the center out to about 0.75, after which the scatter is greater and the points generally higher. This is readily explained by the foreshortening of spots toward the limb. When the spot is reduced to nothing but a narrow line, considerable photospheric light is certain to be mixed with that from the umbra, regardless of how carefully the guiding is done or of the excellence of the seeing.

No correction has been made for skylight superposed upon the umbra. Exposures on the limb equal to those required for the umbra always showed the limb sharply defined against a background of perfectly clear glass.

An upper limit to the intensity of the scattered light can be found, however, from a series of plates taken during the partial eclipse of April 19, 1939. The intensity of the image was cut down 80 per cent by a rotating sector, enough to allow light from off the limb to register properly, without overexposing the disk. These plates show the scattered light at 10″ from the limb to be about 5 per cent as intense as the center of the disk. But in the ten months since the spot plates were taken, the surfaces of the mirrors have greatly deteriorated—a fact which is obvious from a casual inspection of the image. Probably 3 per cent would be a reasonable estimate of the degree of scattered light during June and July of 1938.

A result that was not anticipated is that the scatter is least for the λ 4100 region, increases through the green and orange, and is greatest at λ 6600. One would naturally expect more trouble from diffuse light and errors in focusing a visual lens in the violet rather than in the red. The effect could be attributed to a progressive change in seeing, if special precautions had not been taken to prevent it. On Mount Wilson during the summer the finest solar seeing

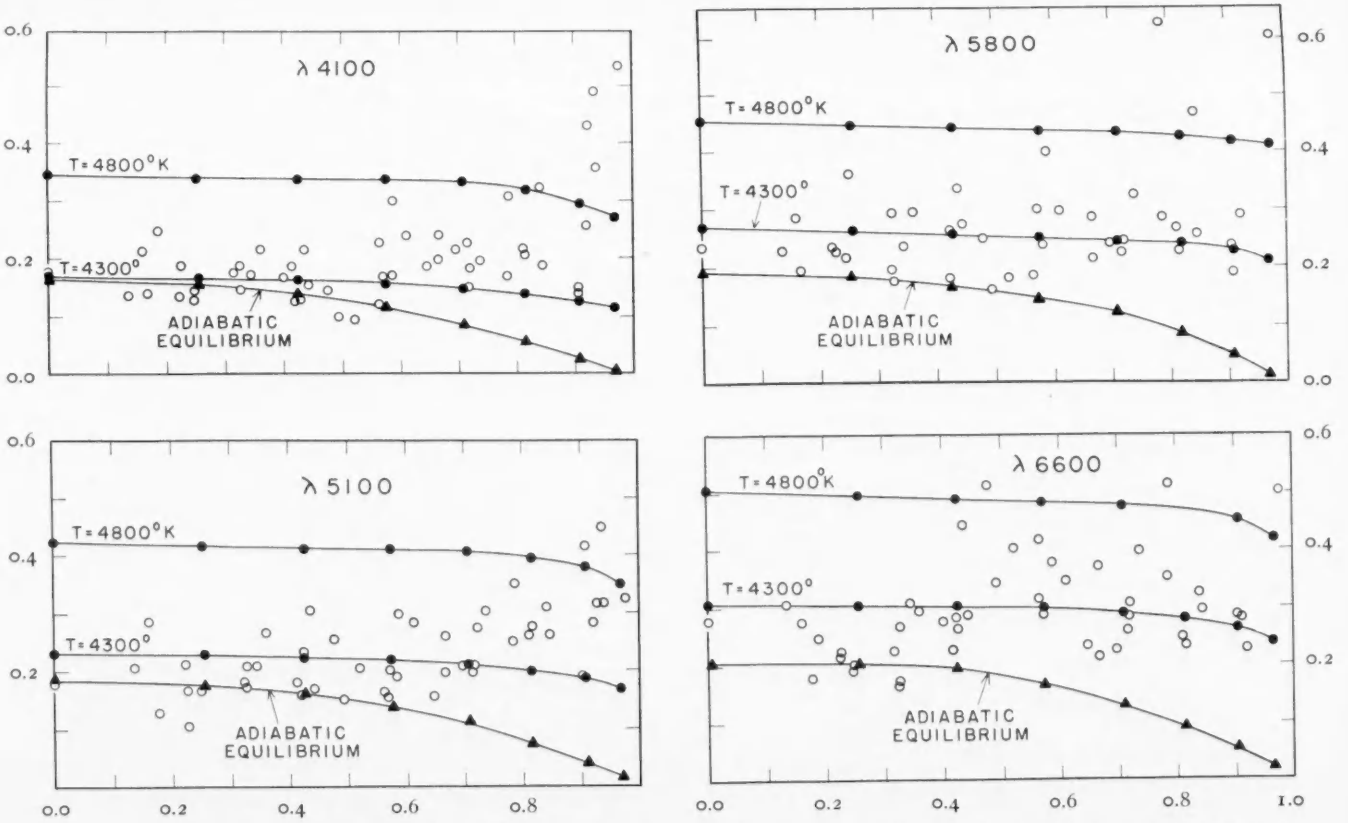

FIG. 1.—Intensity-ratio of spot to disk (ordinates) at different fractional distances from center, for λλ 4100, 5100, 5800, and 6600. Curves represent predicted values for adiabatic equilibrium in the umbra, and for radiative equilibrium at 4300° and 4800° K, respectively. Circles indicate observed values.

occurs soon after sunrise. Over an interval of from thirty minutes to an hour it may be 7, 8, or 9. Then in only half an hour it often falls as low as 2 or 3. Usually there was just enough time to make all four exposures before the seeing began to break up. Had the exposures always been taken in the order λλ 4100, 5100, 5800, and 6600, the one in the violet, on the average, would have been taken with better seeing than that at λ 6600. But the series was purposely reversed on successive days in order to avoid this possibility. No plausible explanation presents itself at this writing.

4. CONCLUSION

In the diagrams the lower curve shows the ratio of intensity, spot to disk, on the assumption that the spot is in adiabatic equilibrium. The curve just above shows this same ratio for a spot in radiative equilibrium at an effective temperature of 4300° K. The assumption of radiative equilibrium gives a good representation of the observations for all wave lengths for points at the center and out to about 0.75. The adiabatic hypothesis predicts a drop in intensity toward the limb that is much too steep, and moreover the predicted intensity does not increase rapidly enough with increasing wave length, at least not over the limited range examined here. Hence, these results confirm the conclusion of Minnaert and Wanders that sunspots behave as if they are in radiative, rather than in adiabatic, equilibrium. This does not necessarily rule out completely the theory of cooling by expansion in sunspots. The gases may be rising so slowly that light from the column is essentially in radiative equilibrium.

The temperature of 4300° K found for the umbra is about 500° lower than that generally given in textbooks, probably taken from the work of Nicholson and Pettit[4] and of Miss Moore.[5] This is clearly due to the exceptionally good seeing with which all the plates were taken. The highest curve shows the ratio of spot to disk for radiative equilibrium at 4800° K. In each diagram it lies far above all except a few scattered points.

CARNEGIE INSTITUTION OF WASHINGTON
MOUNT WILSON OBSERVATORY
April 1939

[4] *Mt. W. Contr.*, No. 397; *Ap. J.*, **71**, 153, 1930.
[5] *Mt. W. Contr.*, No. 446; *Ap. J.*, **75**, 222, 1932.

ON THE DOUBLET RATIO OF INTERSTELLAR H AND K AND THE ABSOLUTE MAGNITUDES OF WOLF-RAYET STARS*

ROSCOE F. SANFORD AND O. C. WILSON

ABSTRACT

Observations.—The total absorptions of the interstellar *Ca* II lines, H and K, have been measured in 40 O and B stars with weak $H\epsilon$ and in 18 Wolf-Rayet stars (Table 1). The difficulty so often encountered in measuring the total absorption of H in the presence of strong $H\epsilon$ in absorption has therefore been largely obviated, and it is hoped that these measures are an improvement upon earlier ones.

Ratio of K to H.—K/H appears to be approximately 2 for very weak lines and to decrease, on the average, as lines of greater strength are considered, reaching 1.56 for H = 0.4 A, with little apparent tendency to diminish thereafter. See Figures 1 and 2.

Ratios D2/K and D1/H.—Twenty-four stars in Table 1 provide measures of the total absorptions of the interstellar D2 and D1 of *Na* I. The mean D2/K and D1/H derived therefrom are 1.63 and 2.18, respectively, which closely check earlier results, 1.6 and the tentative value 2.1, respectively.

Absolute magnitudes of Wolf-Rayet stars.—The curve which relates distance with K-line intensity has been used to derive the distances of the 18 Wolf-Rayet stars from which mean visual absolute magnitudes for 6 stars of the carbon sequence and 12 of the nitrogen sequence have been derived. They are −2.8 and −2.1, respectively.

Masses of the Wolf-Rayet stars.—Plausible values of temperature, together with our derived absolute magnitudes and what appears to be a reasonable allowance for the contribution of bright bands to the apparent magnitudes, give masses approximately thirty times that of the sun. The assumptions and guesses involved make such values highly speculative, even though the mass-luminosity relation itself is unqualifiably accepted.

The ratios of the equivalent widths of the interstellar lines D2 and D1 of *Na* I have already been discussed in a paper by O. C. Wilson and P. W. Merrill.[1] It seems equally important that a similar treatment of the ratios of the interstellar lines K and H of *Ca* II be undertaken.

Although H was measured for a considerable number of the stars given in our Catalogue,[2] it was felt that these values for H were, for the most part, far less reliable than those for K, and that this inferiority was to be attributed to the presence of a strong $H\epsilon$ which provides a very difficult background against which H must be

* *Contributions from the Mount Wilson Observatory, Carnegie Institution of Washington*, No. 613.

[1] *Mt. W. Contr.*, No. 570; *Ap. J.*, **86**, 44, 1937.

[2] *Mt. W. Contr.*, No. 576; *Ap. J.*, **86**, 274, 1937.

measured. It seemed best, therefore, to select with some care a program of stars that would obviate this difficulty as much as possible.

To that end, our spectrograms of stars of types B3 and earlier were carefully scrutinized, and an observing list was thereby formed of stars having $H\epsilon$ weak, or broad and shallow, or virtually absent. To these were added all Wolf-Rayet stars that are accessible from this latitude, which should be ideal for the purpose since there is practically no interference by $H\epsilon$ in absorption. The observation of these selected stars showed that in some of the B and O stars $H\epsilon$ still makes the measurement of H difficult, and that a few Wolf-Rayet stars required excessive exposures. H and K have now been measured in the spectra of 40 B and O stars and of 18 Wolf-Rayet stars. Although shortcomings are admitted, these measures provide, we think, significant results, and it seems fair to expect that even very onerous additional observations would change only the details of the results.

The total absorption of K and of H, expressed in angstrom units, has been derived for each of these stars by methods already described elsewhere.[2] Duplicate tracings were always made, which enabled each of us to obtain an independent measure of each line. Careful comparison revealed no significant systematic or accidental differences between our measures. The stars, with a range from the second to the tenth visual apparent magnitude, have been observed with the dispersion and the photographic emulsion which seemed best adapted to their individual requirements. Consequently, some system of weighting was necessary, and that adopted represents our combined judgment as to the accuracy obtainable from the photometric tracings.

Our results are given in Table 1. The first, second, fourth, and fifth columns are taken from the *Henry Draper Catalogue*. The spectral classes are mostly our own estimates. The galactic co-ordinates are from the Lund tables.[3] The measured equivalent widths, expressed in angstrom units, are in the eighth and ninth columns, followed by their respective weights in parentheses. The final column contains the ratios K/H, which, especially for some stars with weak lines, may differ somewhat from the values corresponding to

[3] *Ann. Obs. Lund*, No. 3, 1932.

TABLE 1

MEASURES OF H AND K

HD No.	Vis. Mag.	Sp.	1900		Galactic		Total Abs.		$\frac{K}{H}$
			R.A.	Decl.	l	b	K	H	
							A	A	
4004	10.2	WN6	0^h37^m5	$+64°14'$	90°	$+2°$	0.38 (2)	0.24 (1)	1.58
9974	10.0	WN5	1 32.4	+57 39	97	− 4	.69 (3)	.45 (1)	1.53
14633	7.7	O8	2 16.7	+41 2	109	−18	.27 (3)	.13 (3)	2.08
16523	10.0	WC6	33.9	+56 18	105	− 2	.67 (4)	.44 (4)	1.52
18326	7.9	Bon	51.6	+60 10	106	+ 2	.38 (4)	.25 (4)	1.54
23180*	3.9	B2	3 38.0	+31 58	128	−17	.08 (3)	.04 (3)	2.00
23800	6.9	B2	42.9	+52 11	116	0	.36 (6)	.24 (6)	1.47
30614*	4.4	O9sea	4 44.1	+66 10	112	+15	.28 (9)	.17 (5)	1.65
35921	6.7	O9	5 23.0	+35 18	140	+ 2	.30 (2)	.18 (2)	1.65
37128*	1.8	Bo	31.1	− 1 16	173	−16	.09 (3)	.05 (3)	1.64
37490*	4.5	B3ne	33.9	+ 4 4	168	−13	.14 (9)	.07 (9)	2.00
41161	6.5	O9n	58.2	+48 15	132	+14	.22 (2)	.12 (2)	1.87
47432	6.1	Bo	33.5	+ 1 42	178	− 1	.35 (3)	.19 (3)	1.83
48099	6.2	O7	36.6	+ 6 27	174	+ 2	.35 (5)	.25 (5)	1.40
50896	6.6	WN6	50.0	−23 48	202	− 9	.18 (2)	.10 (2)	1.80
57061*	4.4	O9	7 14.5	−24 47	206	− 4	.12 (9)	.06 (6)	2.00
60848	7.7	O7ne	31.4	+17 7	170	+19	.23 (2)	.11 (2)	2.09
157857	7.4	O7	17 20.7	−10 55	341	+12	.39 (2)	.18 (1)	2.22
160762*	3.8	B3	36.6	+46 4	39	+30	.10 (2)	.05 (2)	2.00
164794*	5.9	O5	57.7	−24 22	334	− 2	.25 (1)	.14 (1)	1.79
165763	7.8	WC6	18 2.5	−21 16	337	− 2	.60 (2)	.35 (2)	1.72
167771	6.4	O8	11.6	−18 30	340	− 3	.24 (1)	.20 (1)	1.23
178129	8.0	B3	19 2.3	+ 3 17	6	− 3	.87 (3)	.57 (1)	1.54
185859	6.4	Bo	36.1	+20 15	24	− 2	.20 (3)	.14 (2)	1.39
186943	10.0	WN6	42.2	+28 1	32	+ 1	.64 (1)	.49 (1)	1.31
187282	10.0?	WN5	44.1	+17 57	23	− 5	.55 (2)	.40 (2)	1.37
187320	7.6	B2n	44.3	+19 24	25	− 4	.36 (3)	.22 (3)	1.67
188001	6.3	O7f	47.9	+18 25	24	− 6	.29 (2)	.18 (1)	1.57
190429N*	7.2	O5n	59.8	+35 45	40	+ 2	.39 (7)	.21 (6)	1.86
190429S	7.5	O9n	59.8	+35 45	40	+ 2	.38 (4)	.17 (3)	2.24
190603	5.7	cBOeβ	20 0.7	+31 56	37	0	.31 (5)	.21 (3)	1.48
190864	8.2	O6	1.9	+35 19	40	+ 1	.52 (4)	.28 (3)	1.86
Ex 227611	9.5	Bn3	2.0	+35 37	40	+ 1	.49 (3)	.28 (3)	1.72
190918	7.0	WN5	2.2	+35 31	41	+ 1	.57 (7)	.31 (4)	1.84
Ex 227634	7.6	B1	2.3	+35 29	40	+ 1	.48 (2)	.32 (1)	1.52
Ex 227696	9.0	B2	2.8	+35 27	40	+ 1	.44 (4)	.23 (3)	1.96
191612	8.2	O7	5.7	+35 26	40	+ 1	.32 (2)	.20 (1)	1.60
191765	7.8	WN6	6.5	+35 53	41	+ 1	.36 (6)	.21 (4)	1.71
192103	7.9	WC7	8.1	+35 54	41	0	.42 (5)	.24 (5)	1.75
192163	7.4	WN6	8.4	+38 3	43	+ 2	.40 (9)	.27 (9)	1.48
192281	7.5	B3	9.0	+39 58	45	+ 3	.49 (6)	.30 (6)	1.63
192641	7.9	WC7	10.8	+36 21	42	0	.28 (3)	.17 (3)	1.65
193077	8.0	WN5	13.3	+37 7	43	0	.34 (4)	.23 (3)	1.48
193576	8.0	WN5	15.8	+38 25	44	+ 1	.30 (2)	.19 (1)	1.58
193793	6.8	WC6	17.1	+43 32	49	+ 3	.49 (1)	.31 (7)	1.58
193928	9.4	WN5	17.8	+36 36	43	− 1	.56 (4)	.40 (3)	1.40
199579	6.0	O6	53.1	+44 33	54	0	.34 (1)	.24 (1)	1.42
203064*	5.1	O8n	21 14.8	+43 31	55	− 4	.18 (3)	.13 (3)	1.48
206267	5.6	O6n	35.9	+57 2	67	+ 3	0.24 (2)	0.12 (1)	2.00

* Refers to notes at end of table.

TABLE 1—*Continued*

HD No.	Vis. Mag.	Sp.	1900		Galactic		Total Abs.		$\frac{K}{H}$
			R.A.	Decl.		b	K	H	
							A	A	
211853....	9.0	WN_5	22^h15^m0	$+55°37'$	70°	− 1°	0.66 (5)	0.33 (2)	2.00
214167*...	6.6	B2	31.4	+39 7	65	−17	.12 (2)	.06 (2)	2.00
214168*...	5.8	B3ne	31.4	+39 7	65	−17	.16 (2)	.08 (2)	2.00
214263....	6.8	B3	31.9	+37 19	64	−18	.13 (2)	.08 (1)	1.63
214419....	8.9	WN_5	32.9	+56 23	73	− 1	.50 (4)	.31 (3)	1.58
214680*...	4.9	O9	34.8	+38 32	65	−17	.18 (1)	.12 (1)	1.52
215227....	8.7	Ben	38.6	+44 12	68	−13	.38 (4)	.15 (3)	2.53
224599....	6.5	B3ne	23 53.8	+45 52	82	−15	.64 (2)	.44 (1)	1.48
224905....	9.2	B3n	56.6	+59 54	85	− 2	0.56 (5)	0.33 (3)	1.69

NOTES TO TABLE 1

23180 o Per
30614 9 Cam
37128 ε Ori

Beals has found, and we confirm, double interstellar lines. The intensities given in this table relate to the blends.

37490 ω Ori
57061 τ CMa
160762 ι Her
164794 9 Sgr

190429N, 190429S .....

The components of this double star have two K and two H lines, both of which seem to be interstellar. This assumption appears justified, for both stars, though classed as spectroscopic binaries with very poor lines, give the same constant velocities from the *Ca* lines. These are, for the strong components, −11 km/sec and, for the weak components, −80 km/sec. The equivalent widths of the weak components are K = 0.098 A, H = 0.045 A for the N star.

What evidence we have points to an absence of any weak components for D_2 and D_1, although the plates so far obtained for this purpose are rather poor. If this should be definitely confirmed, these stars would stand by themselves, since in all others which have been adequately tested, double *Na* lines have been found where double interstellar *Ca* lines are known.

203064 A Cyg
214167 8 Lac Ft
214168 8 Lac Br
214680 10 Lac

the individual H's and K's as rounded off to two decimals for printing. The weight assigned to K/H is that attached to the corresponding H. Figure 1 is a plot of K against H from Table 1.

The total absorptions of K for the stars appearing in Table 1 may differ somewhat from those in common with our Catalogue,[2] for in

Table 1 they have been derived from spectrograms upon which H, as well as K, could be measured. The differences in most cases, however, are minor.

THE RATIO K/H

Mean values for this ratio have been obtained by using not only the results in Table 1 but also the old Mount Wilson measures already alluded to and those by Beals[4] and by Williams.[5] Overlapping means for groups of 10 stars were formed for the data of Table 1, grouped first according to K and secondly according to H. A similar procedure for the remaining data gave another set of normals. Finally six values were obtained, each of which is the mean of approximately 12 of these normals, double weight having been given to those from Table 1 because of their freedom from interference by $H\epsilon$. These six values of H and K/H are plotted in Figure 2. The adopted curve is judged to be the best compatible with the points and with a value of 2 for K/H at H = 0 A and is equivalent to the formation of the mean of the two regression-curves. Values of K for different values of H, derived by means of the curve of Figure 2, were used to plot the curve in Figure 1. The plotted points from selected stars are apparently quite satisfactorily represented. Evidently the inclusion of measures of H hampered by $H\epsilon$ has not, in

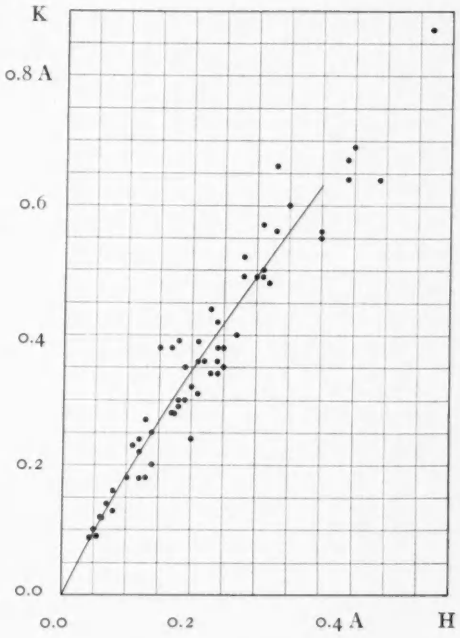

FIG. 1.—Total intensity of K (ordinates) plotted against the total intensity of H from the data in Table 1. Curve based on Fig. 2.

[4] *M.N.*, **96**, 661, 1936.

[5] *Mt. W. Contr.*, No. 487; *Ap. J.*, **79**, 280, 1934.

the mean, systematically interfered with the relation of K/H, although the scatter in the plot of K/H to H for individual stars is large, especially for weak lines.

The mean curve in Figure 2 shows the trend of K/H from H = 0 A to H = 0.4 A, where it has become practically horizontal at K/H = 1.56. For H > 0.4 A our data, in Figure 1, are meager, but they appear to be fairly well represented by the continued use of this

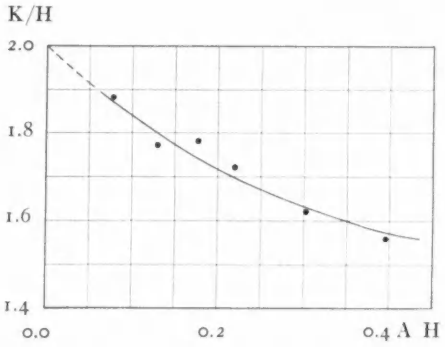

FIG. 2.—Six finally adopted mean values of K/H plotted against the corresponding values of H.

value of the ratio. It seems likely, therefore, that, statistically at least, 1.56 is not far from the minimum of the ratio K/H.

RATIOS OF D2/K AND D1/H

Total absorptions have been measured for all of the four lines D2, D1, K, and H for 24 of the stars in Table 1. They give the following means:

D2 = 0.483	D2/K = 1.63
D1 = .394	D1/H = 2.18
K = .297	K/H = 1.65
H = 0.180	D2/D1 = 1.23

D2 is plotted against K in Figure 3,*a*, and D1 against H in Figure 3,*b*. The foregoing mean values for D2/K and for D1/H are represented by straight lines in Figure 3. The scatter of the plotted points would scarcely justify an attempt to represent them more in detail.

The previously published ratios[6] were D2/K = 1.6, and the tentative value D1/H = 2.1. This large ratio for D1/H is, of course, quite in keeping with the fact that the ratios of K/H never attain as small values as D2/D1.

ABSOLUTE MAGNITUDES OF THE WOLF-RAYET STARS

The statistical relation of the equivalent width of K to distance on the basis of a visual absorption of 0.35 mag/kpc has been given

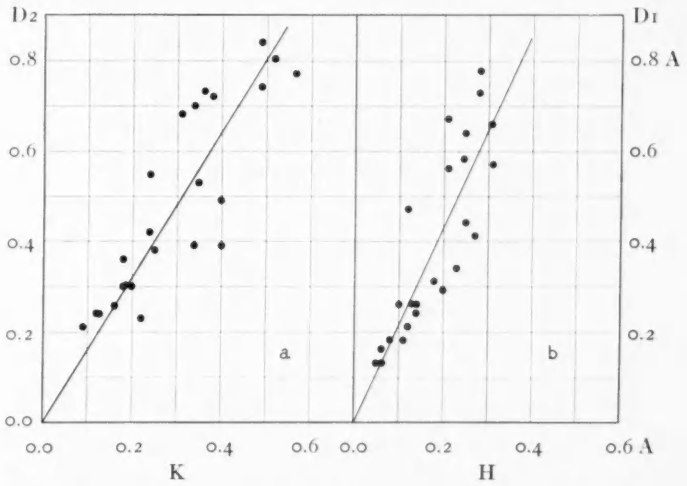

FIG. 3.—(*a*) gives the total absorption of D2 (ordinates) against the total absorption of K for the individual stars in Table 1 which have these data in common. (*b*) is a similar plot of D1 against H. The straight lines represent the linear relations given by the ratios of mean D2 to mean K (*a*) and mean D1 to H (*b*).

elsewhere[7] and has already been used to derive mean absolute magnitudes[6] for O- and B-type stars. K intensities were then available for only 5 Wolf-Rayet stars. For the three Oa stars they gave −3.2, and for the two Ob stars −2.6, as the mean visual absolute magnitudes. The extension of the measures to 18 stars and improved values of the total absorption of the interstellar *Ca* II lines lead to new mean absolute magnitudes of much greater weight.

The distance to each Wolf-Rayet star was read from the afore-

[6] *Mt. W. Contr.*, No. 585; *Ap. J.*, **87**, 118–132, 1938.

[7] *Mt. W. Contr.*, No. 573; *Ap. J.*, **86**, 136, 1937.

mentioned curve by means of its K-line intensity and used to compute the absolute magnitude from the formula[6]

$$M = m + 5 - 5 \log D - 0.00035 D ,$$

where the last term represents the visual absorption. Of the 18 stars, 6 are of the carbon sequence and 12 of the nitrogen sequence, corresponding roughly to types Oa and Ob. The mean visual absolute magnitudes found are -2.8 and -2.1, respectively, as against the earlier values -3.2 and -2.6.

There is some evidence that among these 18 Wolf-Rayet stars the apparently fainter ones are also, on the average, intrinsically fainter than the brighter stars.

This might be explained as due either to a real spread in the individual absolute magnitudes or to a diminution of the density of interstellar calcium at large distances. In view of all the uncertainties it is felt that, at present, significance should be attached only to the foregoing mean absolute magnitudes for the two sequences of Wolf-Rayet stars.

THE MASSES OF THE WOLF-RAYET STARS

The masses of the Wolf-Rayet stars may now be estimated by using the empirical mass-luminosity curve of Kuiper.[8] The corrections necessary to transform visual to bolometric magnitudes have been computed by Pike.[9] The temperatures of the stars must, of course, be known in order to make the reduction to bolometric magnitude; but since the minimum temperatures of the Wolf-Rayet stars appear to be of the order of 65,000°,[10] it is probably sufficiently accurate to take 5.0 mag. as the correction. The absolute bolometric magnitudes of the carbon and nitrogen W–R stars would accordingly be about -7.8 and -7.1, respectively. From Figure 1 of Kuiper's paper the corresponding masses are of the order of thirty to forty times that of the sun. These estimates of mass would be diminished somewhat, though probably not greatly, if accurate account could be taken of the contribution of the emission bands to the visual mag-

[8] *Ap. J.*, **88**, 472, 1938.

[9] *M.N.*, **89**, 538, 1929.

[10] C. S. Beals, *M.N.*, **92**, 684, 1932.

nitude. Apart from this observational point, these estimates of masses seem to rest chiefly upon the assumption that the W–R stars radiate as black bodies. This assumption is used twice in the present case, first in deducing temperatures for the stars by Zanstra's method and secondly in assigning the bolometric corrections. Hence, if the radiation of a Wolf-Rayet star deviates widely from that of a black body, the masses derived above may be seriously in error. And, of course, any supportable objection to the use of the mass-luminosity relation as a means of getting masses in specific cases is valid here.

CARNEGIE INSTITUTION OF WASHINGTON
MOUNT WILSON OBSERVATORY
April 1939

INTERCOMPARISON OF DOUBLET RATIO AND LINE INTENSITY FOR INTERSTELLAR SODIUM AND CALCIUM*

O. C. WILSON

ABSTRACT

If the observed decrease in the doublet ratios K/H and D2/D1 in passing from weak to strong lines is a manifestation of Doppler effect (curve of growth), it is shown that the mean small-scale velocity of the calcium ions must be about three times that of the sodium atoms. This difference is probably difficult to justify physically, and no solution is offered. The question of the relative numbers of sodium atoms and calcium ions in space is discussed briefly.

The purpose of this paper is to compare the observed relationships between line strength and doublet ratio for the D lines of sodium and for the H and K lines of ionized calcium. Such relationships may be conveniently exhibited by plotting D2/D1 against D1 and K/H against H. The resulting diagrams will be referred to as "ratio-curves."

The observed ratio-curves for interstellar sodium[1] and calcium[2] are shown in Figure 1, together with certain computed points to which reference will be made later. The two curves are similar in general characteristics, but it is important to note that the calcium-curve lies always well above that for sodium.

In *Mount Wilson Contribution* No. 570[1] three different assumptions concerning the velocity distribution of the interstellar sodium atoms were investigated in an effort to reproduce the observed behavior of the D lines.[3] In order of increasing complexity these assumptions were:

1. The atoms possess only random velocities which do not vary along the line of sight (homogeneity).

* *Contributions from the Mount Wilson Observatory, Carnegie Institution of Washington*, No. 614.

[1] *Mt. W. Contr.*, No. 570; *Ap. J.*, **86**, 44, 1937, Fig. 4.

[2] *Mt. W. Contr.*, No. 613; *Ap. J.*, **90**, 235, 1939, Fig. 2.

[3] It should perhaps be mentioned that in *all* hypotheses of interstellar line formation the only physical factor which has been introduced as a widening agent (aside from natural line-width) is Doppler effect.

2. In addition to random velocities there is a monotonically varying radial component along the line of sight (galactic rotation).

3. A typical line of sight encounters one or more "clouds" within which the atoms move with random velocities, while the clouds possess relative motions in addition.

The discussion of these three possibilities in the light of the observations led to the rejection of the first two and the adoption of the third. The reasons for this choice are fully set forth in *Contribution* No. 570 and need not be repeated. The point to be emphasized here is that all three hypotheses were equally satisfactory for the weaker lines; only the behavior of the stronger lines permitted a differentiation between them. The reason for this lack of discrimination lies in the inclusion of random small-scale velocities in each of the hypotheses, an inclusion made necessary by the observed drop in the ratio D_2/D_1 from approximately 2 for the weakest lines to about 1.2 for those with $D_1 > 0.3$ A. In effect, in all three cases, the run of the ratio-curve for values of $D_1 \leq 0.3$ A is just that given by a curve of growth.[4] Therefore, in comparing the ratio-curves for sodium and calcium, at least as far as the weaker lines are concerned, we are really comparing the small-scale (temperature or pseudo-temperature) motions of the two kinds of atoms and nothing more.

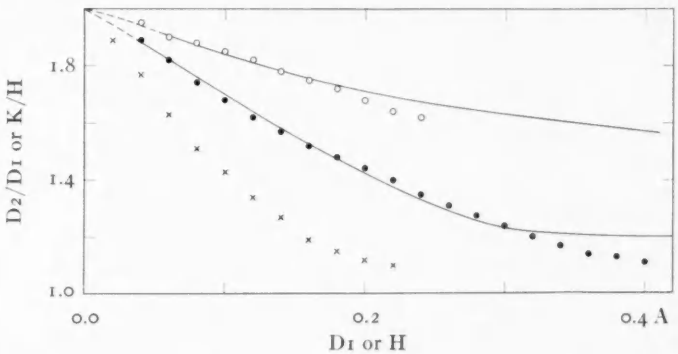

FIG. 1.—Observed ratio-curves for interstellar sodium and calcium (top curve) and points computed from curves of growth.

[4] By the term "curve of growth" we mean specifically the relationship between equivalent width and number of active atoms which holds when the atomic velocity distribution is purely Maxwellian.

Turning to Figure 1, the solid points which fit the left-hand part of the sodium ratio-curve have been read from a curve of growth computed with the value of the parameter $b = 0.12$ A.[5] It will be recalled that

$$b = \frac{\lambda}{c}\sqrt{\frac{2}{3}\overline{v^2}},$$

where $\sqrt{\overline{v^2}}$ is the root mean square speed. In the case of purely thermal motion,

$$\overline{v^2} = \frac{3RT}{\mu} \quad \text{and} \quad b = \frac{\lambda}{c}\sqrt{\frac{2RT}{\mu}},$$

where μ is the molecular weight and T the temperature. Thus, $b = 0.12$ A for the D lines corresponds to $T = 52{,}000°$, or, in terms of velocity, it signifies an average speed of about 7.5 km/sec.

If the foregoing value of T is really a measure of the motions of the individual sodium atoms and if the calcium and sodium are thoroughly mixed in space,[6] it is difficult to avoid the conclusion that equipartition of energy should hold for the two kinds of particles. Accordingly, inserting the proper values of λ and μ into the expression for b, we find $b = 0.061$ A for H and K, corresponding to 0.12 A for the D lines. The crosses in Figure 1 have been computed from a curve of growth for calcium with $b = 0.061$ A and clearly do not fit the observed ratio-curve even approximately.

In order to obtain a fit with the observed H and K ratio-curve it is necessary to take $b_{Ca} \sim 0.24$ A. The open circles in Figure 1 have been computed with this value, which corresponds to the extraordinary temperature $T_{Ca} \sim 860{,}000°$. If, instead of true thermal motions, small-scale turbulence independent of the atomic weight is

[5] In *Contribution* No. 570, b was found, from stars within 10° of the rotational null points, to be 0.11 A. We have made a slight adjustment of this value to get the best fit with the mean ratio-curve from all observed stars.

[6] The statistical evidence indicates such a mixture (Merrill and Sanford, *Mt. W. Contr.*, Nos. 564 and 585; *Ap. J.*, **85**, 73, 1937, and **87**, 118, 1938). In addition, double sodium and calcium lines have been observed in certain spectra with the velocity differences for the two sets of lines in good agreement (Sanford, Merrill, and Wilson, *Pub. A.S.P.*, **50**, 58, 1938, and C. S. Beals, *Ap. J.*, **87**, 568, 1938).

postulated, the average velocity for calcium turns out to be about 22 km/sec, compared to 7.5 km/sec for sodium.

These results are unexpected and, it must be confessed, rather disappointing. At the moment there appear to be only three possibilities of explanation. These are:

1. Some of the observations are seriously affected by systematic errors, and the comparison of the observed ratio-curves is therefore meaningless.

2. The observations and calculations are essentially correct, and a physical picture must be sought which permits the small-scale calcium and sodium velocities to differ considerably.

3. The observations are correct, but the application of the curve of growth to this problem is wrong, and some physical factor other than Doppler effect must be invoked to explain the observed ratio-curves.

Of the foregoing possibilities, the first cannot be ruled out dogmatically; but the large numbers of stars involved in both curves, as well as the care exercised to guard against systematic error, render it unlikely that any observational deficiencies can account for a discrepancy of the magnitude of the present one. The second possibility demands that two species of atoms, apparently coextensive in space, possess mean velocities which stand in the ratio of 3 to 1, with the heavier atoms having the greater velocity. Perhaps such a situation is not physically impossible, but it is certainly contrary to generally accepted ideas of the conditions prevailing in a gaseous mixture. Finally, the third possibility seems the least likely of all, for none of the known physical effects which can modify the total absorption of a line would be of the slightest help under the conditions of extreme low density of matter and radiation in interstellar space. Thus, the problem of the mechanism of the formation of interstellar lines appears to need considerable clarification.

Finally we consider the question of the relative numbers of sodium atoms and calcium ions. This question could be answered unambiguously and with fair accuracy if both ratio-curves could be fitted by curves of growth for which the parameters b had values corresponding to the same T. It would merely be necessary to read values of $\log N$ from the appropriate curves of growth for intensities of D2 and

K measured in the same spectra. This process may still be performed, but it is doubtful whether it has more than a merely formal significance.

There are 17 stars in Table 6 of *Contribution* No. 576[7] for which D1 $\leq$ 0.3 A and for which there are also measures of the intensity of K. For each of these stars the values of log $N_{Ca\,II}$ and log N_{Na} have been read from curves of growth with b = 0.12 A and 0.24 A for sodium and calcium, respectively. The ratios $N_{Ca\,II}/N_{Na}$ range from 0.22 to 2.14, and the mean is 1.0. The significance, if any, to be attached to this result depends entirely upon whether the assumption of unequal velocities for sodium and calcium can be justified.

CARNEGIE INSTITUTION OF WASHINGTON
MOUNT WILSON OBSERVATORY
April 1939

[7] *Ap. J.*, **86**, 274, 1937.

GALACTIC DENSITY GRADIENTS*

BART J. BOK

ABSTRACT

An attempt is made to investigate the gradients of the star density in the galactic plane for two sections of the Milky Way. First a study is made for several subregions of the change of color with distance for stars of known spectral types. Since it has been shown by several investigators that the ratio of total absorption for photographic light to the observed color excess in a given color system is sensibly constant for regions outside conspicuous dark nebulae, it is possible to estimate roughly the increase of the total absorption for photographic light in each subregion. Star counts to faint limits of magnitude and statistics of the distribution of spectral types provide the data from which the change of star density with increasing distance from the sun can be determined.

The basic material for the section in Monoceros ($\lambda = 180°, \beta = 0°$) consists of blue-red color indices of the early-type stars of known spectral type. The fields fall in a part of the Milky Way for which the surface distribution of the stars is extremely regular and unaffected by obvious local obscuration. It is therefore interesting to find that space reddening clearly affects the colors of the fainter stars of early spectral types. If the assumption is made that the total photographic absorption for any given star equals three times the color excess on the blue-red system ($\lambda_1 = 4500$ A, $\lambda_2 = 6200$ A), the photographic absorption is found to increase regularly with distance for distances up to 1500 parsecs. For the fields within three degrees of the galactic equator the rate of increase is measured by the value $A_{pg} = 1^m$/kpc. The corresponding value for the fields at average galactic latitude $+5°$ is $A_{pg} = 0^m4$/kpc. The density analyses for the B8 to A0 and A2 to A5 stars show the presence of considerable negative density gradients. It is important to notice that the rapid drop in the star density apparently is not shared by the stars at large; star counts for Selected Area 98—which falls within the region covered by the analysis—indicate a fairly constant star density for distances up to 1000 parsecs from the sun.

The second section of the Milky Way for which approximate density gradients are determined lies in Cepheus and Cassiopeia. The basic material consists of star counts, spectral types, and color indices for Selected Areas 8, 9, 18, and 19. The Cepheus-Cassiopeia section of the Milky Way is by no means free from local obscuration. S.A. 8 is in a region where the surface distribution is decidedly irregular, S.A. 9 is in a fairly uniform field, S.A. 18 is bordered by obscuration, and S.A. 19 is adjacent to a large dark cloud. The counted areas and the fields for which the colors were measured were adjusted so as to include only uniform fields of smallest obscuration. A factor four is used for the conversion of excesses on the international scale to total photographic absorptions. The resulting minimum values for the corresponding coefficients of absorption are: S.A. 8: $A_{pg} = 1^m2$/kpc for $0 < r < 2000$ parsecs; S.A. 9: $A_{pg} = 1^m6$/kpc for $0 < r < 1500$ parsecs; S.A. 18: $A_{pg} = 0^m5$/kpc for $0 < r < 2000$ parsecs; S.A. 19: $A_{pg} = 0^m0$/kpc for $r < 800$ parsecs, $A_{pg} = 1^m2$/kpc for $800 < r < 2000$ parsecs. S.A. 18, at $\beta = +6°$, is the only area at some distance from the galactic plane. Star densities are computed for intervals B0 to B5, B6 to B9, A0 to A4, A5 to A9, and—from star counts—for all stars combined. It is found that the star density drops generally with increasing distance from the sun for distances up to 2000 parsecs. In contrast to the results for the fields in Monoceros, it is generally

* This paper was presented at the symposium on galactic and extragalactic structure, held in connection with the dedication of the McDonald Observatory May 5–8, 1939.

found that the space densities for the early-type stars and the stars at large drop about equally fast. There is nowhere a definite indication of an increase in space density from the sun outward.

We conclude that our information on interstellar absorption and galactic density gradients for distances up to 2000 parsecs from the sun may be increased rapidly through suitable studies based on spectral types, colors, and star counts. Because of the irregular structure of the Milky Way, we can hope to arrive at a true picture of the stellar distribution in the galactic plane only if such studies are made for every single section of the Milky Way.

INTRODUCTION

A lack of sufficient information about the amount of interstellar absorption for various directions in the Milky Way is mainly responsible for the present uncertainties concerning the structure of the galactic system. Shapley's researches on the distribution of globular clusters and the Oort-Lindblad theory of galactic rotation have revealed the general outlines of the galaxy and the location of our sun with respect to the center; but we are at present still uncertain about the density distribution in the galactic plane, even for distances up to 2000 parsecs from the sun. The situation is by no means hopeless, however. With the accumulation of further data on spectral types, colors, magnitudes, star counts, and the distribution of external galaxies, we may gain detailed information about the properties of the interstellar absorbing material. This knowledge should render possible the study of the variation of star density with increasing distance from the sun for various directions in the galactic plane.

In the present paper an attempt is made to determine galactic density gradients for two sections of the Milky Way: the first in Monoceros, the second in Cepheus-Cassiopeia. The prospects for statistical analysis appear to be nowhere else quite as good as in Monoceros, which is probably the smoothest section of the Milky Way. In view of the suggestion that a considerable fraction of the interstellar absorption might take place in isolated dark nebulae, a study of the absorption properties of the Monoceros field, where no conspicuous dark clouds are present, should be extremely interesting. Blue-red color indices have been determined for early-type stars in regions for which Miss Cannon has very kindly offered the use of the *Henry Draper Charts* in advance of publication.

The section in Cepheus and Cassiopeia was chosen largely because it is one of the most frequently studied sections of the Milky Way.

Particularly for Selected Areas 8, 9, 18, and 19 an abundance of data is available. The published star counts for these areas[1] have been supplemented by unpublished counts by Miss Risley, Dr. R. H. Baker, and Dr. Evans.[2] The spectral types and photographic magnitudes for stars brighter than $m = 13.0$ are given in the first volume of the *Bergedorfer Spektral Durchmusterung*. For some time a program of photovisual-magnitude determination for stars in Selected Areas at $\delta = +60^\circ$ has been under way at the Harvard Observatory, and its completion for Selected Areas 8, 9, 18, and 19 has yielded data on the colors of the stars in these areas.

The basic procedure of the investigation is the following. First, for each separate region a study is made of the change of color excess with distance modulus for successive intervals of spectral type. In order to obtain the total absorption for photographic light, we make use of recent determinations of the ratio of the total photographic absorption to the amount of reddening, applying in particular the results of Greenstein[3] and Oort.[4] The observed color excesses in Cepheus-Cassiopeia are on the International Scale ($\lambda_1 = 4400$ A, $\lambda_2 = 5500$ A), and can be roughly transformed into total absorptions for photographic light by multiplication by a factor four. The factor three has been used for the conversion of the blue-red excesses ($\lambda_1 = 4500$ A, $\lambda_2 = 6200$ A) in Monoceros.

Let us now suppose that a color excess C has been found at apparent magnitude m for a group of stars with an assumed mean absolute magnitude M. If the color excess C refers to the International Scale, the approximate value of K—where K represents the total photographic absorption which the light of the particular group of stars has suffered—is given by the relation

$$K = 4 \times C .$$

It is then possible to compute an approximate value for the average distance of the group of stars, from the formula

$$5 \log r = (m - M) + 5 - K ,$$

[1] van Rhijn, *Groningen Pub.*, No. 43, 1929.

[2] See *Trans. I.A.U.*, **6**, 447, 1938.

[3] *Ap. J.*, **87**, 151, 1938.

[4] *B.A.N.*, No. 308, 1938.

or its equivalent

$$5 \log r = (m - M) + 5 - 4 \times C . \qquad (1)$$

We can then plot the total absorptions against the true distances and obtain the desired information concerning the variation in the total absorption for photographic light with distance. The formula for the blue-red color excesses, corresponding to equation (1), will take the form

$$5 \log r = (m - M) + 5 - 3 \times C' , \qquad (2)$$

where C' is the observed blue-red excess. Star counts to faint limits of magnitude and statistics on the distribution of spectral types provide finally the data from which the gradients of star density can be determined for various directions.

I. THE MONOCEROS REGION

A. THE COLOR DATA AND THEIR ANALYSIS

Through the kindness of Miss Cannon, the *Henry Draper Charts* for the section of the Milky Way from $\alpha = 6^h20^m$ to 7^h10^m and from $\delta = -5°$ to $\delta = +3°$ were placed at our disposal in advance of publication. The present investigation deals with two regions that together cover a total area of 27.8 square degrees—one centered at $\alpha = 6^h45^m$, $\delta = 0°$, the other at $\alpha = 6^h57^m$, $\delta = +1°$. The average galactic longitude is 180°; the extreme values of the galactic latitude are $-1°$ and $+7°$ on the Harvard pole, and $-5°$ and $+3°$ on van Rhijn's pole.[5] The magnitudes and colors were determined from polar comparison plates taken with the 8-inch Ross (IR) camera at the Oak Ridge Station. The blue magnitudes ($\lambda = 4500$ A) were measured on Cramer Hi-Speed plates taken without a color filter; the red magnitudes ($\lambda = 6200$ A) were measured on Eastman I-C special plates taken with a ciné-red filter. The plates were taken largely by Dr. Cuffey, who was responsible also for the measurements. The analysis of the material was carried out in collaboration with Dr. Cuffey and Miss Cherry. As standards of magnitude, the

[5] Unless specifically noted otherwise, all galactic co-ordinates are referred to the Harvard pole ($\alpha = 12^h40^m$, $\delta = +28°0$). The equatorial co-ordinates of van Rhijn's pole are: $\alpha = 12^h56^m$, $\delta = 25°.5$.

polar sequence on the International Photographic Scale[6] and the red polar sequence determined by Mrs. Gaposchkin[7] were used.

Dr. Cuffey's measurements gave the color indices of 1054 stars with known spectral types earlier than Fo. The average probable error of a final color is of the order of $\pm 0^m.05$. For purposes of analysis the field under investigation has been divided into eight subregions; the size of each subregion and its approximate center are listed in Table 1. The diagrams that show the relationship between the individual blue-red color indices and the photo-red magnitudes for small intervals of spectral type are given in Figure 1 for each subregion. The total number of early B stars is too small to warrant the construction of a separate diagram for each subregion. It may be of interest to mention that only one of the twenty Bo to B5 stars with $m_r > 9.0$ has a negative color index.

TABLE 1

POSITION OF CENTER AND TOTAL AREA FOR EACH OF THE SUBREGIONS IN MONOCEROS

Subregion	α	δ	λ	β	Area in Square Degrees
I	6^h40^m	$+1^\circ$	179°	0°	3.27
II	6 40	−1	181	0	3.35
III	6 47	+1	180	+2	2.17
IV	6 47	−1	182	+1	2.81
V	6 53	+2	180	+4	3.74
VI	6 53	0	182	+3	3.53
VII	7 02	+2	181	+6	4.46
VIII	7 02	0	183	+5	4.47

It is at once apparent from Figure 1 that considerable space reddening exists for the distant stars in Monoceros. The effects are most clearly marked in Areas I and II, for which the average galactic latitude is practically zero. Slightly smaller reddening is indicated for Areas III and IV, which form a second more or less homogeneous group with an average latitude of $+2\frac{1}{2}^\circ$. The observed amount of reddening is very much smaller for Areas VII and VIII, with an average latitude of $+5^\circ$.

The relevant data for the color excesses are shown in Table 2,

[6] See *Trans. I.A.U.*, **1**, 71, 1922. [7] *Harvard Ann.*, **89**, No. 5, 1935.

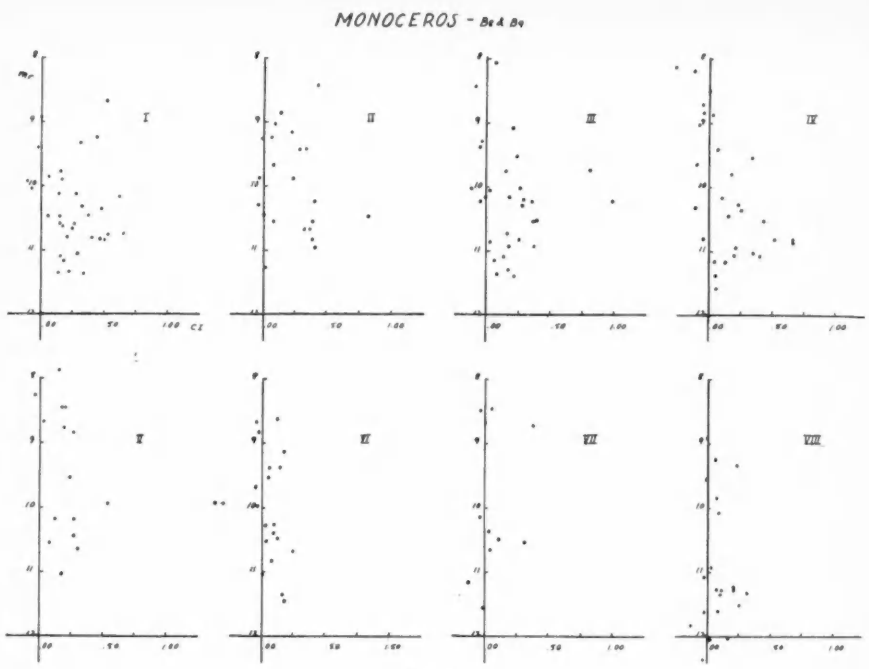

FIG. 1a

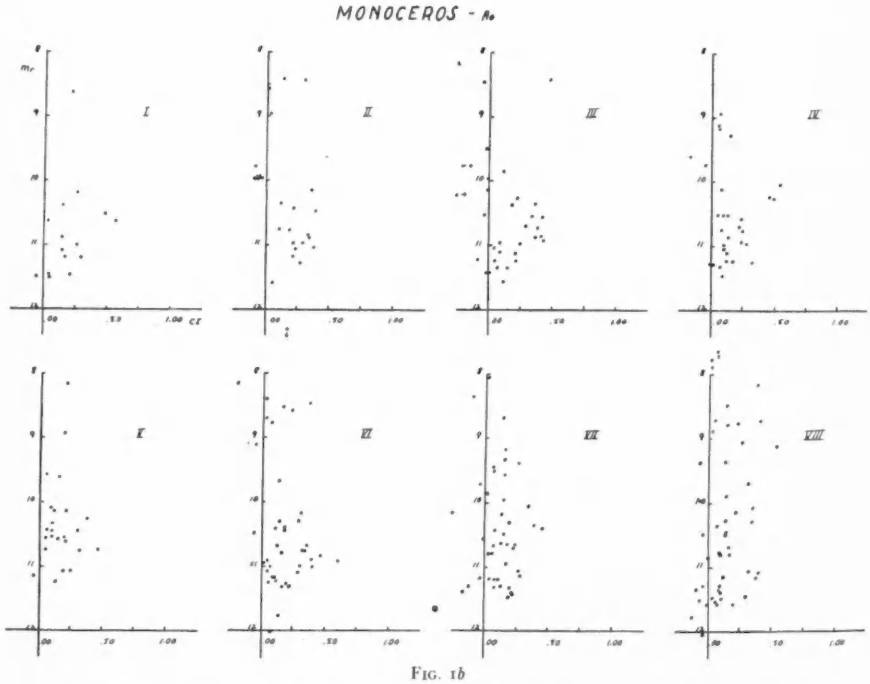

FIG. 1b

FIG. 1.—The relations between the observed color indices (*abscissae*) and the photo-red magnitudes (*ordinates*) for the stars in Monoceros. See also Figs. *c–d*.

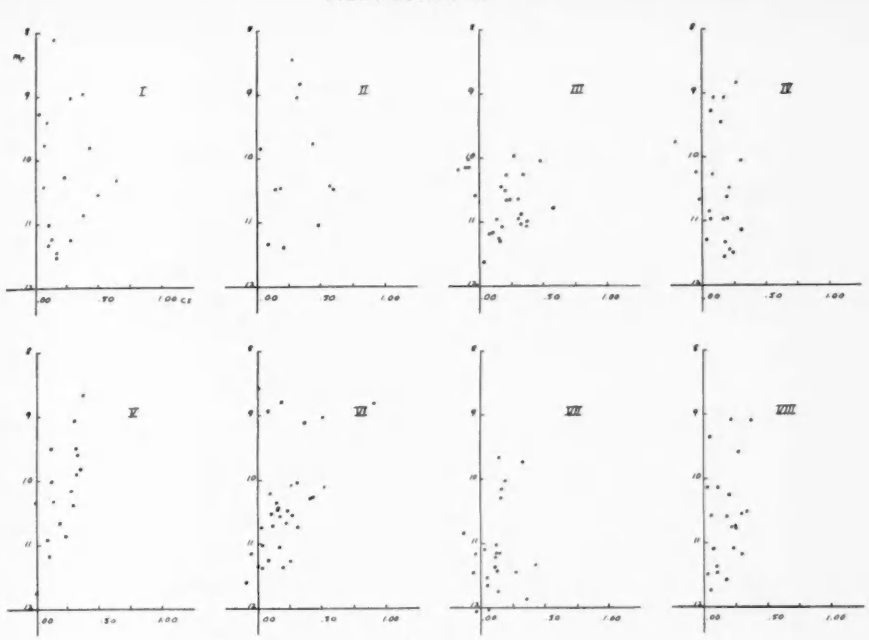

FIG. 1c

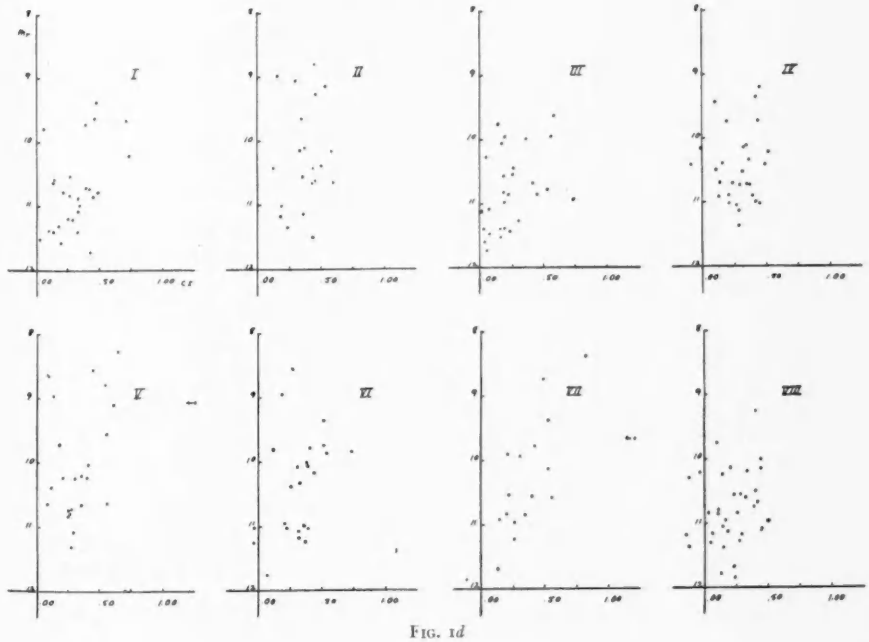

FIG. 1d

FIG. 1.—*Cont.*

where the averages for areas with similar reddening have been combined. From the diagrams in Figure 1 the observed average color index is read for each spectral division at $m = 11.00$. The averages listed in the third column of Table 2 are the basic values used in the later reductions. The figures in the fourth and fifth columns are derived from the following assumptions for the mean absolute magnitudes and normal color indices for each spectral division:

Sp.	$\overline{M}$	C.I. Normal
B8 to B9	−0.5	−0.20
A0	+0.5	− .10
A2	+1.5	.00
A3 to A7	+2.5	+0.20

The total photographic absorptions for successive values of $(m-M)$ are then computed from the relation

$$K = 3 \times C',$$

and finally the corresponding values for the average true distances, given in the last column, are found with the aid of relation (2). The figures of the last two columns are reproduced graphically in Figure 2. The results are generally confirmed by the color excesses of the B0 to B5 stars, which show an average color excess of $+0^m.45$ at $m = 10.0$ at the galactic circle. If we compute the distances for these stars with the aid of equation (2), we find that for $r = 1300$ parsecs $K = 1^m.3$, and therefore $A_{pg} = 1^m.0$/kpc, in agreement with the results from the more numerous B8 to A7 stars.

The results of the analysis of the color indices are summarized as follows:

1. Space reddening, which increases with distance from the sun, is present in a section of the Milky Way in Monoceros, where the surface distribution of the stars is extremely regular.

2. The average amount of reddening on our blue-red photometric system amounts to $0^m.34$/kpc, or approximately $0^m.25$/kpc on the International Scale, at galactic latitudes $-1°$ to $+3°$ on the Harvard pole.

3. The reddening is only half as strong for the regions at $\beta = +5^\circ$ as for those at $\beta = -1^\circ$ to $+3^\circ$.

4. The suggested final values for the coefficient of absorption for photographic light are:

Areas I and II ..... $A_{pg} = 1^m1$/kpc
Areas III–VI ..... $A_{pg} = 0^m9$/kpc
Areas VII and VIII ..... $A_{pg} = 0^m4$/kpc

for distances up to 1200 parsecs from the sun.

TABLE 2

SUMMARY OF COLOR EXCESSES AND ESTIMATES OF ABSORPTION IN MONOCEROS

Area	Sp.	C.I. at $m=11.0$	$m-M$	C.E.	$K=3\times$C.E.	r (pcs)
I and II	B8 to B9	+0.27	11.5	+0.47	1.4	1050
($\bar{\beta}=0^\circ$)	A0	.21	10.5	.31	0.9	830
	A2	.25	9.5	.25	0.8	550
	A3 to A7	.32	8.5	.12	0.4	420
III to VI	B8 to B9	.20	11.5	.40	1.2	1150
($\bar{\beta}=+2.5^\circ$)	A0	.18	10.5	.28	0.8	870
	A2	.16	9.5	.16	0.5	630
	A3 to A7	.29	8.5	.09	0.3	440
VII and VIII	B8 to B9	.02	11.5	.22	0.7	1440
($\bar{\beta}=+5^\circ$)	A0	.05	10.5	.15	0.4	1050
	A2	.15	9.5	.15	0.4	660
	A3 to A7	+0.22	8.5	+0.02	0.1	480

B. THE DENSITY GRADIENTS

It is now possible, from statistics on the surface distribution of the stars, to find the variations in the true space density with distance from the sun. We shall designate by $A'(m)$ the number of stars that have apparent magnitudes between $m - \frac{1}{4}$ and $m + \frac{1}{4}$, reduced to an area of 100 square degrees in the sky. Direct counts on Miss Cannon's *Henry Draper Charts* gave values of $A'(m)$ for $m = 9.0$ to $m = 11.0$. The limiting magnitude of Miss Cannon's classification is 11.5, and the counts are essentially complete to $m = 11.3$. Direct counts in the *Henry Draper Catalogue* for a region of 100 square degrees along the Milky Way in Monoceros

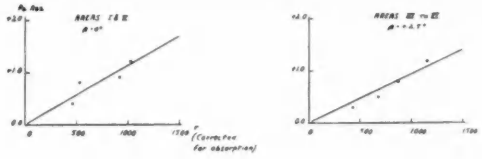

FIG. 2

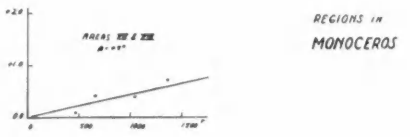

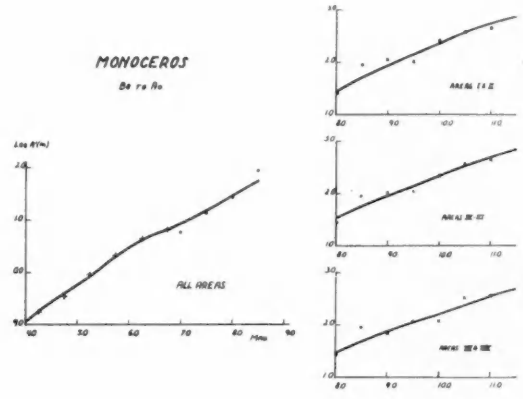

FIG. 3

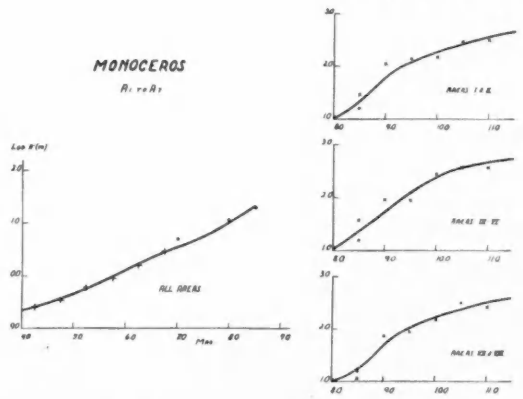

FIG. 4

FIG. 2.—The diagrams show how the total absorption for photographic light (*ordinates*) varies with the distance from the sun (*abscissae*).

FIG. 3.—The curves show the variation of the counted numbers of stars with the apparent photographic magnitude for the B8 to A0 stars.

FIG. 4.—The curves show the variation of the counted numbers of stars with the apparent photographic magnitude for the A1 to A7 stars.

yielded values of $A'(m)$ for $m = 7.0$ to $m = 8.5$; the distribution of the Henry Draper stars was sufficiently similar for all subregions to warrant the use of a single set of average $A'(m)$'s for the whole region. The counts for $m = 4.25$ to $m = 7.25$ were obtained from a paper by Seydl[8] in which total numbers counted in the *Henry Draper Catalogue* are given for the zone $\beta = -10°$ to $+10°$. It is essential to include in the analysis these statistics on the average distribution of the bright stars if one wishes to study the variations in star density from the immediate vicinity of the sun outward. The variation of the observed values of log $A'(m)$ with apparent magnitude and the mean curves used in the analysis are shown in Figures 3 and 4.

The counts for the B8 to A0 and the A1 to A7 stars have been analyzed by the method of Schalén and Lindblad.[9] The average absolute magnitudes were taken as $M = +0.5$ for the B8 to A0 stars and $M = +2.0$ for the A1 to A7 stars; a dispersion $\sigma = \pm 1^m.0$ was assumed in each case. The corrections for absorption were made with the aid of Seeliger's formula.[10] The resulting space densities are reproduced graphically in Figure 5.

The space densities for the early-type stars are found to decrease with distance from the sun. For the fields right in the Milky Way plane the space density at a distance of 600 parsecs is approximately only one-half that near the sun.

Apparently no such steep density gradients are found for the stars at large. Van Rhijn[11] has studied the density distribution for Selected Area 98, which falls within our region. He finds that for this part of the Milky Way the average space density for the stars at large remains sensibly constant for distances up to 1000 parsecs from the sun, if we assume that A_{pg} has the value $1^m.1$/kpc. He shows in the same paper that for the section of the Milky Way between $\lambda = 0°$ and $\lambda = 200°$ the average gradient of the space density has a much larger negative value for the B0 to B2 stars than for stars in general.

[8] *Pub. Nat. Obs. Prague*, No. 6, 1929.

[9] See *Upsala Medd.*, No. 37, 1928.

[10] Bok, *The Distribution of the Stars in Space*, p. 13, University of Chicago, 1937.

[11] *Groningen Pub.*, No. 47, 1936.

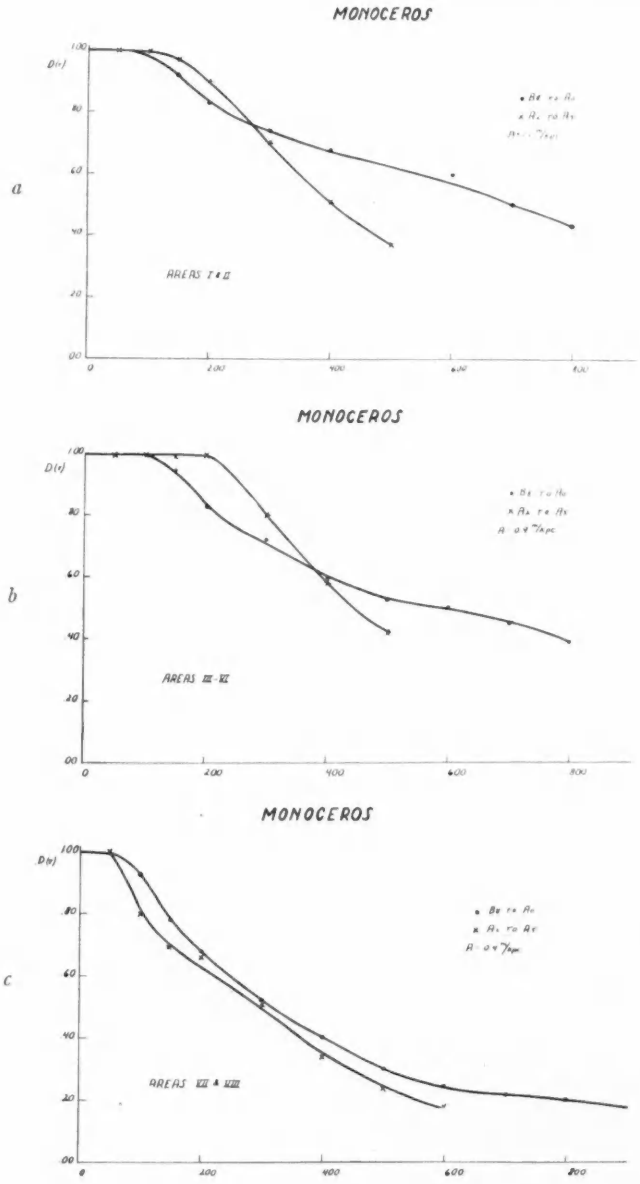

FIG. 5.—The relations between the true space densities $D(r)$ (*ordinates*) and the distance from the sun (*abscissae*) for the fields in Monoceros.

Our present data suggest that for the direction $\lambda = 180°$, the density of the B8 to A0 stars drops much more rapidly than that of the stars in general. It is significant that a *difference* between the density gradients for different groups of stars in a given section of the Milky Way can never be eliminated by choosing a different value for the coefficient of interstellar absorption.

II. THE CEPHEUS-CASSIOPEIA REGION

A. THE COLOR DATA AND THEIR ANALYSIS

Photovisual magnitudes on the International Scale have been obtained for stars of spectral types B0 to A4 and magnitudes 8.0 to 12.0 that are given in the *Bergedorfer Spektral Durchmusterung* for Selected Areas 8, 9, 18, and 19. The magnitudes have been measured on Eastman I-G plates taken with the 16-inch Metcalf (MC) refractor at Oak Ridge, through a yellow filter.[12] The differences between the photographic magnitudes, measured at Groningen, and the Harvard photovisual magnitudes yield color indices with average probable errors of the order of $\pm 0^m.10$. The average color indices obtained in the same way for stars of later spectral type are used to determine the corrections to be applied for zero point and scale errors. In no case have the latter been appreciable, but corrections to the zero point have been indicated and have been applied wherever necessary. The corrected average color indices for all four areas are listed in Table 3. These average color indices are transformed into color excesses on the International Scale by assuming that the normal color indices for average unreddened B0 to B5 and B6 to A4 stars are $-0^m.20$ and $-0^m.10$, respectively. The color excesses are plotted against the differences $(m - M)$, and from these graphs the total photographic absorptions are computed according to the method outlined in the introduction to the present paper. The details and results for each area follow.

Selected Area 8 ($\lambda = 92°$, $\beta = -2°$).—Miss Virginia McKibben and Mr. J. G. Baker have measured the photovisual magnitudes of 150 stars with spectral types between B0 and A4 and 53 stars in the interval A5 to F4. A correction of $+0^m.10$, indicated by the colors of the latter stars, has been applied to the average color indices of the

[12] For details see Bok and Swann, *Harvard Ann.*, **105**, 371, 1937.

early-type stars. The results of the analysis outlined at the beginning of this section show that the coefficient of absorption for photographic light is equal to at least $A_{pg} = 1^m.2$/kpc. The photographic absorption increases very nearly linearly with the apparent magnitude for distances up to 2000 parsecs from the sun.

This value for the coefficient A_{pg} checks well with other determinations. Photoelectric color indices obtained by Stebbins and Huffer[13] yield $A_{pg} = 1^m.4$/kpc for $0 < r < 500$ parsecs, and Zug's[14] colors for stars in distant clusters suggest $A_{pg} = 0^m.9$/kpc in the vicinity of Selected Area 8. Seares[15] finds color excesses of the order of $0^m.6$ for the faint stars in Selected Area 8.

TABLE 3*

AVERAGE COLOR INDICES ON THE INTERNATIONAL SCALE IN FOUR SELECTED AREAS

m_{pg}	S.A.8 ($\beta = -2°$)		S.A.9 ($\beta = +3°$)		S.A.18 ($\beta = +7°$)		S.A.19 ($\beta = -1°$)	
	Bo to B5	B6 to A4	Bo to B5	B6 to A4	Bo to B5	B6 to A4	Bo to B5	B6 to A4
9.00– 9.99	+0.03 (7)	+0.03 (11)	.....	+0.05 (22)	−0.15 (8)	−0.12 (9)	.....	.....
10.00–10.99	.24 (3)	.17 (34)	+0.24 (1)	.20 (38)	+0.12 (3)	− .02 (32)	+0.09 (5)	−0.09 (19)
11.00–11.99	+0.28 (11)	+0.23 (77)	.....	.29 (49)	.....	+0.03 (40)	.....	.00 (30)
12.00–12.99	.....	.....	+0.65 (2)	+0.43 (55)	.....	.....	.....	+0.24 (7)

* The numbers in brackets give the numbers of stars in each average.

Selected Area 9 ($\lambda = 107°$, $\beta = +3°$).—Mr. W. F. Swann has measured the photovisual magnitudes of 164 stars with spectral types B6 to A4 and of 45 supplementary stars with spectral types A5 to F4. The latter show that the zero point needs no correction. Analysis of the color indices indicates that the total photographic absorption increases approximately linearly with the apparent magnitude for distances up to 1500 parsecs; the average value of the coefficient for photographic light is $A_{pg} = 2^m.0$/kpc. The color excesses computed from Stebbins and Huffer's[16] material give a value $A_{pg} = 1^m.6$/kpc for the vicinity of Selected Area 19.

Selected Area 18 ($\lambda = 68°$, $\beta = +7°$).—Miss Barbara Cherry has measured the photovisual magnitudes for 110 stars with spectral types Bo to A4 and for 50 stars with spectral types A5 to K2. The

[13] *Washburn Obs. Pub.*, **15**, No. 4, 1934.

[14] *Lick Obs. Bull.*, No. 454, 1933.

[15] *Proc. Nat. Acad.*, **22**, 327, 1936.

[16] *Op. cit.*

average colors of the late-type stars show that an average constant correction of $-0^{m}.10$ is needed for the reduction of the colors to the International Scale. Analysis of the averages indicates no reddening for distances less than 700 parsecs from the sun, whereas the data between $r = 700$ parsecs and $r = 2000$ parsecs are represented by $A_{pg} = 1^{m}.1/\text{kpc}$.

The low value for A_{pg} is supported by work of Schalén,[17] Sticker,[18] Berg,[19] and Stenquist,[20] who find only very slight color effects for fields at the same galactic longitude as Selected Area 18, but nearer the galactic equator. Miss Slocum[21] finds that the distant stars in Selected Area 18 are very much bluer than similar stars in Selected Areas 8, 9, and 19; Seares[22] finds excesses for a small fraction of all stars in Selected Area 18. The photoelectric colors by Stebbins and Huffer[23] and by Elvey and Mehlin[24]—which are in excellent agreement—show, however, considerable reddening effects for distances up to 700 parsecs. It is extremely difficult to accept their value $A_{pg} = 1^{m}.6/\text{kpc}$ near the sun for Selected Area 18. It seems likely that this area falls in a region of variable reddening and that the stars measured by the photoelectric observers lie in regions of excessive reddening. The density analyses for Selected Area 18 will be carried out on the assumptions that $A_{pg} = 0^{m}.5/\text{kpc}$ and $A_{pg} = 1^{m}.0/\text{kpc}$.

Selected Area 19 ($\lambda = 81^{\circ}$, $\beta = -1^{\circ}$).—Mr. W. P. Bidelman has measured the photovisual magnitudes of 61 stars with spectral types Bo to A4 and for 20 stars with later spectral types. The average color indices of the late-type stars are larger by $0^{m}.30$ than would be expected, and although the material is rather meager, we have applied a systematic correction of $-0^{m}.30$ to all color indices. No appreciable reddening is shown for distances up to 1000 parsecs from the sun. Beyond this distance the absorption rises probably rather sharply, and the value $A_{pg} = 1^{m}.7/\text{kpc}$ is suggested for $1000 < r < 1500$ parsecs.

The somewhat uncertain results of Bidelman's measurements are

[17] *Upsala Medd.*, No. 58, 1934.
[18] *Bonn Veröff.*, No. 30, 1937.
[19] *Poulkovo Bull.*, **15**, 2, 1936.
[20] *Bergstrand Festskrift*, No. 50, 1938.
[21] *Lick Obs. Bull.*, No. 434, 1931.
[22] *Op. cit.*
[23] *Op. cit.*
[24] *Ap. J.*, **75**, 354, 1932.

in striking agreement with those recently published by W. Becker,[25] who finds no perceptible reddening for $r < 900$ parsecs in a field directly north of that studied by Bidelman. Becker's color indices yield a value $A_{pg} = 1^{m}0/\text{kpc}$ for $1000 < r < 2000$ parsecs. Stebbins and Huffer[26] have measured only two stars near Selected Area 19, one of which shows some reddening. Zug's measures[27] of color indices for two distant clusters show considerable reddening.

B. THE DENSITY GRADIENTS[28]

In Figure 6 are shown plots of the counted values of log $A'(m)$ against the corresponding values of the apparent photographic magnitudes. ($A'(m)$ again represents the number of stars with magnitudes between $m - \frac{1}{4}$ and $m + \frac{1}{4}$, reduced to an area of 100 square degrees of the sky.) The data for the stars fainter than $m = 8.0$ have been obtained from direct counts in the *Bergedorfer Spektral Durchmusterung*. The values of log $A'(m)$ for $m = 7.25$ and $m = 7.75$ were found from counts in the *Henry Draper Catalogue* for extended regions centered on the Selected Areas. For $m < 7.0$ the counts were again taken from Seydl's tables[29] for the zone $\beta = -10°$ to $+10°$. The drawing of the smooth curves was, on the whole, straightforward; the only pronounced discontinuity observed was for the Ao to A4 stars in Selected Area 18. The counts from the *Bergedorfer Spektral Durchmusterung* do not generally refer to the whole area covered in the catalogue. The sizes of the counted areas were reduced so that they included only those portions which, from an inspection of long-exposure plates and from star counts made on Harvard plates, were found to be homogeneous in surface distribution with the area for which the colors and faint star counts were available. It was necessary to omit from the regions covered in the catalogue two strips on the sides of Selected Area 8, a corner of Selected Area 18, and approximately one-third of Selected Area 19.

The statistics on the surface distribution for the stars at large were found by combining the data for each area given in *Groningen Pub-*

[25] *Zs. f. Ap.*, **17**, 285, 1939.

[26] *Op. cit.* [27] *Op. cit.*

[28] The analysis in this section was carried out in collaboration with Mrs. Bok.

[29] *Op. cit.*

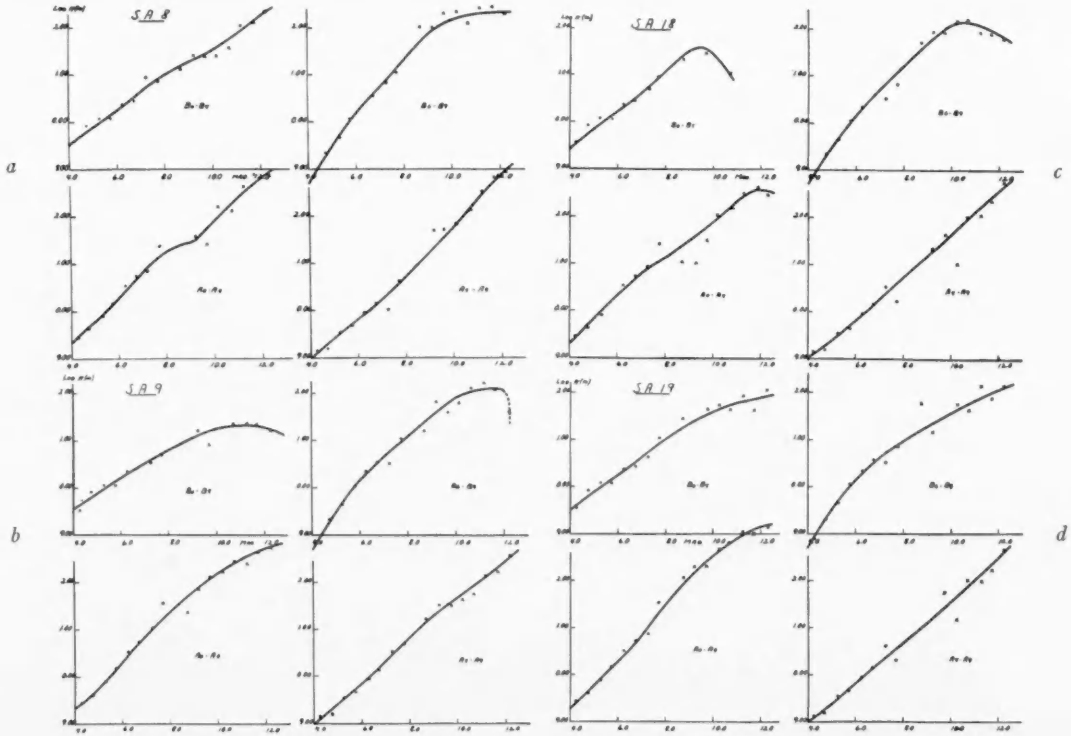

FIG. 6.—The curves show the variation of the counted numbers of stars for successive intervals of spectral types (*ordinates*) with the apparent photographic magnitude (*abscissae*) in each of the Selected Areas.

lications, No. 43, with the total counts from the *Bergedorfer Spektral Durchmusterung* reduced to the same area. The values of log $N(m)$ for $m = 10$ to $m = 15$ were checked from direct counts for the same regions, kindly provided in advance of publication by Miss Risley, Dr. R. H. Baker, and Dr. Evans. The differences between the unpublished Harvard counts and the published data for the Selected Areas were in no case sufficiently large to affect appreciably the space densities listed below, and we decided, therefore, to depend entirely on the combined Bergedorf-Groningen counts.

Because of the uncertainties in the absorption data, the density analyses were carried through for each area on two assumptions for the interstellar absorption. In accordance with the results of the preceding section we have used for Selected Area 8: (1) $A_{pg} = 1^m.2$/kpc, (2) $A_{pg} = 1^m.7$/kpc (to a limiting distance of 2000 parsecs); for Selected Area 9: (1) $A_{pg} = 1^m.6$/kpc, (2) $A_{pg} = 2^m.0$/kpc (to a limiting distance of 1500 parsecs); for Selected Area 18: (1) $A_{pg} = 0^m.5$/kpc, (2) $A_{pg} = 1^m.0$/kpc (to a limiting distance of 2000 parsecs); and for Selected Area 19: (1) $A_{pg} = 0^m.0$/kpc for $r < 800$ parsecs, followed by $A_{pg} = 1^m.2$/kpc for $800 < r < 2000$ parsecs, (2) $A_{pg} = 0^m.0$/kpc for $r < 800$ parsecs, followed by $A_{pg} = 1^m.7$/kpc for $800 < r < 2000$ parsecs.

The variations of the space densities with distance from the sun are reproduced in Tables 4–7. The space densities were computed by the Schalén-Lindblad[30] method for each spectral subdivision and also with the aid of (m, *log* π) tables[31] based on van Rhijn's most recent form for the general luminosity function[32] for the stars at large. The final densities corrected for interstellar absorption were found by using Seeliger's formula. The space densities at a distance of 100 parsecs from the sun have been arbitrarily set equal to 1.00.

The data of Tables 4–7 lead to the following conclusions:

Selected Area 8.—For $A_{pg} = 1^m.2$/kpc the Bo to B5 stars show a fairly steady decrease in space density, which is paralleled for the stars at large by a decrease that is not quite so rapid. The maxima in space density for $300 < r < 600$ parsecs for the B6 to B9

[30] *Op. cit.*

[31] *Harvard Circ.*, No. 371, 1931.

[32] *Groningen Pub.*, No. 47, 1936.

TABLE 4

THE DENSITY DISTRIBUTION FOR THE STARS IN SELECTED AREA 8

r (PARSECS)	B0 TO B5		B6 TO B9		A0 TO A4		A5 TO A9		FROM GENERAL STAR COUNTS	
	(1)*	(2)	(1)	(2)	(1)	(2)	(1)	(2)	(1)	(2)
100	1.00	1.00	1.00	1.00	1.00	1.00	1.00	1.00	1.00	1.00
200	1.00	1.16	1.00	1.23	0.45	0.51	0.94	1.01	0.70	0.75
300	0.76	1.25	1.13	1.45	0.36	0.42	1.06	1.20	0.60	0.63
400	0.57	0.75	1.15	1.58	0.36	0.44	1.10	1.30	0.56	0.58
500	0.57	0.71	1.14	1.52	0.35	0.47	1.06	1.24	0.54	0.58
600	0.49	0.67	1.02	1.44	0.33	0.50	.....	.....	0.52	0.53
700	0.43	0.60	0.82	1.20	0.35	0.42	.....	.....	0.52	0.54
800	0.40	0.64	0.73	0.95	0.29	.....	.....	.....	0.56	0.64
900	0.38	0.62	0.65	0.86	.....	.....	.....	.....	0.62	0.77
1000	0.38	0.60	0.55	0.70	.....	.....	.....	.....	0.70	0.91
1200	0.35	0.64	0.36	0.56	.....	.....	.....	.....	0.72	1.17
1400	0.37	0.71	0.27	.....	.....	.....	.....	.....	0.83	1.18
1600	0.36	0.94	.....	.....	.....	.....	.....	.....	0.65	1.16

* Columns 1 and 2 refer to calculations based on assumptions (1) and (2), respectively, for the absorption coefficient A_{pg} (see text).

TABLE 5

THE DENSITY DISTRIBUTION FOR THE STARS IN SELECTED AREA 9

r (PARSECS)	B0 TO B5		B6 TO B9		A0 TO A4		A5 TO A9		FROM GENERAL STAR COUNTS	
	(1)*	(2)	(1)	(2)	(1)	(2)	(1)	(2)	(1)	(2)
100	1.00	1.00	1.00	1.00	1.00	1.00	1.00	1.00	1.00	1.00
200	1.10	1.10	1.10	1.12	0.78	0.78	0.71	0.72	0.72	0.72
300	0.73	0.74	0.94	1.00	0.60	0.64	0.52	0.55	0.59	0.60
400	0.54	0.59	0.85	0.96	0.44	0.52	0.45	0.52	0.56	0.63
500	0.46	0.56	0.77	0.84	0.35	0.48	0.43	0.54	0.52	0.71
600	0.40	0.43	0.74	0.74	0.29	0.35	.....	.....	0.49	0.49
700	0.38	0.43	0.64	0.66	0.22	.....	.....	.....	0.43	0.45
800	0.28	0.32	0.56	0.66	.....	.....	.....	.....	0.35	0.39
900	0.26	0.36	0.46	0.61	.....	.....	.....	.....	0.34	0.37
1000	0.26	0.29	0.43	0.48	.....	.....	.....	.....	0.26	0.23
1200	0.22	0.29	.....	.....	.....	.....	.....	.....	0.18	0.23
1400	0.16	.....	.....	.....	.....	.....	.....	.....	0.16	0.29
1600	0.11	.....	.....	.....	.....	.....	.....	.....	0.22	.....

* Columns 1 and 2 refer to calculations based on assumptions (1) and (2), respectively, for the absorption coefficient A_{pg} (see text).

TABLE 6

THE DENSITY DISTRIBUTION FOR THE STARS IN SELECTED AREA 18

r (PARSECS)	B0 TO B5		B6 TO B9		A0 TO A4		A5 TO A9		FROM GENERAL STAR COUNTS	
	(1)*	(2)	(1)	(2)	(1)	(2)	(1)	(2)	(1)	(2)
100	.....	.....	1.00	1.00	1.00	1.00	1.00	1.00	1.00	1.00
200	1.00	1.00	1.00	1.09	0.54	0.59	0.68	0.73	0.65	0.68
300	0.67	0.71	1.00	1.14	0.39	0.41	0.55	0.64	0.53	0.59
400	0.50	0.61	0.88	1.03	0.31	0.34	0.48	0.60	0.40	0.50
500	0.45	0.57	0.77	0.96	0.25	0.26	0.44	0.58	0.35	0.44
600	0.40	0.57	0.69	0.89	0.17	0.21	0.42	0.57	0.33	0.45
700	0.38	0.55	0.59	0.74	0.15	0.18	0.39	.....	0.28	0.31
800	0.36	0.52	0.49	0.59	0.12	0.17	0.27	.....	0.22	0.33
900	0.33	0.51	0.38	0.50	0.08	0.16	.....	.....	0.20	0.31
1000	0.31	0.44	0.32	0.39	0.06	.....	.....	.....	0.20	0.26
1200	0.24	0.37	0.22	0.27	.....	.....	.....	.....	0.15	0.29
1400	0.20	0.23	0.13	0.20	.....	.....	.....	.....	0.14	0.31
1600	0.13	0.16	0.10	.....	.....	.....	.....	.....	0.12	0.31

* Columns 1 and 2 refer to calculations based on assumptions (1) and (2), respectively, for the absorption coefficient A_{pg} (see text).

TABLE 7

THE DENSITY DISTRIBUTION FOR THE STARS IN SELECTED AREA 19

r (PARSECS)	B0 TO B5		B6 TO B9		A0 TO A4		A5 TO A9		FROM GENERAL STAR COUNTS	
	(1)*	(2)	(1)	(2)	(1)	(2)	(1)	(2)	(1)	(2)
100	.....	.....	1.00	1.00	1.00	1.00	1.00	1.00	1.00	1.00
200	1.00	1.00	0.72	0.72	0.86	0.86	0.57	0.57	0.61	0.61
300	0.60	0.60	0.46	0.46	0.68	0.68	0.40	0.40	0.43	0.43
400	0.45	0.45	0.34	0.34	0.52	0.52	0.35	0.35	0.30	0.30
500	0.34	0.34	0.25	0.25	0.40	0.40	0.29	0.29	0.28	0.28
600	0.30	0.30	0.20	0.20	0.31	0.31	0.25	0.25	0.26	0.26
700	0.25	0.25	0.16	0.16	0.24	0.24	0.23	0.23	0.24	0.24
800	0.28	0.28	0.17	0.17	0.22	0.22	0.27	0.27	0.30	0.30
900	0.29	0.33	0.18	0.18	0.22	0.23	.....	.....	0.38	0.41
1000	0.28	0.38	0.15	0.20	0.20	0.26	.....	.....	0.39	0.49
1200	0.27	0.38	0.15	0.19	.....	.....	.....	.....	0.36	0.48
1400	0.23	0.39	0.10	0.17	.....	.....	.....	.....	0.31	0.61
1600	0.22	0.38	0.09	0.18	.....	.....	.....	.....	0.37	0.77

* Columns 1 and 2 refer to calculations based on assumptions (1) and (2), respectively, for the absorption coefficient A_{pg} (see text).

and the A5 to A9 stars may be significant, but it should be pointed out that the A0 to A4 stars show a deficiency at the same distances, and that an inconsistency in the spectral classification may well be the cause of the irregularities. The average space density at a distance of 1500 parsecs is not in excess of three-quarters of that near the sun. A somewhat different picture is obtained if we assume $A_{pg} = 1^m.7/\text{kpc}$; it is then found that for the stars at large the average space densities remain approximately constant and equal to those found for the vicinity of the sun for distances to $r = 2000$ parsecs. The negative gradient for the early-type stars persists in spite of the increase in the coefficient of absorption.

Selected Area 9.—The space densities for the separate spectral subdivisions and the stars in general run parallel. There can be little doubt about the reality of consistent negative density gradients for this particular direction. At a distance of 1500 parsecs from the sun the space density has decreased apparently to approximately one-quarter of its value for the vicinity of the sun.

Selected Area 18.—This area is located in galactic latitude $+7°$, and it is not surprising to find that the space density drops rapidly with increasing distance from the sun for all spectral subdivisions separately as well as for the stars at large. Again there are no indications that the space densities for the early-type stars drop more rapidly than those for stars of all types together. The average space density at a distance of 1500 parsecs from the sun does not exceed one-third of its value near the sun.

Selected Area 19.—The gradual drop in the star density with increasing distance from the sun is again marked. There is some indication that the space densities for the B0 to B5 stars drop somewhat more rapidly than those for the stars in general, but the difference is not very conspicuous. The average space density at a distance of 1500 parsecs from the sun does not exceed one-half the value for the solar neighborhood.

CONCLUSIONS

It should be emphasized that it is impossible to come to any general conclusions about galactic structure on the basis of studies for two selected sections of the Milky Way. The present study shows

that it should be possible to obtain a picture of the stellar distribution near the galactic plane for distances up to 2000 parsecs from the sun if spectral surveys for sections of the Milky Way are followed by work on colors and magnitudes and general star counts.

The most significant result from the Monoceros field is that considerable space reddening has been detected for a region that is free from obvious obscuration; the large value $A_{pg} = 1^{m}0/\text{kpc}$ at the galactic equator is worth noting. Negative density gradients are found for the early-type stars, but the density for the stars in general is found to be very nearly constant.

The absorption characteristics for the Selected Areas in the Cepheus-Cassiopeia section of the Milky Way show conspicuous differences from one area to another. Strong reddening is found for Selected Areas 8 and 9, the effect is small for Selected Area 18 ($\beta = +7°$), and for Selected Area 19 absorption sets in apparently not nearer than 1000 parsecs from the sun. The space densities are found to decrease for separate spectral subdivisions as well as for the stars in general in at least three of the four areas. Selected Area 8 is the only possible exception, but the uncertainties about the value of the coefficient of absorption make it impossible to arrive at a definite conclusion for this field. No marked differences are found between the density gradients for the stars in general and the gradients for separate spectral subdivisions in the Cepheus-Cassiopeia section.

HARVARD COLLEGE OBSERVATORY
May 1939

PHYSICAL PROCESSES IN THE GASEOUS NEBULAE

VII. THE TRANSFER OF RADIATION IN THE LYMAN CONTINUUM

JAMES G. BAKER,[1] LAWRENCE H. ALLER,[1] AND DONALD H. MENZEL

ABSTRACT

The differential equations for the transfer of radiation in the Lyman continuum are derived. In order to take into account the varying quality of the radiation as it passes through the nebula and also the variation of the electron temperature, it is necessary to consider the transfer in each element of the continuum rather than to treat the continuum as a single level. The equation of transfer, as written down for a particular frequency in the continuum, therefore contains a term that describes the "interlocking" between the elements of the continuum. The application of these equations to a numerical example is deferred to a later paper.

In the preceding paper[2] we have given the equations of transfer for bound-bound, bound-free, and free-free transitions. For the case of a gaseous nebula exposed to dilute temperature radiation, these equations admit of certain simplifications and modifications. In this paper we shall consider the transfer of radiation in the Lyman continuum for a model planetary nebula consisting of a shell whose thickness is small compared with its radius. For this problem it is not necessary to suppose that the nebular shell is in static equilibrium. The rates of expansion of the planetary nebulae, as observed by Campbell and Moore,[3] introduce Doppler shifts of only negligible importance in the continuum. In the case of the Lyman lines, however, the problem of transfer as discussed in paper VI is further complicated by these internal motions in the nebular shell. Even for the simple case of a homogeneous gaseous shell expanding at a constant rate, the boundary conditions for the differential equations of transfer become involved.

[1] Society of Fellows, Harvard University.

[2] "Physical Processes in the Gaseous Nebulae," I, *Ap. J.*, **85**, 330, 1937; II, *ibid.*, **86**, 70, 1937; III, *ibid.*, **88**, 52, 1938; IV, *ibid.*, p. 313; V, *ibid.*, p. 422; VI, *ibid.*, **89**, 587, 1939. The papers of this series are referred to in the text as papers I, II, III, etc.

[3] *Pub. Lick Obs.*, **13**, 77, 1918.

The transfer equation for the bound-free transitions for a particular frequency ν may be written as given in equation VI (5):

$$\cos\theta \frac{dI_\nu}{dx} = -\frac{1}{4\pi}\sum_{n'}(E_{n'\kappa} - E_{\kappa n'}) . \tag{1}$$

Since the same frequency may be emitted by the capture of a very fast electron on the second or higher level as by the capture of a much slower electron on the first level, we have summed over n'. This overlapping effect will be of importance, however, only for extremely high temperatures. Ordinarily, for a given spectral region and almost certainly for the frequencies in the Lyman continuum, only the first term of the summation need be retained. Since the energy absorbed or emitted is related to the number of transitions by means of the formula $E_{1\kappa}d\nu = F_{1\kappa}h\nu d\nu$, the equation of radiative transfer becomes:

$$\cos\theta \frac{dI_\nu}{dx} d\nu = -\frac{1}{4\pi}[F_{1\kappa} - F_{\kappa 1}]h\nu d\nu . \tag{2}$$

In order to solve this equation we must find a relation between $F_{1\kappa}$ and $F_{\kappa 1}$. Note that equation (2) is written for an element $d\nu$ of the continuum. Previous investigators of the transfer problem have introduced the approximation of considering the continuum as a single level. The absorption coefficient was taken as constant over the level. We shall remove this severe restriction. If we are to study the variation of electron temperature and of the radiation field through the nebula, it will be necessary to consider the transfer problem in each element of the continuum rather than to treat the continuum as a single level.

In a steady state the number of electrons entering the continuum must be equal to the number of electrons leaving it. As we have shown in paper V, the number of ionizations from the second and higher levels is very small compared with the number of ionizations from the first, the reason being the small number of atoms in the higher levels as well as the much weaker radiation intensity in the visible and infrared regions of the stellar spectrum. Hence, neglecting ionizations from the higher levels, we find that the electrons are supplied to the continuum from the ground level. The converse

process, however, may be a recapture on any one of the discrete levels. Therefore, for statistical equilibrium,

$$\int_{\nu_1}^{\infty} F_{1\kappa} d\nu = \sum_{n=1}^{\infty} \int_{\nu_n}^{\infty} F_{\kappa n} d\nu \,. \tag{3}$$

The summation should be extended to a certain maximum value of n depending on the density in a manner which we shall discuss in a later paper. For purposes of simplification we here make the approximation of summing to infinity. The error introduced by this approximation will be of small importance in the transfer problem of the Lyman continuum. Of the totality of captured ν-electrons, the fraction p_ν entering the first level is given by

$$p_\nu = \frac{F_{\kappa 1} d\nu}{\sum_1^{\infty} F_{\kappa n} d\nu} = \frac{\sigma_{\kappa 1}}{\sum_1^{\infty} \sigma_{\kappa n}} \,, \tag{4}$$

where $\sigma_{\kappa n}$ is the target area of the nth level. For an electron moving with a velocity v, κ is given by

$$\tfrac{1}{2} m v^2 = \frac{hRZ^2}{\kappa^2} \,. \tag{5}$$

The expression for $\sigma_{\kappa n}$ for hydrogen is

$$\sigma_{\kappa n} = \frac{2^4}{3\sqrt{3}} \frac{\epsilon^2 h}{m^2 c^3} \frac{1}{\left(\frac{1}{n'^2} + \frac{1}{\kappa^2}\right)} \frac{\kappa^2}{n'^3} g_{\text{II}} \,, \tag{6}$$

where h, m, and c have their usual meanings and g_{II} is the correction factor to Kramers' formula for bound-free transitions. The quantity κ, a real positive number not necessarily integral, is related to the frequency of the emitted radiation by

$$\nu_{n'\kappa} = RZ^2 \left(\frac{1}{n'^2} + \frac{1}{\kappa^2}\right),$$

where n' is integral and R is the Rydberg constant. For the first level

$$\frac{\nu_{1\kappa}}{RZ^2} = \frac{1}{\kappa^2} + 1 \,,$$

and we obtain finally

$$p_\nu = \frac{\dfrac{g_{\mathrm{II}}}{1+\dfrac{1}{\kappa^2}}}{\displaystyle\sum_{n'=1}^{\infty} \frac{g_{\mathrm{II}n'}}{\left(\dfrac{1}{n'^2}+\dfrac{1}{\kappa^2}\right)n'^3}} = \frac{\dfrac{RZ^2}{\nu}}{\displaystyle\sum_{n'=1}^{\infty} \frac{\dfrac{g_{\mathrm{II}n'}}{g_{\mathrm{II}}}}{\left\{n'+\left(\dfrac{\nu}{RZ^2}-1\right)n'^3\right\}}} . \qquad (7)$$

The dependence of g_{II} on the frequency is known. For the purposes of the present discussion we have found it permissible to take the ratio $g_{\mathrm{II}n'}/g_{\mathrm{II}_1}$ as constant. Values of p_ν were then adopted as follows:

ν/ν_1	p_ν	ν/ν_1	p_ν
1.001	0.21	1.40	0.64
1.01	0.31	1.60	0.68
1.03	0.38	2.00	0.72
1.06	0.44	2.50	0.75
1.10	0.48	3.00	0.77
1.20	0.57	6.00	0.80

Previous investigators have employed p_ν as a parameter in their equations. In this manner they have evaded the troublesome task of determining a properly weighted mean value of p_ν consistent with their treatment of the continuum as a single discrete level.

Equation (3) imposes the condition that the number of electrons entering the continuum per second must be equal to the number leaving it per second. We have yet to consider the requirement that each element $d\kappa$ of the continuum must be in a steady state; that is, the number of atoms entering the range $d\kappa$ per second by all possible processes must be equal to the number leaving that element per second by all processes. We may express this condition as follows:

$$\left.\begin{aligned} F_{1\kappa}d\kappa + \int_{\kappa}^{\infty} F_{\kappa'\kappa}d\kappa''d\kappa + C_1(\kappa)d\kappa \\ = \sum_{n=1}^{\infty} F_{\kappa n}d\kappa + \int_{0}^{\infty} F_{\kappa\kappa'}d\kappa + C_2(\kappa)d\kappa . \end{aligned}\right\} \qquad (8)$$

The left-hand side of the equation expresses the totality of ways in which an electron may enter the element $d\kappa$ of the continuum. The respective terms represent photo-ionizations from the ground state, free-free transitions from a higher state, and collisional processes involving radiationless impact. The right-hand side of the equation enumerates the totality of ways by which an electron can leave the element $d\kappa$ of the continuum, by capture on the nth level of an atom, by a free-free transition to a lower level, or by a collision with another electron. We denote the collisional terms by $C_1(\kappa)$ and $C_2(\kappa)$, respectively, and shall find that we do not need to evaluate them explicitly. From equation (4) we have

$$F_{\kappa 1} = p_\nu \sum_1^\infty F_{\kappa n} . \tag{9}$$

We re-write equation (8) in the form

$$\sum_1^\infty F_{\kappa n} d\kappa = F_{1\kappa} d\kappa + \eta d\kappa , \tag{10}$$

where

$$\eta = \left\{ \int_\kappa^\infty F_{\kappa'' \kappa} d\kappa'' - \int_0^\kappa F_{\kappa\kappa'} d\kappa + C_1(\kappa) - C_2(\kappa) \right\} .$$

Equation (10) is taken as a definition of η. Now equation (3) requires that

$$\int_0^\infty \eta d\kappa = 0 , \tag{11}$$

an expression that proves to be a useful check on the accuracy of the calculations of the transfer problem. Physically, η is a measure of the extent to which the electron velocities are reshuffled by collisions and by free-free transitions among the various elements $d\kappa$ of the continuum. Previous writers have usually considered the continuum as a single level, in which case η has no significance. We shall find η to be of importance in the solution of the equations of transfer. From equations (9) and (10) we have

$$p_\nu [F_{1\kappa} + \eta] = F_{\kappa 1} . \tag{12}$$

Using equation (2), we obtain

$$\cos\theta \frac{dI_\nu}{dx} = -\frac{1}{4\pi}[1 - p_\nu]F_{1\nu}h\nu + \frac{p_\nu \eta h\nu}{4\pi}. \tag{13}$$

The element of optical depth is now introduced as

$$d\tau_\nu = N_1 a_{1\nu} dx, \tag{14}$$

where N_1 is the number of atoms in the ground state and a_ν is the absorption coefficient at the frequency ν. In the notation of previous papers we have

$$d\tau_\nu = b_1 \frac{N_i N_e}{4\pi\sigma} \frac{KZ^4}{T_e^{3/2}} hg e^{X_1} dx, \tag{15}$$

where $\sigma = 2h\nu^3/c^2$. We must remark that the optical depth of any given nebula will vary with the frequency of the radiation with which it is measured. The optical depth will decrease with increasing frequency roughly as ν^{-3}. It is convenient to define a τ_{ν_1} which represents the optical depth at the Lyman limit.

Our method of discussion will be to set up the differential equation of transfer for each frequency element of the continuum. The equations of transfer will contain the terms in η representing the "interlocking" between the various elements of the continuous levels. It is in the introduction of η that our method differs from that of Ambarzumian,[4] who treated the continuum as a single level. Our equations will be similar to his in form, but we find it necessary to introduce for each ν the total optical depth at that frequency. The relation between the optical depth at a given frequency and the frequency at the Lyman limit is known. The geometrical thickness of the shell is, of course, constant.

Let us consider the radiation field to which an elementary volume of the nebula is exposed. First of all, there is the direct radiation from the star. If τ_ν is measured outward from the inner surface of the nebular shell, the incident stellar radiation at a given level will be $S_\nu e^{-\tau_\nu}$, where S_ν is the flux of direct stellar radiation incident upon the inner face of the nebula. The direct beam from the star is de-

[4] *M.N.*, **93**, 50, 1932; see also Chandrasekhar, *Zs. f. Ap.*, **9**, 266, 1935.

pleted in an exponential manner as it passes through the gaseous shell. We assume the geometrical portion of the dilution factor for the stellar radiation to be constant through the shell. Therefore, this part of the dilution factor cancels out of our equations and need not be considered. To take properly into account, in any given case, the variation of this geometrical factor, we should have to know the thickness and radius of the shell.

In the second place, we must consider the Lyman continuum radiation originating in the nebula itself. This energy has been absorbed from the direct beam and reradiated in the nebula in all directions. We denote the intensity of this diffuse radiation at frequency ν by J_ν. Our problem is to find J_ν as a function of both optical depth and frequency. The number of transitions from the first state to the element $d\kappa$ of the continuum corresponding to the frequency ν will be determined by the number of atoms in the ground level, the absorption coefficient for a frequency ν, and the total intensity of the diffuse and direct radiation of frequency ν. Thus,

$$F_{1\kappa} h\nu d\nu = N_1 a_\nu [J_\nu + S_\nu e^{-\tau_\nu}] d\nu \,. \tag{16}$$

We substitute equation (16) into equation (13), multiply by $2\pi \sin\theta d\theta$, integrate to obtain the differential equation for the total ν-flux, F'_ν, and obtain

$$\frac{dF'_\nu}{dx} = -[1 - p_\nu] N_1 a_\nu [J_\nu + S_\nu e^{-\tau_\nu}] + p_\nu \eta h\nu \,. \tag{17}$$

For the direct beam from the star, the flux and intensity are both given by $S_\nu e^{-\tau_\nu}$. The radiation absorbed and re-emitted in the Lyman continuum in the nebula, i.e., the diffuse flux, is to be found by integrating the equation of transfer. Let

$$F'_\nu = F_\nu + F^*_\nu \,, \tag{18}$$

where $F^*_\nu = S_\nu e^{-\tau_\nu}$ and F_ν is the diffuse flux. The equation for the latter is, therefore,

$$\frac{dF_\nu}{dx} = -J_\nu N_1 a_\nu + p_\nu N_1 a_\nu [J_\nu + S_\nu e^{-\tau_\nu}] + p_\nu \eta h\nu \,. \tag{19}$$

By introducing the definition of the optical depth, we get:

$$\frac{dF_\nu}{d\tau_\nu} = -J_\nu + p_\nu[J_\nu + S_\nu e^{-\tau_\nu}] + R_\nu , \tag{20}$$

where

$$R_\nu = \frac{p_\nu \eta h\nu}{N_1 a_\nu} . \tag{21}$$

The expression for R_ν is obtained with the aid of equations (12), I (23), (14), and (4) and V (2). It is:

$$R_\nu = \frac{e^{X_1} 8\pi h\nu^3 e^{-h\nu/kT_e}}{c^2 G_{T_e}} \int_{y_1}^{\infty} W_{1\kappa} \frac{dy}{y(e^y - 1)} - p_\nu W_{1\kappa} \frac{8\pi h\nu^3}{c^2} \frac{1}{e^y - 1} , \tag{22}$$

where $y = h\nu/kT_1$. To solve equation (20) we use the relation between F_ν and J_ν given by the Eddington approximation, namely:

$$F_\nu = -\frac{1}{3} \frac{\partial J_\nu}{\partial \tau_\nu} , \tag{23}$$

and our differential equation becomes

$$\frac{d^2 J_\nu}{d\tau_\nu^2} = 3(1 - p_\nu) J_\nu - 3p_\nu S_\nu e^{-\tau_\nu} - 3R_\nu . \tag{24}$$

To simplify matters we find it convenient to recast the equations in units of S_ν, the direct radiation from the star upon the inner surface of the nebular shell. Let $\mathfrak{J}_\nu$ denote the diffuse intensity and $\mathfrak{R}_\nu$ the interlocking term. With this new unit we obtain

$$\frac{d^2 \mathfrak{J}_\nu}{d\tau_\nu^2} = \lambda_\nu^2 \mathfrak{J}_\nu - 3p_\nu e^{-\tau_\nu} - 3\mathfrak{R}_\nu , \tag{25}$$

where

$$\lambda_\nu^2 = 3(1 - p_\nu) . \tag{26}$$

We also get from equation (22)

$$\mathfrak{R}_\nu = \frac{(e^{h\nu/kT_1} - 1)}{G_{T_e}} e^{-h(\nu-\nu_1)/kT_e} \int_{y_1}^{\infty} (\mathfrak{J}_\nu + e^{-\tau_\nu}) \frac{dy}{y(e^y - 1)} - p_\nu(\mathfrak{J}_\nu + e^{-\tau_\nu}) . \tag{27}$$

Since W is the dilution factor for both diffuse flux and direct starlight, we have in the new units:

$$W_{1K} = \mathfrak{J}_\nu + e^{-\tau_\nu}.$$

Now $\mathfrak{J}_\nu$ is a function of both τ_ν and ν, and therefore we should properly use partial derivatives. From equations (25) and (27) we find

$$\frac{\partial^2 \mathfrak{J}_\nu}{\partial \tau_\nu^2} = 3\mathfrak{J}_\nu - \frac{3(e^{h\nu/kT_1} - 1)}{GT_e} e^{-h(\nu-\nu_1)/kT_e} \int_{y_1}^{\infty} (\mathfrak{J}_\nu + e^{-\tau_\nu}) \frac{dy}{y(e^y - 1)}. \quad (28)$$

We have still to indicate the dependence of the optical depth upon the frequency. If we neglect the g-factor, we obtain the result:

$$\frac{\tau_\nu}{\tau_{\nu_1}} = \left(\frac{\nu_1}{\nu}\right)^3 = \left(\frac{y_1}{y}\right)^3 \qquad \text{or} \qquad \tau_\nu = \left(\frac{y_1}{y}\right)^3 \tau_{\nu_1}. \quad (29)$$

The equation of transfer for any frequency ν, expressed in terms of the two independent variables τ_{ν_1} and ν, becomes:

$$\left.\begin{aligned} &\frac{\partial^2 \mathfrak{J}_\nu}{\partial \tau_{\nu_1}^2} \left(\frac{y}{y_1}\right)^6 \\ &\quad = 3\mathfrak{J}_\nu - \frac{3(e^y - 1)}{GT_e} e^{(y_1 - y)T_1/T_e} \int_{y_1}^{\infty} (\mathfrak{J}_\nu + e^{-\tau_\nu}) \frac{dy}{y(e^y - 1)}. \end{aligned}\right\} \quad (30)$$

There is no rigorous solution of this equation readily obtainable in terms of elementary functions. The boundary conditions for the problem have been given by Milne.[5] Since no diffuse radiation is created within the nebular shell, the net diffuse flux must vanish at the inner boundary of the shell. In other words, the inward and outward fluxes just balance. The total optical depth of the nebula at frequency ν is expressed by $\tau_{0\nu}$. For the outer boundary condition we make use of the approximate relationship

$$J_\nu = 2F_\nu. \quad (31)$$

This boundary condition has often been used in treating problems of radiation transfer in stellar atmospheres. In the case of plane-

[5] *Zs. f. Ap.*, 1, 98, 1930.

parallel layers of radiating material, this means that there is no appreciable back radiation.

The transfer problem for the free-free transitions is extremely simple. We note, in the equation of transfer VI (17),

$$\cos\theta \frac{dI_\nu}{dx} = -\frac{N_i N_e}{4\pi\sigma} \frac{KZ^4}{T_e^{3/2}} \frac{kT_e}{2hRZ^2} \bar{g} \{[1 - e^{-h\nu/kT_e}]I_\nu - 1\}, \quad (32)$$

that the first term contains I_ν and therefore contains the dilution factor $W_{\kappa\kappa'}$ for the radiation in question. This first term is, accordingly, very small compared with unity and may be neglected. The transfer equation then becomes

$$\cos\theta \frac{dI_\nu}{d\tau_\nu} = \frac{kT_e}{2hRZ^2} \frac{\bar{g}}{g} \frac{\int_{y_1}^{\infty} W_{1\kappa} \frac{dy}{y(e^y - 1)}}{G_{T_e}}, \quad (33)$$

where we have used equation V (2) to express b_1 in terms of the parameters of the electron temperature and the radiation field. The equation falls into this form because of our definition of the optical depth.

The integration of equation (33) can be carried through numerically as soon as the functional dependence of T_e and $W_{1\kappa}$ on optical depth is known from the solution of the equations for the Lyman continuum. The boundary conditions of the problem will be the same as for the diffuse Lyman flux.

In the next paper the solution of the foregoing equations of transfer will be carried out numerically for the case of a model nebula of total optical depth $\tau_{0\nu_1} = 3.0$, with a central star radiating as a black body at a temperature of 80,000°.

HARVARD COLLEGE OBSERVATORY
May 15, 1939

CONTRIBUTION TO THE EFFECTIVE STELLAR TEMPERATURE SCALE

ZDENĚK KOPAL

ABSTRACT

The effective temperatures of eclipsing binaries, divided into groups of similar spectra, have been studied on the basis of their mean parallaxes derived from their proper motions and radial velocities. The main result is that the effective temperatures of B- and A-type components of eclipsing binary systems are found to be about 10 per cent lower than those given by Kuiper's recent effective-temperature scale, based primarily on simple stars. The results for a few stars for which individual trigonometric parallaxes are available lead to similar conclusions.

The physical parameter known as the "effective temperature" is defined by

$$L = 4\pi acR^2T_{\text{eff}}^4 ,$$

where L is the luminosity and R the radius of a star with effective temperature T_{eff}, a is Stefan's constant, and c the velocity of light. Measures of effective temperatures thus depend upon the luminosities and radii of the respective stars and can be determined only if these values are ascertainable in absolute units. The only stars where the radii can be determined without recourse to the temperature—with the exception of the sun and a few supergiants whose disks are measurable with the interferometer—are the eclipsing binaries for which both the spectroscopic and the visual elements are known. But determinations of effective temperatures still involve a knowledge of the absolute brightness, and such systems can be used only when the absolute dimensions and the parallaxes are also known.

The first attempt to determine an effective temperature scale by use of the components of eclipsing binaries was made by S. Gaposchkin.[1] His scale agreed roughly with the ionization temperatures, but it has been criticized in several respects.[2] The largest uncertainty in his determinations arises from doubt regarding the values for the parallaxes. Most stars used by Gaposchkin were distant sys-

[1] *A.N.*, **248**, 213, 1933.

[2] Cf. Woolley, *M.N.*, **94**, 721, 1934; or Pilowski, *Zs. f. Ap.*, **11**, 267, 1936.

tems; for a large number the probable errors of the necessarily small parallaxes exceeded the numerical values of the parallaxes many times. The number of eclipsing systems with parallaxes that can be regarded as reliable is, unfortunately, very limited and scarcely permits a temperature scale to be based exclusively on them.

There is, however, another way in which the temperatures of eclipsing binaries may be derived. A determination of the individual parallaxes of such distant systems is no doubt difficult, but it is possible to obtain their mean parallaxes with the aid of their proper motions and radial velocities. Dividing the whole material into groups according to their spectral class, and averaging their apparent brightnesses, we can determine their absolute magnitudes; we can then combine these values with the average radii and obtain the temperatures for the mean spectral class of each group.

In the following tables the material available for the discussion has been assembled. The radial velocities are taken, without exception, from Moore's *Fourth Catalogue of Spectroscopic Binary Stars*.[3] The majority of the proper motions are those given by Boss; for a number of systems with well-determined dimensions and radial velocities, but not included in Boss's *General Catalogue*, the proper motions were compiled from other sources (reduced to the Boss system) or were derived by the writer using the sources for the positions given below.

Successive columns in Table 1 give the name; the number from Boss's *General Catalogue* (if lacking, the proper motion was determined by the writer or taken from another source); the proper motion in right ascension (in seconds); the proper motion in declination (in seconds of arc); their weight (if the probable errors in both co-ordinates are smaller than the absolute values of the respective proper motion, they are assigned weight 2; if the probable error of the proper motion in one co-ordinate exceeds 100 per cent, weight 1; stars with probable errors exceeding 100 per cent in both co-ordinates were omitted); and (the last column) the radial velocity of the center of mass of each system (in kilometers per second) taken from Moore's *Catalogue*.

Tables 2, 3, and 4 contain the material grouped according to

[3] *Lick Bull.*, No. 483, 1936.

TABLE 1

Star	No.	Proper Motion		Wt.	Rad. Vel.
		α	δ		
		sec			km/sec
AN And	32447	−0.0008	−0″.051	2	− 4.87
S Ant	13173	− .0056	+ .034	2	− 5.0
σ Aql	27185	− .0002	− .002	2	− 5.00
TT Aur	.....	− .0018	+ .011	2	+10.2
WW Aur	8474	− .0017	− .021	2	− 5.8
AR Aur	6476	+ .0013	− .033	2	+25.1
β Aur	7543	− .0048	− .004	2	−18.1
R CMa	9758	+ .0110	− .132	2	−39.70
RS CVn	Palmér*	− .0041	− .000	1	− 8.9
RZ Cas	3345	+ .0008	+ .037	2	−38.32
TV Cas	.....	− .0110	+ .026	2	+ 0.54
YZ Cas	891	− .0044	− .022	2	+ 9.97
AR Cas	32683	+ .0023	+ .007	2	−14.78
U Cep	1202	+ .0116	+ .002	1	− 6.0
AH Cep	31826	+ .0002	+ .005	1	−20.6
U CrB	20574	− .0024	− .016	2	− 7.65
Y Cyg	20114	+ .0016	− .008	1	−51.8
GO Cyg	.....	− .0014	− .064	1	+ 3.2
MR Cyg	.....	+ .0018	− .047	1	−26.0
Z Her	24450	− .0018	+ .070	2	−46.5
RX Her	25274	− .0005	+ .009	1	−24.9
TX Her	Palmér*	− .0013	− .019	2	− 6.4
u Her	23359	− .0010	− .010	2	−21.16
AR Lac	30985	− .0028	+ .031	2	−36.25
CM Lac	.....	− .0052	+ .002	1	−17.5
δ Lib	20195	− .0044	− .012	2	−35.38
RR Lyn	8281	− .0023	+ .019	2	−13.74
β Lyr	25847	+ .0001	− .007	2	−19.02
U Oph	23317	− .0001	− .020	1	−11.5
VV Ori	6884	− .0003	− .002	1	+20.77
AG Per	4943	− .0013	− .006	2	+15.84
β Per	3733	− .0005	+ .001	1	+16.30
U Sge	26639	− .0012	− .001	1	−15.1
X Tri	.....	− .0076	+ .067	1	0.0
TX UMa	14783	+ .0015	− .002	1	−11.2
W UMi	.....	− .0023	− .091	1	− 7.7
AG Vir	.....	− .0018	− .040	1	−16
Z Vul	26710	− .0013	− .009	2	−15.08
RS Vul	26611	+0.0007	+0.001	1	−22.04

* Frida Palmér, *Lund Medd.*, Ser. 2, No. 66, 1932. The sources for the positions used in determining the proper motions of the rest of the stars (not included by Boss) are:

Star	Source	No.	Ep.
TT Aur	*Astr. Cat. Helsingfors*, 2, Cl. 211	452	1893.2
	A.G. Lund	2538	1879.9
TV Cas	*A.G. Helsingfors*	205	1872.9
	Holmberg, *Lund Medd.*, Ser. 2, No. 98	1	1933.9
GO Cyg	*A.G. Lund*	9539	1885.1
	Holmberg, *Lund Medd.*, Ser. 2, No. 98	86	1933.7
MR Cyg	Argelander, *Oeltzen's Katalog*	23162	1842.4
	A.G. Bonn	16204	1876.2
CM Lac	*A.G. Bonn*	16233	1873.3
	Holmberg, *Lund Medd.*, Ser. 2, No. 98	94	1933.9
X Tri	*A.G. Cambridge*	1093	1878.0
	Holmberg, *Lund Medd.*, Ser. 2, No. 98	9	1933.9
W UMi	Schwerd, *Oeltzen's Katalog*	198	1826.5
	Second Radcliffe Catalogue	1609	1860.0
AG Vir	*A.G. Leipzig*	4463	1869.8
	Holmberg, *Lund Medd.*, Ser. 2, No. 98	67	1933.3

TABLE 2

Star	Sp.	Radius	Mag.	P.M.	Rad. Vel.
					km/sec
Y Cyg A.....	O9.5	5.9⊙	7^m5	0".021	51.8
Y Cyg B.....	O9.5	5.9	7.5	.021	51.8
AH Cep A.....	Bo	5.5	7.0	.006	20.6
AH Cep B.....	Bo	7.3	8.1	.006	20.6
VV Ori A.....	B2	7.5	5.5	.004	20.77
TT Aur A.....	B3	3.8	8.6	.025	10.2
TT Aur B.....	B3	3.5	9.6	.025	10.2
U CrB A.....	B3	3.0	7.8	.035	7.65
u Her A.....	B3	4.6	4.9	.016	21.16
AG Per A.....	B3	3.7	6.9	.017	15.84
AG Per B.....	B3	2.6	7.8	.017	15.84
Z Vul A.....	B3	4.2	7.2	.019	15.08
β Lyr A.....	B5	18	3.9	.007	19.02
U Oph A.....	B5	3.2	6.3	.020	11.5
U Oph B.....	B5	3.2	6.5	.020	11.5
σ Aql A.....	B8	3.4	5.6	.002	5.00
σ Aql B.....	B8	3.4	5.9	.002	5.00
β Per A.....	B8	4.1	2.2	.006	16.30
RS Vul A.....	B8	4.3	7.1	.009	22.04
GO Cyg A.....	B9	2.0	8.4	.066	3.2
U Sge A.....	B9	3.4	6.6	.017	15.1
TX UMa A.....	B9	3.8	7.1	0.018	11.2

TABLE 3

Star	Sp.	Radius	Mag.	P.M.	Rad. Vel.
					km/sec
AR Aur A.....	Ao	1.9⊙	6^m5	0".030	25.1
AR Aur B.....	Ao	2.0	6.6	.034	25.1
β Aur A.....	Ao	2.8	2.8	.048	18.1
β Aur B.....	Ao	2.8	2.8	.048	18.1
TV Cas A.....	Ao	2.5	7.5	.092	0.54
U Cep A.....	Ao	2.5	7.1	.035	6.0
GO Cyg B.....	Ao	1.3	10.0	.066	3.2
MR Cyg A.....	Ao	1.0	8.7	.050	26.0
RX Her A.....	Ao	2.0	7.9	.012	24.9
RX Her B.....	Ao	1.8	8.0	.012	24.9
δ Lib A.....	Ao	3.4	4.9	.048	35.38
W UMi A.....	Ao	3.6	8.7	.091	3.6
AG Vir A.....	Ao	1.3	8.7	.048	16
RZ Cas A.....	A2	1.6	6.4	.039	38.32
TX Her A.....	A2	1.6	8.8	.024	6.4
TX Her B.....	A2	1.6	9.4	.024	6.4
CM Lac A.....	A2	1.3	8.3	.037	17.5
YZ Cas A.....	A3	3.1	5.8	.029	9.97
X Tri A.....	A3	2.0	8.9	0.125	0.0

spectral class. Tables 2 includes the B stars; Table 3, A0–A4; Table 4, A5–F5. Successive columns in Tables 2–4 give the designation (A and B referring to the primary, or more massive, and the secondary component, respectively); the spectrum; the radius in solar units (for ellipsoidal components, the geometric mean of the semimajor axes); the apparent magnitude; the total proper motion defined by

$$\mu''^2 = \mu_\alpha''^2 \cos^2 \delta + \mu_\delta''^2 ;$$

and the radial velocity, both values regardless of sign.

TABLE 4

Star	Sp.	Radius	Mag.	P.M.	Rad. Vel.
					km/sec
RR Lyn A	A6	2.4⊙	$6^m.5$	0".048	13.74
AN And A	A7	3.3	6.3	.052	4.87
WW Aur A	A7	2.3	6.2	.031	5.8
WW Aur B	A7	2.0	6.6	.031	5.8
S Ant A	A8	1.3	6.9	.082	5.00
S Ant B	A8	1.0	7.5	.082	5.00
R CMa A	A9	0.7	5.5	.203	39.7
RS CVn A	F4	1.6	8.1	0.037	8.9

The mean parallaxes are given by the well-known formula

$$\pi = 3.016 \frac{\bar{\mu}''}{\overline{RV}} .$$

Its validity requires that the peculiar tangential velocities and the radial velocities possess a Maxwellian distribution. Whether this is or is not the case has not yet been the subject of any specific discussion. But Wallenquist,[4] analyzing the radial velocities of spectroscopic and eclipsing binaries, found that they yield nearly the same value for the solar apex and space velocity as other stars of the same spectral type and that the axes of their velocity ellipsoid coincided nearly with those found for stars in general. Hence, the Maxwellian distribution of their peculiar velocities is very probable.

[4] *Lembang Ann.*, **4**, 1, 1929.

When the mean parallaxes have been determined, the mean absolute magnitudes follow from

$$M = m + 5 + 5 \log \pi .$$

If we adopt $+4.73$ as the absolute magnitude[5] of the sun and use the mean radii, the surface brightnesses can be determined in solar units; the surface temperatures T_0 follow from

$$\frac{J_*}{J_\odot} = \frac{e^{c_2/\lambda T_\odot} - 1}{e^{c_2/\lambda T_*} - 1} ,$$

and

$$T_{\text{eff}}^4 = 2T_0^4 .$$

This procedure avoids any recourse to the bolometric corrections. If we take $c_2 = 1.432$ cm grad, $\lambda_{\text{vis}} = 5290$ A, and $T_{\text{eff}\odot} = 5713^\circ$ (Unsöld),[6] we arrive at the effective temperatures given in the last row of Table 5.

TABLE 5

	Group		
	I	II	III
Spectral range	B0–B9	A0–A4	A5–F5
Number of stars	23	19	8
Mean spectrum	B4±3	A1±1	A8±1
Mean apparent visual magnitude	6.1±1.3	7.2±1.5	6.0±0.9
Mean μ''	0″.0156	0″.0467	0″.064
Mean $\lvert RV \rvert$	17.3 km/sec	16.1 km/sec	10.0 km/sec
Mean π	0″.0029	0″.0087	0″.019
Mean absolute visual magnitude	−1.6	+1.9	+2.4
Mean radius	4.9⊙	2.1⊙	2.0⊙
Mean effective temperature	14,600°	8800°	8000°

A glance at these values shows that they are systematically lower than those given by Kuiper's recent effective-temperature scale,[7]

[5] Kuiper, *Ap. J.*, **88**, 438, 1938.

[6] *Physik der Sternatmosphären*, pp. 37 and 53, Berlin, 1938.

[7] Kuiper, *op. cit.*, p. 446.

based mainly upon the properties of simple stars; this may be illustrated by the following comparison:

Sp.	T_{eff} Eclipsing	T_{eff} Kuiper
B4	14,600	17,000
A1	8,800	10,200
A8	8,000	8,200

Thus, the defect of the eclipsing-binary temperature scale with respect to Kuiper's scale amounts to about 10 per cent—with the exception of the A8 group, which is based on the smallest number of stars and for which the better agreement may be accidental.

Before entering into a discussion of the possible significance of this result, let us examine what can be inferred from the individual parallaxes. For the four following early-type stars the parallaxes appear to be reliably known:

Star	π	Source
β Aur	$0''.037 \pm 0''.004$	*Yale Catalogue of Parallaxes*, 1935, No. 1889
VV Ori	.0051	Kapteyn, *Ap. J.*, **47**, 176
β Per	$.031 \pm 0.004$	*Yale Catalogue*, No. 918
μ^1 Sco	0.0074	Kapteyn, *Ap. J.*, **40**, 43

The parallaxes of β Aurigae and β Persei are trigonometric; those of VV Orionis and μ^1 Scorpii are group parallaxes. Following exactly the same procedure as above, we obtain:

Star	Sp.	$m$vis	Mvis	R	Teff	Source of Visual Elements
β Aur A	A0	2.8	−0.7	$2.8\odot$	10,000°	Stebbins, *Ap. J.*, **33**, 395
β Aur B	A0	2.8	0.7	2.8	10,000	
VV Ori A	B2	5.5	1.0	7.5	9,200	Schneller, *Kl. Veröff. B.B.*, No. 17
β Per A	B8	2.2	0.4	4.1	11,000	Danjon, *Strasb. Ann.*, **2**, 163
μ^1 Sco A	B3	3.8	2.0	5.3	16,000	Rudnick and Elvey, *Ap. J.*, **87**, 556
μ^1 Sco B	[B6]	4.1	−1.7	5.9	13,000	

The radius of the primary component of Algol is not yet known with sufficient accuracy, and the radius of VV Orionis seems to be exceptionally large; but one sees at once that, on the average, the tem-

peratures are sensibly lower than Kuiper's values. A rough mean of the B stars would appear to indicate B6 $\pm$ 3, $T_{\text{eff}} = 12,300°$—in qualitative agreement with the preceding results based on statistical parallaxes.

The aim of this paper has been to present the facts as they stand and not to attempt any specific discussion regarding their significance. Whether the effective temperatures of close binaries as a class (i.e., rapidly rotating stars) are lower than those of simple stars, whether the discrepancies point to departures from black-body radiation or whether Kuiper's scale for high-temperature stars needs further correction is hard to say. It is likely that for the early-type stars the effective temperature will not be a single-valued function of their spectral class, and the scatter of individual values may be such that the establishment of any effective-temperature scale will be very difficult. It is also possible that the temperature defect we found for distant B-type stars may be interpreted as an indication of the existence of nonselective interstellar absorption. A detailed discussion of the individual alternatives would exceed too widely the scope of the present paper.

HARVARD COLLEGE OBSERVATORY
CAMBRIDGE, MASSACHUSETTS
February 1939

S SAGITTAE

ARTHUR L. BENNETT

ABSTRACT

S Sagittae was observed from April 24 to November 14, 1938, with the infrared photometer on the Loomis telescope. Energy of effective wave length near λ 8000 was used. The range of variation is c^m459, the second maximum is very nearly equal to the first, and minimum occurs 2.35 days before maximum.

S Sagittae (BS 7609), a typical Cepheid of period 8^d4, spectrum[1] F8–G7, was observed from April 24 to November 14, 1938, with the infrared photoelectric photometer on the Loomis telescope. This star and RT Aurigae (to be published later) were put on the observing program at the request of Dr. Martin Schwarzschild, who is investigating the theory of Cepheid variation.[2] S Sagittae is of particular interest because of the pronounced "hump" shortly following the maximum which gives the light-curve the appearance of a double maximum. The advantage of the infrared spectral region is the greater certainty of the reduction to bolometric magnitude.

The phases were computed with Luizet's elements[3] as modified by Hellerich,[4] who found that the epoch should be corrected by -0^d5, as follows:

$$\text{Max} = \text{J.D. } 240{,}9862.82 + 8^d38209E\,.$$

Heliocentric Greenwich astronomical time is used.

The photometer, which is sensitive from λ 3000 to λ 11,000, was used with a Wratten No. 25 filter, which absorbs all the light of $\lambda < 5400$ and transmits uniformly for $\lambda > 6600$. From measures made with an objective grating very kindly lent by Dr. John S. Hall in 1935, the following effective wave lengths for this combination were derived: α Lyrae, λ 7580; α Boötis, λ 8080; α Tauri, λ 8080.

[1] ten Bruggencate, *Die veränderlichen Sterne*, p. 31, 1931. The spectral type is derived from the gradient.

[2] *Harvard Circ.*, No. 431, 1938.

[3] *A.N.*, **168**, 341, 1905.

[4] *A.N.*, **264**, 249, 1937; *Mitt. Hamburg*, **7**, 258, 1938.

It was impossible to find a single comparison star of both spectrum and magnitude near the median of the variable. Two stars were therefore chosen approximately at the limits of the range in magnitude and spectrum:

$$a = \text{BS } 7672\,, \qquad m_v = 5.89\,, \qquad \text{G}_1 \text{ (Mt. W.)}\,;$$

$$b = \text{BS } 7463\,, \qquad m_v = 5.67\,, \qquad \text{G8 (Mt. W.)}\,.$$

A set consisted of eight readings on the variable and a total of eight on the comparison stars, in this order: $2a$, $4v$, $4b$, $4v$, $2a$. Each pointing was followed by half as many readings on the sky. Since a reading is taken every 30 seconds and about one minute is required for the shift from one star to the next, a set was observed in 16–18 minutes.

The readings for each star, corrected for sky, were reduced to apparent magnitude with the same arbitrary zero point. The mean magnitude of the comparison stars was then subtracted from that of the variable; this difference is Δm.

For the derivation of the extinction, a considerable number of sets were taken at large hour-angles. Mean coefficients were derived for each estimated value of the transparency;[5] T10 and T9, $0^m.096$; T8, $0^m.156$; T7, $0^m.212$; T6, $0^m.280$. Intermediate steps were used. The function of the hour-angle of the variable, $\sec z_v - (\sec z_a + \sec z_b)/2$, was derived for each observation. The product of this function and the extinction coefficient subtracted from Δm gave Δm_1, the magnitude difference at the zenith. The difference in the coefficients of the comparison stars has been neglected, as well as the change of the variable's coefficient with phase.

The individual observations are given in Table 1. Seven sets in which the effect of clouds or smoke was obvious have been rejected. A free-hand light-curve was drawn, and residuals read off. Weights derived from the average residuals for transparency 9, 8, and 7 are 1.0, 0.6, and 0.4, respectively. For T9 the weights are 1.0, 0.5, and 0.4 for hour-angles less than 3^h, 3^h to 4^h, and greater than 4^h. The observations at J.D. 9014.840, 9022.800, 9022.820, 9022.844,

[5] T10 represents a perfect night; T5 extreme haziness.

TABLE 1

J.D. Hel. G.A.T.	Phase	Δm_1	p	T	J.D. Hel. G.A.T.	Phase	Δm_1	p	T
9012.812	2284.632	+.056	0.3	8	9151.741	2301.207	−.316	0.0	8
.840	.636	+.063	0.6		.755	.209	−.323	0.0	
.859	.638	+.062	0.6		9153.581	.426	−.149	0.6	8
9013.844	.755	+.103	0.6	8	.595	.428	−.152	0.6	
9014.840	.874	−.092	0.2	7	.608	.430	−.150	0.6	
9022.800	2285.824	+.021	0.4	8	9155.606	.668	+.083	0.4	7
.820	.826	+.011	0.4		.625	.670	+.085	0.4	
.836	.828	−.002	0.4		.638	.672	+.088	0.4	
.844	.829	−.007	0.2		9158.608	2302.026	−.346	0.4	7
9029.752	2286.653	+.071	0.3	8	.623	.028	−.353	0.4	
.764	.655	+.089	0.3		9165.617	.862	−.068	0.6	8
.836	.663	+.082	0.6		9166.690	.990	−.344	0.5	9
.848	.665	+.084	0.6		.704	.992	−.343	0.4	
9032.780	2287.015	−.353	1.0	9	.717	.994	−.347	0.4	
.796	.016	−.350	1.0		9167.575	2303.096	−.309	1.0	9
.815	.019	−.357	1.0		.588	.097	−.305	1.0	
9035.804	.375	−.162	0.6	8	.605	.099	−.301	0.6	
.819	.377	−.177	0.6		.618	.101	−.307	1.0	
.832	.379	−.170	0.6		9168.574	.215	−.340	0.4	7
.844	.380	−.179	0.6		.591	.217	−.337	0.4	
9049.769	2289.041	−.352	0.6	8	9170.587	.455	−.137	0.4	6
.783	.043	−.345	0.6		.622	.459	−.137	0.4	
.795	.044	−.338	0.6		9173.572	.811	+.033	0.6	8
.810	.046	−.345	0.6		.615	.816	+.030	0.6	
9050.788	.163	−.294	0.4	7	9174.564	.930	−.211	0.6	8
.800	.164	−.284	0.4		.596	.934	−.218	0.6	
.813	.166	−.286	0.4		9176.563	2304.168	−.300	0.5	<8
9059.748	2290.232	−.349	0.4	7	.578	.170	−.293	0.5	
.774	.235	−.341	0.4		.630	.176	−.308	0.4	
.803	.238	−.346	0.4		.645	.178	−.301	0.4	
9079.731	2292.616	+.038	0.5	>7	9179.586	.529	−.067	1.0	9
.744	.617	+.030	0.5		.601	.531	−.058	1.0	
.757	.619	+.038	0.5		.657	.537	−.060	0.4	
9083.706	2293.090	−.310	0.6	8	.671	.539	−.064	0.4	
.723	.092	−.310	0.6		9181.543	.762	+.095	0.5	<8
.737	.094	−.304	0.6		.559	.764	+.088	0.5	
.828	.105	−.290	0.6		.622	.772	+.089	0.4	
839	.106	−.309	0.6		.638	.774	+.084	0.4	
9086.804	.460	−.122	0.4	7	9182.555	.883	−.107	1.0	9
.815	.461	−.134	0.4		.569	.885	−.117	1.0	
9090.630	.916	−.172	0.4	7	.587	.887	−.117	1.0	
.642	.918	−.194	0.4		.642	.893	−.120	0.5	
.654	.919	−.181	0.4		.655	.895	−.124	0.4	
9095.734	2294.525	−.069	0.4	7	9188.592	2305.603	+.021	0.4	7
.749	.527	−.071	0.4		.608	.605	+.019	0.4	
.763	.529	−.049	0.4		.620	.607	+.009	0.4	
9146.608	2300.594	+.020	0.4	7	9189.529	.715	+.113	0.4	6
.628	.597	+.029	0.4		.545	.717	+.098	0.4	
9151.589	2301.189	−.302	0.6	8	.606	.724	+.108	0.0	
.607	.191	−.321	0.6		.621	.726	+.093	0.0	
.621	.193	−.320	0.6		9190.609	.844	−.029	0.4	6

TABLE 1—*Continued*

J.D. Hel. G.A.T.	Phase	Δm_1	p	T	J.D. Hel. G.A.T.	Phase	Δm_1	p	T
9190.626	2305.846	−.026	0.4	6	9203.501	2307.382	−.180	0.5	<8
9194.560	2306.315	−.256	0.2	6	.541	.387	−.154	0.2	7
9197.483	.664	+.095	0.6	8	.554	.388	−.161	0.2	
.495	.665	+.086	0.6		.575	.391	−.171	0.2	
.513	.668	+.084	0.6		9204.514	.503	−.096	0.5	<8
9198.493	.784	+.081	0.4	7	9212.494	2308.455	−.138	1.0	9
.505	.786	+.067	0.4		.509	.457	−.141	1.0	
.556	.792	+.061	0.4		.525	.459	−.141	0.5	
.568	.793	+.060	0.4		.584	.466	−.116	0.4	
9202.505	2307.263	−.354	0.6	8	.598	.467	−.119	0.4	
.521	.265	−.340	0.6		9213.462	.570	−.008	0.4	8
.535	.267	−.333	0.6		.477	.572	−.016	0.6	
.549	.268	−.353	0.6		9217.491	2309.051	−.343	1.0	9
.562	.270	−.351	0.3		.506	.053	−.341	1.0	
.574	.271	−.350	0.3		.522	.055	−.332	0.5	
.589	.273	−.333	0.3		.547	.058	−.343	0.5	
9203.489	.380	−.178	0.5	<8	.589	.063	−.323	0.4	

TABLE 2

WEIGHTED NIGHT MEANS

$\overline{\text{Phase}}$	$\overline{\Delta m_1}$	Σp	$\overline{\text{Phase}}$	$\overline{\Delta m_1}$	Σp	$\overline{\text{Phase}}$	$\overline{\Delta m_1}$	Σp
2287.017	−.353	3.0	2301.428	−.150	1.8	2305.716	+.106	0.8
2302.027	−.350	0.8	2303.457	−.137	0.8	2284.755	+.103	0.6
2289.044	−.345	2.4	2308.459	−.134	3.3	2304.767	+.089	1.8
2309.054	−.338	3.4	2293.460	−.128	0.8	2306.789	+.067	1.6
2293.097	−.305	3.0	2307.503	−.096	0.5	2303.814	+.032	1.2
2303.098	−.306	3.6	2294.527	−.063	1.2	2285.826	+.008	1.4
2289.164	−.288	1.2	2304.532	−.062	2.8	2305.845	−.028	0.8
2304.173	−.301	1.8	2308.571	−.013	1.0	2302.862	−.068	0.6
2301.191	−.314	1.8	2300.596	+.024	0.8	2284.874	−.092	0.2
2303.216	−.338	0.8	2305.605	+.016	1.2	2304.887	−.116	3.9
2290.235	−.345	1.2	2392.617	+.035	1.5	2293.918	−.182	1.2
2307.267	−.345	3.3	2284.636	+.061	1.5	2303.932	−.214	1.2
2306.315	−.256	0.2	2286.661	+.082	1.8	2302.992	−.345	1.3
2287.378	−.172	2.4	2306.666	+.088	1.8			
2307.384	−.173	1.6	2301.670	+.085	1.2			

9167.605 and 9194.560 contain only half the usual number of readings and received weight 0.6. The combined weights are given. The probable error of an observation of unit weight, if eleven unknowns are assumed, is $0^m.0030$.

In Table 2 are given the weighted means for each night; these values are plotted in Figure 1. The range of variation is $0^m.459$, much less than the photographic range of $1^m.39$ found by Hertzsprung[6] with

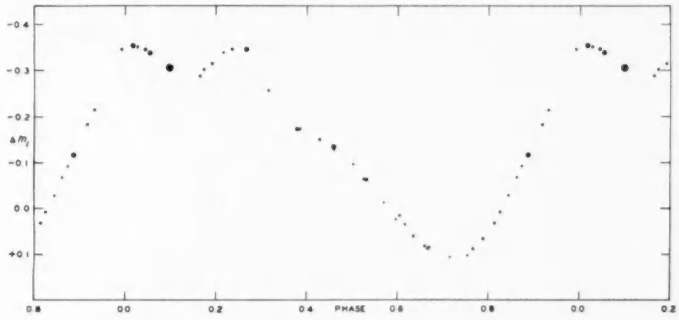

FIG. 1.—S Sagittae. Infrared photoelectric observations. The weight of each night's observations is indicated by the size of the dot.

the U–V triplet at Potsdam. Aside from the range, the features of the light-curve are similar to the photographic one, except that in my light-curve the second maximum is very nearly equal to the primary one. The phase of the second maximum is very nearly the same, but minimum occurs somewhat later, at phase 0.720, i.e., $M - m = 2^d.35$.

YALE OBSERVATORY
May 1939

[6] *A.N.*, **205**, 281, 1917.

REMARKS ON LORETA'S HYPOTHESIS CONCERNING R CORONAE BOREALIS

JOHN A. O'KEEFE

ABSTRACT

It is shown that the shape of the light-curve of R Coronae Borealis and its spectral variations at minimum can be accounted for by supposing it to eject matter which condenses at a considerable distance and forms obscuring clouds. The solid matter is believed to be principally carbon. This hypothesis is shown to be consistent with physical principles.

The star R Coronae Borealis, typical member of a small group of irregular variables, presents a series of phenomena which are not explained by the usual theories of stellar variability. The observational data are summarized in the book *Variable Stars* by C. P. and S. Gaposchkin.[1] We may state the problem which confronts the astrophysicist as follows: The constancy of the spectral type at minimum, and some other features, suggests strongly some sort of obscuration. On the other hand, we cannot suppose that this obscuration is due to the obvious thing, namely, dark nebulae, because of the correlation of the R Coronae Borealis type of variation with spectral class. An escape from this dilemma was proposed by E. Loreta[2] in 1934. Loreta suggested that the obscuring clouds originated in the star itself. He pointed out that eruptions of luminous matter were well known and suggested that, by some process analogous to that in the novae, dark clouds of material were ejected. The writer reached similar conclusions independently. The present paper is an attempt to show that this hypothesis is not inconsistent with what is known about these stars.

Suppose that R Coronae ejects matter from its atmosphere, in somewhat the same way that the sun does, in the form of prominences of the eruptive type.[3] Such a prominence would be composed principally of carbon, because of the exceptionally large abundance

[1] Harvard Observatory Monographs, 1938.

[2] *A.N.*, **254**, 151, 1934.

[3] We may note, in support of this idea, that Berman found from his curve of growth a velocity of turbulence of 10 km/sec. (*Ap. J.*, **81**, 369, 1935).

of this element in R Coronae Borealis. As the cloud recedes, it cools, until the vapor pressure of the solid carbon is less than that of the gas, and graphite forms in small crystals. These, even in small quantities, produce an obscuration sufficient to block out the light of the star. Radiation pressure then drives them away, gradually dissipating the cloud.

In this way, the distinctive features of the typical R Coronae light-curve are accounted for. The sharp drop to minimum corresponds to the formation of solid carbon; the slow recovery, to the gradual dissipation of the cloud. The association of R Coronae Borealis stars with great abundance of carbon is indicated by this hypothesis, since only the comparatively rare element tungsten has as low a vapor pressure. The spectral peculiarities at minimum are likewise explained; the emission lines observed by Joy and Humason[4] are formed in the cloud which is expelled; their velocity of approach of 20 km/sec represents the velocity of the cloud. The absence of change of spectral type is quite intelligible, since, for the star as a whole, the eruption is unimportant.

We shall endeavor to show that these ideas do not involve any obvious contradiction with physical principles. In the first place, we note that in thermodynamic equilibrium, at a given temperature, the solid and the gaseous phases of a substance are in equilibrium at one and only one pressure—the vapor pressure. If the pressure falls below this, the solid will sublime; if it increases, the gas will condense. In order, therefore, to find whether or not carbon can condense, it is necessary to find the vapor pressure as a function of the temperature.[5]

The vapor pressure is calculated from the free energies. It is known that the condition for equilibrium among several substances is that their free energies per mole shall be equal. We calculate the free energies of the monatomic and the diatomic carbon gas by means of the equation

$$\frac{F}{T} = Nk \log_e Q - Nk \log_e N ,$$

[4] *Pub. A.S.P.*, **35**, 325, 1923.

[5] The liquid phase does not come into consideration for carbon, except at considerable pressures.

where N is the number of particles, T the temperature, F the free energy, k Boltzmann's constant, and Q the partition function per atom. The free energies of the gases involve the pressures through the translational part of the partition function. For a perfect gas we may write

$$\frac{F}{T} = \frac{F^0}{T} + R \log_e P ,$$

where F is now the free energy per mole, F^0 the standard free energy, or free energy per mole at one atmosphere, P the pressure, and R the gas constant. In the second and third columns of Table 1 we give the standard free energy for monatomic and diatomic carbon. That for the diatomic carbon is taken from a formula given by A. R. Gordon.[6] The values for the monatomic carbon were computed by the writer. For the dissociation energy of C_2, necessary for the free energy of the diatomic vapor, the value 90 kilocalories per mole was taken from G. Herzberg.[7] For the solid state, the free energies tabulated by J. O. Clayton and W. F. Giauque[8] were used, together with the value of -124 kilocalories per mole[9] for the free energy at absolute zero. The fourth column of the table gives the total free energy at one atmosphere for one mole of C.

It follows at once from the definition of the standard free energy that

$$F^0_{\text{solid}} - F^0_{\text{gas}} = RT \log_e P ,$$

where P is the vapor pressure. The free energies must be measured per mole for both solid and gas; hence, for the molal free energy of the solid, the value used in comparing with the diatomic vapor must be twice that used in comparing with the monatomic vapor. The pressures thus determined are given in the fifth column of Table 1.

We shall make use of these vapor pressures to test the hypothesis. First, we shall estimate the density of the gaseous carbon. Then we shall determine the temperature at which gas of this density would condense. If we should find that the required temperature is exceedingly low, so that it would only be reached at several hundred

[6] *J. Chem. Phys.*, **5**, 350, 1937.

[7] *J. Phys. Chem.*, **41**, 325, 1937.

[8] *J. Amer. Chem. Soc.*, **54**, 2623, 1932.

[9] Herzberg, *loc. cit.*

astronomical units from the star, we must consider this as strong evidence against the idea. If, however, we can show that condensation can take place within 20 radii of the star, we may conclude that the process is physically reasonable.

In order to estimate the density of the gas, we work backward from the density of the solid particles. The transition from gas to solid takes place so rapidly, in the pressure range with which we shall be concerned, that the intervening stage may be neglected. Thus, between 1800° and 1600° the vapor pressure falls by a factor of 80, which implies that if condensation had set in at 1800° it would be practically complete at 1600°. For lower temperatures the transi-

TABLE 1

VAPOR PRESSURE OF CARBON

Temperature	F_g^0/T for C (k cal mol^{-1} deg^{-1})	F_g^0/T for C_2 (k cal mol^{-1} deg^{-1})	F_g^0/T per Mole of C(k cal mol^{-1} deg^{-1})	log Vapor Pressure (Atmospheres)
1000° K	−38.82	−140.9	−126.8	−19.2
1200	39.72	127.3	106.7	14.6
1400	40.49	117.8	92.5	11.4
1600	41.15	110.8	82.0	8.9
1800	41.74	105.5	73.8	7.0
2000	−42.26	−101.3	− 67.4	− 5.5

tion is even more rapid. It is, therefore, unlikely that we shall make any serious error in equating the density of the gas immediately before condensation to the density of the solid matter immediately after, i.e., at the bottom of the minimum.

It is possible to compute, on quite general assumptions, the quantity of solid carbon per square centimeter of the star's surface. Greenstein[10] points out that for conducting particles whose circumference is less than half the wave length of light the absorption coefficient is proportional to the quantity of matter per cubic centimeter and is independent of the size of the individual particles. He gives the formula

$$k_\lambda = \frac{6\pi}{\lambda} F_\lambda ,$$

[10] *Harvard Circ.*, No. 422, 1937.

where λ is the wave length of the light, k_λ the absorption coefficient in square centimeters per cubic centimeter of the absorbing medium, and

$$F_\lambda = \frac{6a_\lambda b_\lambda}{(a_\lambda^2 - b_\lambda^2 + 2)^2 + (2a_\lambda b_\lambda)^2}.$$

Here a_λ is the refractive index n of the International Critical Tables, and b_λ is their nk. Now graphite, although not a metal, is a fair conductor of electricity. Taking the optical constants from the International Critical Tables, we find $k_{5500} = 7.46 \times 10^4$ square centimeters per cubic centimeter of graphite. For particles about 1 μ in diameter the absorption coefficient is only slightly less than this, or about 3×10^4. Since we do not know the exact proportion of large to small particles, we shall take a round figure of 5×10^4 cm^2/cm^3. Taking a density of 2.26 gm/cm^3 for graphite, we find that 3×10^{-4} grams of carbon per square centimeter of the star's surface will produce an absorption of 8 mag. This corresponds to 1.7×10^{19} atoms per cm^2, which may be compared with Berman's figure of 3×10^{21} atoms of C per cm^2 in the atmosphere. It is clear that no large portion of the atmospheric mass is required to account for the loss of light.

In order to pass from the density per square centimeter to the density per cubic centimeter of the cloud, we must have an estimate of its thickness. This we shall take to be of the order of the diameter of the star.[11] From Berman's value of -1.4 for the absolute magnitude, and 5300° for the effective temperature, we find, by the well-known relation[12]

$$\log R = \frac{5900}{T} - 0.20M_v - 0.02$$

the value 20 $R_\odot$ for the radius of R Coronae. Distributing the 3×10^{-4} grams per square centimeter along a column of twice this length, we find a density of about 10^{-16} gm/cm^3.

[11] It can be shown that the growth due to diffusion in the period of forty days or so before condensation takes place is negligible; hence this value is not too small.

[12] Russell, Dugan, and Stewart, *Astronomy*, **2**, 738, 1927.

We are now in a position to answer the question: "Will gaseous carbon at this very low density condense at a reasonable distance from the star?" From the gas equation we can determine P as a function of T for this density. From the vapor-pressure table we have another relation between P and T. Between these two, P and T can be evaluated. We find

$$P = 9 \times 10^{-13} \text{ atmospheres}$$
$$T = 1360^\circ .$$

These are the values at which condensation would be expected to set in in thermodynamic equilibrium. We now wish to know how far we must go from the star to reach a point where the temperature could reasonably take the value of 1360°. We find that, at 7.6 times the radius of the star, the black-sphere temperature will be 1360°.

The foregoing reasoning might be questioned on the ground that, although the solid carbon will probably take a temperature not far from the black-sphere temperature, the gas will almost certainly be hotter. Let us assume, for instance, a temperature 80 per cent of the effective temperature of the star, or 4200°. We shall show that this will cause the carbon to condense slightly more rapidly than otherwise.

The vapor pressure is that pressure at which the number of particles leaving the solid material per unit time is equal to the number striking and sticking. Now, it is known that in the case of carbon almost every atom which strikes, sticks.[13] A simple calculation shows that increasing the temperature to 4200° increases the number of collisions by a factor of 1.8. This could be balanced by a 10° rise in the temperature of the solid, which is negligible. A more serious question is whether or not the gas will condense with sufficient speed. This depends on two factors: first, the rate of formation of nuclei and, second, the rate of condensation upon nuclei already formed. It can easily be shown that the second process has sufficient speed. As to the first, there are reasons for supposing that most two-body collisions cannot produce a nucleus, because the colliding particles do not stick. Three-body collisions, which are more favorable,

[13] Herzberg, *loc. cit.*

are rarer by a factor of 2×10^{16}. If we suppose that all nuclei are formed by three-body collisions, we shall have one nucleus per atom in 4×10^{19} seconds. Since we require one nucleus for each particle—that is, one nucleus per 10^{13} atoms—if the particles are 1 μ in diameter, we shall have enough nuclei in 4×10^{6} seconds, or about forty days. If, however, the particles are 0.1 μ in diameter, the corresponding numbers are 10^{10} atoms and one hundred years.

We assume here that the light extinguished is either scattered or absorbed by a cloud lying between the earth and the star. If the cloud lies in some other direction, part of the light should be scattered toward the earth. This fraction will be small, since most of the extinction is by consumptive absorption; it is probably not larger than those small variations in the maximum brightness which Jacchia[14] considers established.

The author wishes to express his gratitude to Dr. Bryce L. Crawford, of the Department of Chemistry of Harvard University, for help in the calculation of the vapor pressures; to Dr. D. H. Menzel and Dr. C. P. Gaposchkin for advice and suggestions; and to Mr. Leon Campbell for the use of A.A.V.S.O. data.

YERKES OBSERVATORY
March 1939

[14] *Pub. Oss. Bologna*, **2**, 14, 1933.

OBSERVATIONS MADE WITH THE NEBULAR SPECTROGRAPH OF THE McDONALD OBSERVATORY. III*

OTTO STRUVE, C. T. ELVEY, AND W. LINKE

ABSTRACT

A series of thirty spectrograms in various parts of the sky reveal a number of new emission regions. Attention is called to the fact that [*O* II] 3727 is relatively strong in Monoceros and Canis Major and weak in Sagittarius, Scorpius, and other regions situated in the summer Milky Way. The large star clouds in Sagittarius and neighboring regions are relatively poor in emission.

The present series of observations is a continuation of those published in former issues of this *Journal*.[1] The new observations confirm our suspicion[2] that the ratio [*O* II]/ *Hα* is relatively large in Monoceros and Canis Major and small in Cygnus, Cepheus, Scorpius, and Sagittarius. This seems to hold for the large, faint emission regions. There are, of course, many strong and compact nebulae in all parts of the Milky Way in which this ratio is substantially the same. One of the most surprising results of the present series is the small number of emission regions in Sagittarius and the neighboring regions. The absence of O-type stars in the star clouds of Sagittarius (regions Nos. 66 and 67) may be a sufficient explanation. Some of these regions have a nebulous appearance on the photographs of the Ross *Atlas*, and there can be no doubt that strong emission lines would have been observed if the spectra of these nebulosities were similar to those in Cygnus and Cepheus. We are inclined, therefore, to believe that these nebulosities are of the reflection type and that they are, in effect, identical with the "galactic light" discovered by Elvey and Roach.[3]

No. 49.—NGC 2237. 1939 Feb. 7/8 Exp. 2^h30^m. Comparison mirror $\Delta\delta = +40°$. Slit eq. 40 mm. This large nebula was observed

* *Contributions from the McDonald Observatory, University of Texas*, No. 9.

[1] *Ap. J.*, **89**, 119, 1939; **89**, 517, 1939.

[2] *Ibid.*, 517, 1939.

[3] *Ap. J.*, **85**, 213, 1937.

TABLE 1

OBSERVATIONS MADE WITH THE NEBULAR SPECTROGRAPH

No.	Object	Guiding Star	Date	Identification	Result
49	NGC 2237	.....	1939, Feb. 7/8	Ross 35; 136 mm from right; 85 mm from bottom	Very strong emission
50	Milky Way	BD−15°1810	Feb. 8/9	Ross 37; 156 mm from right; 88 mm from bottom	Probably weak emission
51	Region outside of Milky Way	BD+17°1623	Feb. 9/10	.....	No emission
52	Milky Way	BD+6°1309	Feb. 10/11	Ross 35; 157 mm from right; 104 mm from bottom	Emission
53	Milky Way	γ Velorum	Feb. 10/11	.....	Emission
54	Milky Way	BD−3°1643	Feb. 11/12	Ross 36; 105 mm from right; 121 mm from bottom	No emission
55	Milky Way	BD+6°1351	Feb. 13/14	Ross 35; 175 mm from right; 107 mm from bottom	Strong emission
56	Nebulosity	BD−11°1760	Feb. 14/15	Ross 37; 75 mm from right; 157 mm from bottom	Very strong emission
57	Milky Way	BD−8°1734	Feb. 14/15	Ross 37; 80 mm from right; 134 mm from top	Emission
58	Region outside of Milky Way	BD−44°2920	Feb. 15/16	.....	Probably no emission
59	Milky Way	ζ Puppis	Feb. 15/16	.....	Probably no emission
60	Milky Way	BD−23°4553	Feb. 19/20	Ross 38; 137 mm from right; 161 mm from bottom	No emission
61	Milky Way	o^2 Can Maj	Mar. 11/12	Ross 38; 168 mm from right; 163 mm from bottom	No emission

TABLE 1—*Continued*

No.	Object	Guiding Star	Date	Identification	Result
62	Milky Way	η Can Maj	1939, Mar. 12/13	Ross 38; 95 mm from left; 77 mm from bottom	Emission
63	Milky Way	3 Puppis	Mar. 14/15	Ross 38; 27 mm from left; 80 mm from bottom	Probably weak emission
64	B 35	1 1939 Orionis	Mar. 15/16	Ross 33; 134 mm from left; 164 mm from bottom	Emission
65	I.C. 5592	ν Scorpii	Mar. 25/26	Ross 2; 141 mm from right; 19 mm from top	Probably no emission
66	Milky Way	44 Ophiuchi	Mar. 27/28	Ross 3; 120 mm from left; 109 mm from top	No emission
67	Milky Way	45 Ophiuchi	Mar. 28/29	Ross 3; 120 mm from left; 137 mm from bottom	No emission
68	Milky Way	BD$-41°10972$	Apr. 15/16	Ross 1; 132 mm from right; 51 mm from bottom	Weak emission
69	Milky Way	BD$-32°12935$	Apr. 17/18	Ross 1; 72 mm from left; 144 mm from top	Strong emission
70	Milky Way	BD$-37°11206$	Apr. 19/20	Ross 1; 166 mm from right; 114 mm from bottom	Weak emission
71	Milky Way	μ Scorpii	Apr. 20/21	Ross 1; 130 mm from right; 110 mm from bottom	No emission
72	Cluster h3651	.....	Apr. 21/22	Ross 1; 144 mm from right; 72 mm from bottom	Emission
73	Milky Way	μ Normae	Apr. 22/23	Ross 1; 81 mm from right; 14 mm from bottom	Probably no emission
74	Cluster Dunlap 568	.....	Apr. 24/25	Ross 1; 13 mm from left; 150 mm from bottom	Probably no emission
75	Milky Way	N Scorpii	Apr. 25/26	Ross 1; 61 mm from right; 158 mm from bottom	No emission

TABLE 1—*Continued*

No.	Object	Guiding Star	Date	Identification	Result
76...	Milky Way	χ Lupi	1939, May 11/12	Ross 2; 75 mm from right; 82 mm from bottom	Probably no emission
77...	Milky Way	15 Sagittarii	May 15/16	Ross 4; 139 mm from left; 46 mm from top	Emission
78...	Milky Way	44 Cygni	May 21/22	Ross 17; 140 mm from right; 122 mm from bottom	Emission

by Hubble[4] and our observation agrees with his in showing strong emission lines of $H\alpha$, $H\beta$, $H\gamma$, $H\delta$, $N_1 + N_2$, and [*O* II] 3727.

No. 50.—Guiding star BD −15°1810. 1939 Feb. 8/9. Exp. 3^h. Comparison mirror $\Delta\delta = +40°$. Slit eq. 40 mm. This region is east of Sirius. There seems to be a faint trace of [*O* II] 3727, but no indication of $H\alpha$.

No. 51.—Guiding star BD +17°1623 = HD 60848, Sp. O8e. 1939 Feb. 9/10. Exp. 3^h17^m. Comparison mirror $\Delta\delta = +40°$. Slit eq. 40 mm. This region is well outside the Milky Way, the galactic latitude being +18°. There is no emission.

No. 52.—Guiding star BD +6°1309 = HD 47129, Sp. O8e. 1939 Feb. 10/11. Exp. 2^h45^m. Comparison mirror $\Delta\delta = +40°$. Slit eq. 40 mm. This region lies between NGC 2237 and S Monocerotis. $H\alpha$ and [*O* II] 3727 are conspicuous in emission.

No. 53.—Guiding star γ Velorum = HD 68273, Sp. O6w. 1939 Feb. 10/11. Exp. 2^h55^m. Comparison mirror $\Delta\delta = +90°$. Slit eq. 40 mm. This region was so close to the horizon that many night-sky lines appear stronger than in the comparison spectrum. However, making due allowance for this atmospheric effect, $H\alpha$ seems to be in emission. There is no emission at [*O* II] 3727.

No. 54.—Guiding star BD −3°1643 = HD 50891, Sp. O9. 1939 Feb. 11/12. Exp. 3^h. Comparison mirror $\Delta\delta = +40°$. Slit eq. 40 mm. The plate is weak. There is no emission.

No. 55.—Guiding star BD +6°1351 = HD 48099, Sp. O6. 1939

[4] *Ap. J.*, **56**, 176, 1922.

Feb. 13/14. Exp. 3^h. Comparison mirror $\Delta\delta = +40°$. Slit eq. 40 mm. This region is south of S Monocerotis. [*O* II] 3727 is very strong, especially near the eastern end of the slit; *Hα* is strong; *Hβ* and $N_1 + N_2$ are both weak and approximately equal.

No. 56.—Guiding star BD$-11°1760$ = HD 53179, Sp. O9e. 1939 Feb. 14/15. Exp. 3^h. Comparison mirror $\Delta\delta = +40°$. Slit eq. 40 mm. This region is involved in the nebulosity the strongest part of which is designated as IC 2177. It is southwest of region No. 45. [*O* II] 3727 and *Hα* are very strong, especially near the guiding star. The intensity of the lines decreases toward both ends of the slit. *Hβ* and $N_1 + N_2$ are very weak and approximately equal.

No. 57.—Guiding star BD$-8°1734$ = HD 53667, Sp. O8. 1939 Feb. 14/15. Exp. 3^h. Comparison mirror $\Delta\delta = 40°$. Slit eq. 40 mm. This region is north of No. 45, well outside of the conspicuous nebulosity IC 2177. *Hα* and [*O* II] 3727 are in emission, fading somewhat toward the eastern end of the slit.

No. 58.—Guiding star $-44°2920$ = HD 49798, Sp. O5. 1939 Feb. 15/16. Exp. 3^h. Comparison mirror $\Delta\delta = +5°$. Slit eq. 40 mm. This region is outside the Milky Way. There is a slight strengthening of the spectrum near *Hα*, but this may be caused by night-sky lines near the horizon. There is certainly no trace of [*O* II] 3727.

No. 59.—Guiding star ζ Puppis = HD 66811, Sp. O5. 1939 Feb. 15/16. Exp. 3^h. Comparison mirror $\Delta\delta = +40°$. Slit eq. 40 mm. There is a marked strengthening of the spectrum at *Hα*, but this may be caused by night-sky lines near the horizon. There is no trace of [*O* II] 3727.

No. 60.—Guiding star $-23°4553$ = HD 50896, Sp. WI. 1939 Feb. 19/20. Exp. 3^h. Comparison mirror $\Delta\delta = +40°$. Slit eq. 40 mm. This region is in a group of bright Milky Way stars, south of Sirius. The plate is weak, but there is no indication of emission except in the spectrum of the guiding star.

No. 61.—Guiding star o^2 Canis Majoris. 1939 Mar. 11/12. Exp. 3^h. Comparison mirror $\Delta\delta = +40°$. Slit eq. 40 mm. East of region No. 60. No emission.

No. 62.—Guiding star η Canis Majoris. 1939 Mar. 12/13. Exp. 2^h5^m. Comparison mirror $\Delta\delta = +40°$. Slit eq. 40 mm. [*O* II] 3727 is strong, but *Hα* is weak in emission.

No. 63.—Guiding star 3 Puppis. 1939 Mar. 14/15. Exp. 3^h. Comparison mirror $\Delta\delta = +40°$. Slit eq. 40 mm. East of region No. 62. [*O* II] 3727 seems to be in emission.

No. 64.—Guiding star 1. 1939 Orionis. 1939 Mar. 15/16. Exp. 2^h39^m. Comparison mirror $\Delta\delta = +2°$. Slit eq. 40 mm. The guiding star is the nova-like object discovered by Wachmann[5] located in the dark nebula B 35. The nova produced a strong nebulosity, and the purpose of this exposure was to ascertain the character of the spectrum of this small nebulosity. There are strong emission lines of *Hα*, *Hβ*, and [*O* II] 3727, but they are of uniform brightness along the entire length of the slit (1°.5) and show no strengthening in the neighborhood of the guiding star. Hence the spectrum of the small nebulosity must be continuous.

No. 65.—Guiding star *ν* Scorpii. 1939 Mar. 25/26. Exp. 3^h15^m. Comparison mirror $\Delta\delta = +20°$. Slit eq. 30 mm. This star is surrounded by a large nebula, IC 5592, which was found by Hubble[6] to have a continuous spectrum. Our plate shows no emission lines.

No. 66.—Guiding star 44 Ophiuchi. 1939 Mar. 27/28. Exp. 2^h50^m. Comparison mirror $\Delta\delta = +20°$. Slit eq. 40 mm. This region is in the vicinity of *θ* Ophiuchi. The background of the Milky Way looks milky and strongly suggests the existence of nebulosity on the photographs of the Ross *Atlas*. There is no trace of emission, and the milky nebulosity must have a continuous spectrum. It is probable that we are concerned here with the phenomenon described by Elvey and Roach[7] as the galactic light.

No. 67.—Guiding star 45 Ophiuchi. 1939 Mar. 28/29. Exp. 3^h. Comparison mirror $\Delta\delta = +20°$. Slit eq. 45 mm. There is conspicuous nebulosity in this region on Ross's photograph No. 3. The spectrum shows little or no evidence of emission.

No. 68.—Guiding star $-41°10972$ = HD 151932, Sp. WI. 1939 Apr. 15/16. Exp. $2^h\ 50^m$. Comparison mirror $\Delta\delta = +40°$. Slit eq. 40 mm. Weak emission at *Hα*.

No. 69.—Guiding star $-32°12935$ = HD 159176, Sp. O7. Exp. $3^h\ 20^m$. 1939 Apr. 17/18. Comparison mirror $\Delta\delta = +40°$. Slit eq. 40 mm. This region shows a large, faint nebulosity on Ross's photo-

[5] *I.A.U. Circ.*, No. 738, 1939.

[6] *Op. cit.*, p. 181. [7] *Loc. cit.*

graph No. 1. *Hα* and [*O* II] 3727 are conspicuous in emission over the full length of the slit. *Hβ* and *Hγ* are weak. ($N_1 + N_2$) is weak and fades out toward the eastern end of the slit.

No. 70.—Guiding star −37°11206 = HD 153919, Sp. O6W. Exp. 3^h. 1939 Apr. 19/20. Comparison mirror $\Delta\delta = +40°$. Slit eq. 40 mm. Weak emission at *Hα*.

No. 71.—Guiding star μ Scorpii. 1939 Apr. 20/21. Exp. 3^h. Comparison mirror $\Delta\delta = +40°$. Slit eq. 40 mm. North of region No. 70. No emission.

No. 72.—Guiding star in cluster Herschel No. 3651. 1939 Apr. 21/22. Exp. 3^h. Comparison mirror $\Delta\delta = +40°$. Slit eq. 40 mm. 1939 May 17/18. Exp. 3^h. Comparison mirror $\Delta\delta = +40°$. Slit eq. 40 mm. This cluster is enveloped in nebulosity and lies north of a conspicuous group of O-type stars, centered around region No. 68. The spectrum shows emission at *Hα* and [*O* II] 3727, the latter rather weak.

No. 73.—Guiding star μ Normae = HD 149038, Sp. O9e. 1939 Apr. 22/23. Exp. 3^h. Comparison mirror $\Delta\delta = +40°$. Slit eq. 40 mm. There is a slight strengthening of the spectrum at *Hα*, but this is probably caused by night-sky lines near the horizon.

No. 74.—Guiding star in cluster Dunlap No. 568. 1939 Apr. 24/25. Exp. 1^h35^m. Comparison mirror $\Delta\delta = +40°$. Slit eq. 40 mm. The plate is weak, but there seems to be no emission. The cluster is enveloped in a large star cloud having a distinctly milky background on Ross's photographs Nos. 1 and 3.

No. 75.—Guiding star −34°6528 = Scorpii. 1939 Apr. 25/26. Exp. 2^h. Comparison mirror $\Delta\delta = +40°$. Slit eq. 40 mm. No emission.

No. 76.—Guiding star χ Lupi. 1939 May 11/12. Exp. 2^h25^m. Comparison mirror $\Delta\delta = +40°$. Slit eq. 40 mm. 1939 May 19/20. Exp. 3^h. Comparison mirror $\Delta\delta = +40°$. Slit eq. 40 mm. Probably no emission.

No. 77.—Guiding star 15 Sagittarii = HD 167264, Sp. O9. 1939 May 15/16. Exp. 3^h. Comparison mirror $\Delta\delta = +40°$. Slit eq. 40 mm. 1939 May 18/19. Exp. 3^h. Comparison mirror $\Delta\delta = +40°$. Slit eq. 40 mm. *Hα* is in emission.

No. 78.—Guiding star 44 Cygni. 1939 May 21/22. Exp. 1^h22^m.

Comparison mirror $\Delta\delta = +40°$. Slit eq. 40 mm. This star is enveloped in a small bright nebulosity superposed over a large field of milky nebulosity extending from the large Cygnus cloud and from the nebulosities near γ Cygni. The spectrum of 44 Cygni shows marked supergiant characteristics, according to Morgan, and the plate was taken to ascertain whether the small nebulosity near the star is of the emission type. The spectrogram shows *Hα* in emission, of uniform intensity along the entire length of the slit. This emission is evidently a part of the large emission region in Cygnus previously observed by us. There is no strengthening of *Hα* in the immediate vicinity of 44 Cygni. Hence, we conclude that the spectrum of the small nebula is probably continuous.

McDonald Observatory
and
Yerkes Observatory
June 1939

NOTES ON ATMOSPHERIC SODIUM

S. CHAPMAN

ABSTRACT

It is suggested that sodium atoms in the high atmosphere may have a long, though intermittent, free life, despite frequent combination with oxygen atoms to form NaO, through the reaction $NaO + O = Na + O_2$. The source of energy of the light emitted by sodium at night is ascribed to the dissociation energy of oxygen. The level of emission of this light is also discussed.

1. The observation of the D lines of sodium in the night-sky spectrum and with enhanced intensity near sunrise and sunset is now well established,[1,2] and the origin and excitation of the sodium atoms have already been discussed by various writers.[3–6] Such discussion is necessarily speculative at present. The following notes touch on various points, some of them being comments on previous discussions.

THE ORIGIN OF THE SODIUM

2. Among the possible sources of the sodium are (*a*) salt particles from the oceans carried up by ascending currents,[1,3] (*b*) volcanic dust shot up to heights of 10–30 km,[1] (*c*) meteors,[2] (*d*) interstellar sodium swept up by the earth as it moves through space with the solar system,[3] and (*e*) solar streams of gas, such as those whose ionized constituents produce geomagnetic storms.[4]

3. It is obviously difficult to confirm any such suggestions quantitatively, because even if we knew the supply which any particular source could afford, we are unable at present to estimate the rate of removal of the sodium from the levels at which it emits light. This may occur by combination with other atoms and molecules,

[1] R. Bernard, *Ap. J.*, **89**, 133, 1939, and earlier papers.

[2] J. Cabannes, J. Dufay, and J. Gauzit, *Ap. J.*, **88**, 164, 1938, and earlier references there given.

[3] C. Fabry, *M.N.*, **98**, 672, 1938.

[4] S. Chapman, *Meteorol. Mag.*, **73**, 137, 1938.

[5] H. N. Russell, *Sci. Amer.*, **160**, 88, 1939.

[6] J. Franck and C. A. Rieke, *Ap. J.*, **89**, 463, 1939.

leading finally to settlement to the ground (partly in rain), or in other ways.

4. It has been estimated[2] that the meteorites received by the earth supply 2.5×10^3 atoms of sodium per sec per cm^2; I understand this to be the supply to the ground, leaving doubtful the supply to the atmospheric levels where meteor trails are chiefly seen and where the sodium may by vaporization be provided as free atoms. If the two amounts are of the same order, the annual supply per cm^2 column of air would be of order 10^{10} or in 10^9 years of order 10^{19}, corresponding to about $\frac{1}{3}$ cm of sodium gas at N.T.P. If these estimates are roughly correct, it is clear that most of the free sodium thus supplied would have had to be removed from the free atomic state in the atmosphere, since the terrestrial sodium absorption of sunlight is, I understand, very weak, whereas Fabry (*op. cit.*, p. 685) has emphasized[3] how small an amount of sodium vapor ($< 10^{-3}$ cm at N.T.P.) produces easily detectable absorption.

5. In connection with hypothesis (*a*) of § 2, it has been pointed out[6] that *NaCl* molecules would be dissociated by absorption of sunlight in the region 1600–2000 A. This, of course, would occur only by day. The remark was added: "Dissociation during the night could be attributed to electron impacts"; it appears that dissociation of *NaCl* is here referred to. But if, as is most likely, the *NaCl* (combined or dissociated) in the upper atmosphere is a rare constituent, once it has been dissociated by absorption of sunlight its atoms will have small chance of recombining to form the same compound; so that either the *Na* would remain free from the daytime onward into the night or else it would combine with some other atmospheric constituent, and it would be the nocturnal dissociation of the latter that would need consideration.

6. It is most unlikely, however, that dissociation of either *NaCl* or any other compound of sodium could be produced to any significant extent by electron impact during the night, on account of (*a*) the relative scarcity of electrons (even by day, and there are fewer in the ionosphere at night), (*b*) the very small fraction of these which at night could gain the kinetic energy of several volts necessary for the dissociation, and (*c*) the small chance that any such fast electrons would give up their energy to the rare sodium com-

pound molecules, in the presence of the many other atoms and molecules that might absorb this energy, at a single collision or by small steps at many collisions.

THE CONTINUED FREE LIFE OF THE SODIUM ATOMS

7. Russell[5] has emphasized the mystery of the continued free life of the sodium atoms in the upper atmosphere in the presence of the oxygen atoms known to exist there. As regards this, in my opinion the fate of the sodium is likely to depend largely on its relations with its most abundant neighbors, which are molecular nitrogen and oxygen; the latter is molecular at lower and atomic at higher levels. Sodium can form nitrides (Na_3N and NaN_3), but owing to the absence or scarcity of nitrogen *atoms* in the upper atmosphere, these nitrides are unlikely to be formed there to any important extent. It is likely, however, that at levels where there are many free oxygen atoms the following reaction will occur:

$$Na + O + M = NaO + M\,, \qquad (1)$$

where M denotes a third body, usually N_2 or O. At lower levels, where there is little atomic oxygen but some ozone, the following reaction is likely:

$$Na + O_3 = NaO + O_2\,. \qquad (2)$$

8. I have been unable to find any determination of the heat of dissociation of NaO, though it could probably be worked out from known data by considering a cyclical process. If the attachment of the Na to the O atom is similar to that of the H atom in HO, the probably greater distance between the two nuclei in NaO, as compared with HO, suggests that the dissociation energy of Na will be rather less than that of HO (namely, 4.8 volts),[7] which is itself somewhat less than that of O_2 (namely, 5.09 volts).[8] Hence in reac-

[7] H. S. Taylor, *Phys. Chem.*, p. 321.

[8] Dr. W. C. Price suggests that the dissociation potential of NaO may be estimated, to within half an electron volt, as half that of Na_2O, as follows. The heat of formation of Na_2O, at 18° C in its natural state from the elements in their natural states is given as 99.4 k. cal./mole (Bichowski and Rossini, *Thermochemistry of Chemical Substances*, New York, 1936, p. 137). To this must be added $2 \times 25.9(Na) + 59.1(O)$, giving 210.4 k. cal., for the heat of formation of 1 gm molecule of (crystalline) Na_2O from Na atoms and

tion (1) the excess energy (< 5 volts) would seem to be more readily transferred to the third body M if this is an O atom than if it is a nitrogen molecule, whose first electronic level is 6.2 volts above the ground state, whereas the O atom has levels 1.96 ($^1D_2$) and 4.3 volts ($^1S_0$) above the ground state.

9. The free life of the sodium atom having been terminated by one or the other of reactions (1) and (2), it may be renewable by the two-body reaction

$$NaO + O = Na + O_2 , \tag{3}$$

if the attraction of two oxygen atoms for each other exceeds that between Na and O atoms, as the suggested difference between the dissociation energies might indicate. This proposed explanation of the continued (or constantly renewed) free life of the Na atoms is of course tentative, to be checked by definite knowledge of these atomic and molecular collision processes when available. According to this view the sodium atom is able to exist in the free state for an important fraction of a long life, because though union with oxygen atoms is readily contracted, separation follows at no long interval. The Na atom would thus merely act as a convenient intermediary in promoting an $O + O$ recombination; but the energy of this recombination would be transformed in two stages instead of at one only.

THE NOCTURNAL EXCITATION OF THE SODIUM ATOMS

10. The rapid fading of the sodium light at sunset is naturally interpreted as indicating that the sodium is excited to luminescence by sunlight, a process which seems inevitable. It is less evident how the emission is produced at night. It has been suggested[5] that impact of electrons or ions is the cause; but to me this seems improbable, for substantially the same reasons as are urged in § 6 against nocturnal dissociation of sodium compounds by impact.

O atoms (see Table 10.2, p. 54, of Pauling, *Nature of the Chemical Bond*). To obtain the heat of formation of N_2O (gas), the heat of sublimation of Na_2O must be subtracted; this is not known, but in $LiCl$, $NaCl$, and KCl the heat of sublimation is about half that of formation. For Na_2O a smaller fraction, say 30 k. cal., may be taken, since crystalline Na_2O is less symmetrical than the alkali halide crystals. Thus finally we get $210 - 30 = 180$ k. cal. for Na_2O; taking half this for NaO, we have 90 k. cal. or approximately 4 volts.

11. Another suggestion[2] is that the D radiation is a "luminescent phenomenon accompanying the fall of meteorites; in this case each sodium atom would undergo eight thousand transitions before definitely dying out." Though meteorites may possibly be an important source of atmospheric sodium, there seems no special reason why the sodium should emit light only while the meteorite is falling. It seems to me more likely (*a*) that a steady state has been reached between the sodium supply and its final disappearance from the free state, by formation of $NaOH$ or (probably more rarely) Na_2O, and sinking to low levels, and (*b*) that the emission of light occurs by transformation of some atmospheric store of energy always present at night.

12. As I have suggested elsewhere,[4] and originally[9] in connection with the emission of the green oxygen line λ 5577, the only form in which much energy (transformable into radiation) can be stored up by the atmosphere at night, from the energy of sunlight during the day, is dissociation energy; all energy of excitation must disappear very shortly after sunset. The energy of dissociation will be that of dissociation products in their lowest state, for any excitation energy they may initially possess will be short lived. In the upper atmosphere the main dissociation products are probably oxygen atoms and electrons and ions; the latter pairs individually store more energy than the pairs of oxygen atoms, but they are far less numerous. Hence the dissociation energy of oxygen is the store which deserves first consideration in connection with the emission of the night-sky light.

13. I have attempted[10] to show how this energy can be transformed into the observed light of the night sky (the oxygen lines λλ 5577, 6300, 6364, and the Vegard-Kaplan, the first positive, and, with less intensity, other nitrogen bands). As regards the sodium D light, several possibilities may be mentioned; one is that a part of the oxygen dissociation energy is transformed into the excitation energy (2.10 volts) of the ^2P level of Na, at the stage (3) of the sodium reactions discussed in §§ 7–9; to check this suggestion it is necessary to have knowledge as to the energy released in this reaction.

14. The night-sky emission of the oxygen lines λλ 5577, 6300, and

[9] *Proc. R. Soc.*, Ser. A, **132**, 353, 1911. [10] *Phil. Mag.*, Ser. 7, **23**, 657, 1937.

6364 implies the presence, at high levels, of many O atoms in the metastable $^1D_2$ state, which is the final state in the former emission and the initial state for the two red lines; it has a very long life (about 100 seconds) and an excitation energy of 1.96 volts. The excitation energy of the ^2P level of Na is 2.10 volts. It seems possible that in a two-body collision of Na (in its lowest state) with O (in the $^1D_2$ state), not leading to combination, the excitation energy of the O atom, together with the necessary extra 0.14 volts, if available, from the translatory kinetic energy of the two atoms, may raise the Na atom to the ^2P level; the transfer probability is likely to be low, though the necessary amount of kinetic energy, which would correspond to the mean kinetic energy of a single atom in a gas at about 1000° K, is not impossibly high. As regards reaction (3) of § 9, possibly when the free atom of O concerned therein is a $^1D_2$ atom, there is a greater chance of the freed Na atom being excited to the ^2P level. The number[2] of D quanta emitted by atmospheric sodium per cm² column of air per sec (namely 2×10^7), is about one-tenth the number of quanta of the light of λ 5577, so that some emission process involving a considerable supply of energy to the Na atoms must be involved; and oxygen atoms, because of their abundance and their energy store, seem to be the most likely source of this energy.

THE LEVEL OF THE EMISSION OF THE SODIUM D LIGHT

15. Bernard has suggested that the sodium D light is emitted in a relatively thin layer at about 60–80 km height, because when the sun's rays, at sunset, rise past this level, the D-light intensity falls within a minute or two to about 1 per cent of its former value. He concludes also, from the absence of the D lines of Na in the auroral spectrum, that the Na itself is absent in the auroral region.

16. Assuming, with Bernard, that the enhanced D_2 light of Na at twilight is due to "an optical resonance under the action of sunlight," any lower limit that can be set to its level of resonance emission must be interpreted as indicating a rapid downward decrease, at that height, in its absolute concentration;[11] it would not be sur-

[11] Provided that the collision interval at this height exceeds the free life (about 10^{-8} sec) of the ^2P stated of the Na atoms; this condition is fulfilled at all heights above about 30 km.

prising that at about 60 km there should be such a downward decrease in the number-density of free sodium atoms, because at that level the amount of atomic oxygen is decreasing rapidly downward, while that of ozone is increasing downward; thus, though sodium may be oxidized by combination with O_3 (or O), the chance of a molecule of NaO being dissociated again by meeting an O atom is rapidly decreasing downward.

17. It is also possible that in the layer 60–80 km the Na number-density reaches its maximum; but I see no reason to suppose that its concentration ratio should decrease at all rapidly above the level of maximum; it may even increase, because Na atoms are lighter than N_2 molecules. Thus the number density of Na atoms may be proportional to the whole density of the air, above the level of maximum Na. If so, the resonance luminescence would vary with height in the same way. A rise of the lower level of sunlight near sunset from 60 to 80 km would correspond to the eclipse of about $\frac{9}{10}$ of the free sodium present, if this is distributed as suggested above the 60-km level. This seems to offer an explanation of at least the greater part of the rapid decrease in the D light at sunset, observed by Bernard.

18. His inference that Na is absent at auroral levels does not seem to me to be required by the fact of the absence of the D lines in the auroral spectrum. The auroral light is probably[10] excited by the impact of fast-incoming solar particles: in such circumstances it seems likely that the luminescence produced by the different kinds of atmospheric particle present, viz., N_2, N_2^+, $N, O, Na, \ldots$, is roughly proportional to the number-density of each such particle along the track of the exciting rays; of course, this number density need not there be the same as at points outside this track, as the incoming particles probably suddenly increase the numbers of N_2^+ and N, and probably also of O^+ and Na^+, along their track. The fact that no D light of Na is observed in the auroral spectrum may merely signify that along the auroral ray the Na atoms are either largely ionized by impact or are present in very small proportion but not necessarily in a smaller proportion than at 60-km level where the twilight resonance emission of the D light mainly occurs, according to Bernard. For example, suppose (purely for illustration)

that along the auroral ray there is only one *Na* atom to each 1000 N_2 molecules and *O* atoms and that each of these three kinds of particle has, under the corpuscular excitation, roughly the same chance of emitting a quantum of visible radiation, the *Na* contribution to the auroral light will be insignificant. Yet in the twilight this small proportion of *Na* atoms may emit an easily observable amount of radiation by absorbing and re-emitting suitable light quanta, each atom undergoing many thousand (or million) transitions (by absorption and emission) per second.

19. There seems to be no necessary contradiction between Bernard's twilight-height estimate of 60 km and the estimate by Cabannes, Dufay, and Gauzit that the main level of D emission at night is 130 km, though of course the criticisms by Bernard and Déjardin of the accuracy of this estimate need careful consideration. The twilight emission, if due to optical resonance, will be most intense where the number-density of *Na* atoms is greatest; the night-sky emission, due to a totally different type of excitation, may well be at a higher level, where the absolute number-density of *O* atoms is greater than at 60 km.

IMPERIAL COLLEGE OF SCIENCE AND TECHNOLOGY
June 1939

NOTES

SPECTROPHOTOMETRIC OBSERVATIONS OF ζ AURIGAE NEAR THE BEGINNING OF ITS 1937 ECLIPSE

On eight different nights in the spring of 1937 ζ Aurigae was observed with a photoelectric photometer attached to the 24-inch telescope of the Sproul Observatory. Four of these nights preceded and four followed the beginning of the eclipse.

The position of this eclipsing variable was such that ε Aurigae was the only star of comparable brightness which could be used as a comparison star. The corrections for differential extinction for other comparison stars would have been prohibitive, even though the observations were to be made in the red and infrared regions of the spectrum. Photoelectric observations of ε Aurigae by Guthnick and Pavel[1] on twenty-five nights in 1921 showed no variation greater than $0^m.01$. Those of C. M. Huffer[2] and M. Güssow[3] indicate that this star outside eclipse may have constant periods of several weeks, although at times its departure from its mean magnitude in the violet may be as large as $0^m.10$. Presumably these secondary variations are characteristic of the brighter component and are much smaller in the deep red than in the violet.

Spectra were produced by means of a fine-wire objective grating. A grating spectrometer in the focal plane separated the first-order spectra into definite energy units 966 A wide and reflected them to the photocell.[4] Four different effective wave lengths were used: the shortest was at 6540 A and the longest at 9280 A.

Two stop-watch readings were made at each spectral region for each setting of the telescope. A standard lamp was swung into position, and its intensity was measured at the beginning and at the end of the group of readings made on each star. This enabled me to cor-

[1] *A.N.*, **215**, 395, 1922.
[2] *Ap. J.*, **76**, 1, 1932.
[3] *A.N.*, **250**, 75, 1933.
[4] *Ap. J.*, **84**, 372, 1936.

rect for the gradual changes in the sensitivity of the photometer with changes in the position of the telescope and to determine the extinction coefficients.

The stars ζ and ϵ Aurigae are less than 3° apart. On the first four nights the observations were made at relatively small zenith distances, and consequently the corrections for differential extinction were very small or negligible. The extinction coefficients were determined and applied to the observations in each wave length on each of the last four nights. Since the zenith distances were never

TABLE 1

OBSERVED DIFFERENCES IN MAGNITUDE (ζ *minus* ϵ AURIGAE)

1937 E.S.T.	JD 2428	6540 A		7460 A		8380 A		9280 A		MEAN DIFF.
		Δm	p	Δm	p	Δm	p	Δm	p	
Mar. 27.87	620.58	+0^m.28	1.3	−0^m.04	1.3	−0^m.11	1.3	−0^m.23	1.3	0^m.000
Mar. 29.86	622.57	.30	1.3	+ .02	1.3	.10	1.3	.25	1.3	+ .018
Apr. 16.85	640.56	.23	3.0	− .07	1.3	.15	1.3	.19	1.3	− .024
Apr. 19.83	643.54	+0.34	1.0	−0.04	1.3	−0.14	1.3	−0.19	1.3	+0.015
Weighted mean (p.e.)	.....	+0.270±0.016		−0.032± .013		−0.125± .008		−0.215± .010		.....
Apr. 22.88	646.59	+0.36	1.0	+0.06	4.0	−0.10	3.0	−0.18	3.0	+0.003
Apr. 30.86	654.57	.33	3.4	.00	2.4	.11	2.0	.19	2.0	− .022
May 1.86	655.57	.37	3.0	+ .08	2.0	.07	2.4	.11	2.0	+ .036
May 2.86	656.57	+0.32	3.0	+0.07	2.0	−0.10	2.0	−0.24	2.0	−0.018
Weighted mean (p.e.)	.....	+0.342± .008		+0.052± .011		−0.094± .006		−0.180± .017		.....
Change in Δm	.....	+0.072± .018		+0.084± .017		+0.031± .010		+0.035± .020		.....

greater than 72° and since the two stars were observed at nearly the same zenith distance, these differential corrections never exceeded a few hundredths of a magnitude.

The observations are given in Table 1. The first column gives the mean date of observation in Eastern Standard or Seventy-fifth Meridian time. The final column shows the weighted mean departure of each night from the weighted mean magnitude differences of each of the two groups of four nights each. The weights are so arranged that unit weight signifies that each star was observed but once in that particular spectral region. A weight of 1.3, therefore, means that one star was observed twice and the other once. No observations have been rejected. All nights were of good transparency with

the exception of April 22, when the observations were interrupted by clouds.

Some observers have found reason to suspect that ζ Aurigae is also slightly variable outside eclipse, while equally accurate observations by others have failed to confirm this suspicion. The figures in the last column of Table 1 show that the difference in magnitude between these two stars was sensibly constant during the two intervals of four nights each. Taylor[5] reached the same conclusion from a discussion of his visual comparisons of these same two stars. These were made on many nights in common with mine at the near-by Flower Observatory. The fact that the residuals of the second group are larger than those of the first in the final column of Table 1, despite the fact that they are based on more numerous observations, may be attributed to atmospheric disturbances which are nearly always present at such large zenith distances.

Although we cannot be absolutely sure that the brighter component of either binary did not vary between JD 643.54 and 646.59, the observed changes in magnitude occurring between these two dates seem to agree reasonably well with those that might be expected from the depths of the minimum found by others in shorter wave lengths. According to Guthnick, Schneller, and Hachenberg,[6] the 1937 eclipse began at JD 2428644.60. Christie and O. C. Wilson[7] have found that the partial phase lasts 1.7 days. The observations in the deep red given in Table 1 indicate that the partial phase had not made itself evident 1.1 days previous to the time of its beginning found by Guthnick *et al.*[6] in the photographic region of the spectrum. Also, the partial phase was evidently more than 0.3 day after the time predicted by the Babelsberg[6] and Mount Wilson[7] results. This is, therefore, evidence that the deep-red light from the B8 star passing through the outer atmosphere of the K4 star is cut off at approximately the same time as is its violet light.

Numerous values found for the depths of the primary minimum of ζ Aurigae by several observers in different spectral regions are given in Table 2. Published visual amplitudes vary from $0^m.10$ to $0^m.35$. A

[5] *A.N.*, **262**, 436, 1937.

[6] *A.N.*, **262**, 430, 1937.

[7] *Ap. J.*, **81**, 438, 1935.

value of $0^m.16$ would fit the other observations if we assume that the visual effective wave length is at 5500 A. An attempt to represent the data of Table 2 by assuming that the B8 and K4 stars have black-body temperatures of 15,000° and 3000°, respectively, indi-

TABLE 2

LOSS OF LIGHT AT PRIMARY MINIMUM

Wave Length	m	Observer	Wave Length	m	Observer
3780	$2^m.14$	Guthnick *et al.**	5090	$0^m.25$	Himpel‖
4140	1.03	Guthnick	5500	.22	Taylor**
4260	0.77	C. M. Huffer†	5640	.10	Guthnick
4300	0.70	K. Walter‡	5820	.10	Himpel
4450	0.559	Guthnick	5900	.105	Guthnick
4500	0.50	Huffer	6100	.095	Walter
4500	0.448	Smart and Green§	6540	.07	Hall
4640	0.43	Guthnick	7460	.08	Hall
4770	0.36	Huffer	8380	.03	Hall
4950	0.274	Guthnick	9280	0.03	Hall

* *Abh.d. Akad. Berlin*, No. 1, 1935.
† *Ap. J.*, **81**, 292, 1935.
‡ *Zs. f. Ap.*, **14**, 62, 1937.
§ *M.N.*, **95**, 31, 1934.
‖ *A.N.*, **258**, 251, 1936.
** *A.N.*, **262**, 436, 1937.

cates that the first and last three magnitude differences are too large to be compatible with those between. It is hoped that these data will be considerably improved by the 1939–1940 eclipse. Apparently the time of eclipse can be determined with reasonable accuracy as far to the red as 7500 A.

JOHN S. HALL

AMHERST COLLEGE OBSERVATORY
August 19, 1939